

https://dspace.org/

Application of indicator kriging and conditional simulation in assessment of grade uncertainty in Hunters road magmatic sulphide nickel deposit in Zimbabwe

Chiwundura, Phillip

2017

https://hdl.handle.net/10539/24082

Chiwundura, Phillip (2017) Application of indicator kriging and conditional simulation assessment of grade uncertainty in Hunters road magmatic sulphide nickel deposit in Zimbabwe,University of the Witwatersrand, <https://hdl.handle.net/10539/24082>

Downloaded from a DSpace repository. https://dspace.org/

APPLICATION OF INDICATOR KRIGING AND CONDITIONAL SIMULATION IN ASSESSMENT OF GRADE UNCERTAINTY IN HUNTERS ROAD MAGMATIC SULPHIDE NICKEL DEPOSIT IN ZIMBABWE.

PHILLIP CHIWUNDURA

A research project report submitted to the Faculty of Engineering and the Built Environment, University of the Witwatersrand, in fulfilment of the requirements for the degree of Masters of Science in Engineering.

Johannesburg, 2017

DECLARATION

I declare that this research report is my own, unaided work. It is being submitted to the Degree of Master of Science in Engineering to the University of the Witwatersrand, Johannesburg. It has not been submitted before for any degree or examination to any other University.

_____ _____

Signature Date

ABSTRACT

The assessment of local and spatial uncertainty associated with a regionalised variable such as nickel grade at Hunters Road magmatic sulphide deposit is one of the critical elements in the resource estimation. The study focused on the application of Multiple Indicator Kriging (MIK) and Sequential Gaussian Simulation (SGS) in the estimation of recoverable resources and the assessment of grade uncertainty at Hunters Road's Western orebody. The Hunters Road Western orebody was divided into two domains namely the Eastern and the Western domains and was evaluated based on 172 drill holes. MIK and SGS were performed using Datamine Studio RM module. The combined Mineral Resources estimate for the Western orebody at a cut-off grade of 0.40%Ni is 32.30Mt at an average grade of 0.57%Ni, equivalent to 183kt of contained nickel metal. SGS results indicated low uncertainty associated with Hunters Road nickel project with 90% probability of an average true grade above cut-off, lying within +/-3% of the estimated block grade. The estimate of the mean based on SGS was 0.55%Ni and 0.57% Ni for the Western and Eastern domains respectively. MIK results were highly comparable with SGS E-type estimates while the most recent Ordinary Kriging (OK) based estimates by BNC dated May 2006, overstated the resources tonnage and underestimated the grade compared to the MIK estimates. It was concluded that MIK produced better estimates of recoverable resources than OK. However, since only E-type estimates were produced by MIK, post processing of "composite" conditional cumulative distribution function (ccdf) results using a relevant change of support algorithm such as affine correction is recommended. Although SGS produced a good measure of uncertainty around nickel grades, post processing of realisations using a different software such as Isatis has been recommended together with combined simulation of both grade and tonnage.

DEDICATION

To my late father

STEPHEN CHIWUNDURA

1960 - 2017

ACKNOWLEDGMENTS

I would like to thank Bindura Nickel Corporation (BNC) management for funding this project. Furthermore, I would like to thank my supervisor Prof Richard Minnitt for his guidance and support. My workmates at BNC and all my friends who supported me tirelessly throughout my studies need special mention. My last regards goes to my wife Angela, my mother, Gorginah Muzembi and my two daughters Natasha and Samantha for their support and understanding.

TABLE OF CONTENTS

DECLARATION i
ABSTRACT ii
DEDICATION iii
ACKNOWLEDGMENTS iv
LIST OF FIGURES viii
LIST OF TABLES xi
LIST OF SYMBOLS xiii
LIST OF ABBREVIATIONS xiv
CHAPTER 1: INTRODUCTION 1
1.1 Introduction 1
1.2 Location of the Project 1
1.3 Background Information 1
1.4 Problem Statement 3
1.5 Significance of the Work 4
1.6 Research Objectives 5
1.7 Chapter Summary 5
CHAPTER 2: LITERATURE REVIEW 6
2.1 Introduction 6
2.2 Linear Geostatistical Estimation Methods 6
2.2.1 Ordinary Kriging 7
2.3 Estimation of Recoverable Resources: Non-Linear Resource Estimation Techniques 10
2.3.1 Indicator Kriging 11
2.3.2 Multiple Indicator Kriging (MIK) and Median Indicator Kriging(MeIK) 13
2.3.3 Change of Support 14
2.3.4 Order Relations Problem 15
2.4 Assesment of Spatial Uncertainty : Conditional Simulation 16
2.4.1 Sequential Gaussian Simulation 17
2.5 Normal Score Transformation 21
CHAPTER 3: HUNTERS ROAD GEOLOGICAL SETTING 24
3.1 Introduction 24
3.2 Regional Geology 24
3.2.1 Local Geology 26
3.2.2 Nickel Mineralisation 28

3.2.3 Geozones 30
3.3 Chapter Summary 32
CHAPTER 4: EXPLORATORY DATA ANALYSIS (EDA) 33
4.1 Introduction 33
4.2 Validation of Historical Data. 33
4.2.1 Summary of Findings 34
4.3 Orebody Wireframe Validation 40
4.4 QAQC 42
4.5 Relative Density 43
4.6 Statistical Analysis of the Data 44
4.6.1 Compositing and Declustering 44
4.6.2 Descriptive Statistics 48
4.7 Normal Score Statistical Analysis 51
4.8 Summary of Findings 54
CHAPTER 5: VARIOGRAPHY 55
5.1 Introduction 55
5.2 Indicator Variography 56
5.2.1 Indicator Variograms for Eastern Domain 58
5.2.2 Indicator Variogram for Western Domain 61
5.2.3 Cross Validation of Indicator Semi Variogram Models 64
5.3 Normal Scores Semi Variogram Models 66
5.3.1 Cross validation of NS semi variogram 70
5.4 Summary of the Findings 72
CHAPTER 6: RESOURCE ESTIMATION 74
6.1 Introduction 74
6.2 Indicator Kriging Estimation Parameters. 74
6.2.1 Multiple Indicator Kriging Search Volume Parameters 75
6.2.2 Block Size Dimensions 77
6.2.3 Mineral Resource Estimates 77
6.2.4 Cross Validation of the Block Model 82
6.3 Comparison of MIK Estimates and Historical OK Estimates. 86
6.3.1 Analysis of Mineral Resources per Domain 88
6.4 Summary of the Findings 93
CHAPTER 7: CONDITIONAL SIMULATION 95
7.1 Introduction 95

7.2 SGS Steps in Datamine Studio RM 95
7.2.1 SGSIM Results..... 97
7.2.2 SGSIM Validation of Input Variogram (NS) 99
7.3 Analyses of SGS Results..... 119
7.3.1 Eastern Domain Analysis 119
7.3.2 Western Domain Analysis 120
7.4 Chapter Summary..... 122
CHAPTER 8: DISCUSSION 123
8.1 Introduction..... 123
8.2 Estimation of Recoverable Resources Using Indicator Kriging (IK) 123
8.3 Assessment and Quantification of Grade Uncertainty at Hunters Road 124
8.4 Comparison of Historical OK Estimates with Current Estimates 125
CHAPTER 9: CONCLUSION AND RECOMMENDATION..... 128
9.1 Conclusion..... 128
9.2 Recommendation..... 130
10 REFERENCES..... 132

APPENDIX 1: QAQC control charts for 1992 to 1993 exploration program. 138

APPENDIX 2: Variogram models for the Eastern Domain of the Western orebody of Hunters Road nickel project. 144

APPENDIX 3: Variogram models for the Western Domain of the Western orebody of Hunters Road nickel project. 152

APPENDIX 4: Mineral resources per bench for the EASTERN and western domains. 161

LIST OF FIGURES

Figure 1: Location map BNC nickel mines and projects (in red) including ... Hunters Road nickel project in Zimbabwe. 2
Figure 2: Quantile to quantile transformation using cumulative distribution function (Source: Rossi and Deutsch, 2014, p. 22) 22
Figure 3: Regional setting of Hunters Road nickel deposit (extracted from Prendergast, 2001) 25
Figure 4: Local geology for Hunters Road nickel deposit extracted from Prendergast (2001). 26
Figure 5: Geological map showing the location of the Western orebody (West Pit Area) of Hunters Road nickel deposit. 29
Figure 6 : Geological map showing the Eastern and Western domains of the Western Orebody of Hunters Road nickel deposit. 31
Figure 7: Geological map showing the location of boreholes with validation problems. 36
Figure 8: Map showing the location of the 14 holes which did not intersect nickel mineralisation. 38
Figure 9 : Map showing geographical location of the 172 boreholes used in the current study. 39
Figure 10: 3D image of the Eastern and Western domain of the Western orebody 40
Figure 11 : A section showing orebody outlines and drill hole intersections based on indicator grades. 41
Figure 12: PP and QQ plot of eastern and western domain of the Western orebody of Hunters Road nickel deposit. 47
Figure 13: Histogram and cumulative frequency curve for the Eastern domain before declustering. 49
Figure 14: Histogram and cumulative frequency curve for the Western domain before declustering. 50
Figure 15: Histogram and descriptive statistics before and after NS transformation for the Eastern domain samples. 52

Figure 16: Histogram and descriptive statistics before and after NS transformation for the Western domain samples..... 53
Figure 17: Indicator semi variogram for the Eastern Domain using a 0.49%Ni COG. 60
Figure 18: A plot of indicator semi variogram model for the Western Domain using a COG of 0.53%Ni. 63
Figure 19: Scatter plot of actual versus estimated grades for the Eastern and Western domains. 65
Figure 20: NS variogram for the Eastern domain showing directional variogram and downhole variogram. 68
Figure 21: NS variogram for the Western domain showing directional variogram and downhole variogram. 69
Figure 22: Cross validation results for NS variogram for the Eastern and Western domain. 71
Figure 23: Block model for the Eastern and Western domain showing grades determining through MIK. 78
Figure 24: MIK Grade Tonnage curve for the Eastern Domain - Block size 25m x 25m x 10m) 80
Figure 25: MIK Grade Tonnage curve for the Western Domain - Block size 25m x 25m x 10m) 81
Figure 26: A sectional plot of block grades and drill hole sample grades for the Western and Eastern domain. 83
Figure 27: SWATH plot of sample values versus estimated values along the three principal direction for the Eastern domain. 84
Figure 28: SWATH plot of sample values versus estimated values along the three principal direction for the Western domain. 85
Figure 29: NS histogram showing a comparison of sample and 25 simulation realisation distribution for the Eastern domain. 98
Figure 30 : NS histogram showing a comparison of sample and 25 simulation realisations distribution for the Western domain. 98
Figure 31: Eastern Domain downhole and directional semi variogram generated from 25 realisations (downhole variogram). 100

Figure 32: Directional variogram for the 25 simulations of Eastern Domain 100
Figure 33 : Western Domain downhole and directional semi variogram generated from 25 realisations..... 101
Figure 34: Directional variogram for the 25 simulations of Western Domain 102
Figure 35: P10 probability map and block model for the Eastern and Western domains 104
Figure 36: P50 probability map and block model for the Eastern and Western domains. 105
Figure 37: P90 probability map and block model for the Eastern and Western domains. 106
Figure 38: Map and block model showing conditional variances for the Eastern and Western domains. 108
Figure 39: Confidence graph for parent cells of the Eastern domain block model. 110
Figure 40: Confidence graph for parent cells of the Western domain block model 112
Figure 41: Block model grade confidence level plot for the Eastern domain. 115
Figure 42: Block model grade confidence level plot for the Western domain. 117
Figure 43: Grade tonnage curve based on various cut off grades of 118
Figure 44: Grade tonnage curve based on various cut off grades of 119

LIST OF TABLES

Table 1: A summary of drill holes that were excluded from the database used in the current research. 35
Table 2: Declustering statistics for the Eastern and Western domains. ... 45
Table 3: A summary of the cut off grades used in calculating indicator variograms for the Eastern and Western domains. 57
Table 4: The double structured spherical models for the indicator semi variograms of the Eastern Domain at various cut-offs. 59
Table 5: The double structured spherical models for the indicator semi variograms of the Western Domain at various cut-offs. 62
Table 6 : NS semi variogram parameters for the Eastern and Western domain 70
Table 7: Search volume parameters for MIK for Eastern and Western domains. 76
Table 8: Mineral Resource MIK Estimates for Eastern and Western domains without COG. 78
Table 9 : Mineral Resource MIK Estimates for the Eastern and Western domain based on a 0.40%Ni COG. 79
Table 10: Mineral Resource MIK Estimates for the Eastern domain per search volume (SVOL) based on 0.40% Ni COG. 79
Table 11: Mineral Resource MIK Estimates for the Western domain per search volume (SVOL) based on 0.40% Ni COG. 80
Table 12: MIK Grade, Tonnage and Metal content for the Eastern domain at various cut-off grades (Block size 25m x 25m x 10m). 81
Table 13 : Grade, Tonnage and Metal content for the Western domain at various cut-off grade. 82
Table 14: A summary of Hunters Road Western orebody nickel resource estimates 87
Table 15: A summary of Mineral Resources Estimates above and below 0.40% cut-off grade for the Eastern Domain 88
Table 16: A summary of Mineral Resources Estimates above and below 0.40% cut-off grade for the Western Domain 88

Table 17: Hunters Road West orebody resource summary as at May 2006(BNC estimate) 89
Table 18: A summary of AACS January 2001 resource estimates for the two domains at 0.40% Ni cut-off grade. 90
Table 19: MIK Mineral Resource Estimates for the Eastern domain split by elevation interval. 91
Table 20: MIK Mineral Resource Estimates for the Western domain split by elevation interval and 0.40% COG. 92
Table 21: Statistical summary of 25 simulations and the samples used in the simulation in NS space 99
Table 22: Statistical parameters for simulated points of 100 realisations. 103
Table 23: Confidence levels for Eastern domain parent cells at various grade intervals. 109
Table 24: Confidence levels for Western domain parent cells at various grade intervals. 111
Table 25: Block model grade confidence levels per cut-off grade for the Eastern domain. 114
Table 26 : Block model grade confidence levels per cut-off grade for the Western domain. 116

LIST OF SYMBOLS

t	tonnes
%	percent
m^3	volume
t/m^3	Insitu density
σ	Standard deviation
μ	mean
Mt	million tonnes
kt	kiloton
wt%	percentage by weight

LIST OF ABBREVIATIONS

AACS	Anglo American Corporation of South African
ASL	Above sea level
BIF	Banded Iron Formations
BNC	Bindura Nickel Corporation
Ccdf	cumulative conditional distribution function
COG	cut-off grade
E1	E-Type 1
E2	E-Type 2
EDA	Exploratory Data Analysis
FSUF	Fife Scott Ultramafic formation
IMF	Ingwenya Mafic Formation
KKFF	Kwekwe Felstic Formations
LOM	Life of mine
MeIK	Median Indicator Kriging
MIK	Multiple Indicator Kriging
MinRED	Mineral Resource Evaluation Department
NNE	North North East
NS	Normal Scores
OK	Ordinary Kriging
QAQC	Quality Assurance Quality Control
RJF	Redcliff Jaspilite Formations
SGS/SGSIM	Sequential Gaussian Simulation
SK	Simple Kriging
SRK	SRK Consulting
WNW	West North West

CHAPTER 1: INTRODUCTION

1.1 Introduction

Hunters Road nickel project is a large low grade komatiite-hoisted nickel deposit (Prendergast, 2001) located in the Midlands Province of Zimbabwe within a sheared serpentinised Archean ultramafic sequence (SRK Consulting Zimbabwe, 2002). The prospect is owned by Bindura Nickel Corporation (BNC), a subsidiary of Asa Resources PLC, formerly Mwana Africa. BNC has mining rights covering approximately 2818 hectares occupying the Clearwater and Rietfontein farms. A review of historical documents showed that the deposit was discovered by JCI in 1969 and further explored by Donnington Ventures (Union Corporation) between 1971 and 1974. The claims were transferred to Trojan Nickel Mine in 1989, a subsidiary of Bindura Nickel Corporation, which was owned by Anglo American Corporation, in June 1966 (Anglo American Corporation, 1987.BNC was sold to Mwana Africa in 2003, which has changed name to Asa Resource Group since October 2015.

1.2 Location of the Project

Hunters Road nickel deposit is located approximately 25km south of Kwekwe and 37km north of Gweru in Midlands Province. A map showing the location of Hunters Road project in relation to other nickel deposits owned or formerly owned by BNC is shown in Figure 1.

1.3 Background Information

Anglo American Corporation, through its 2002 life of mine (LOM) plan, forecasted the closure of Shangani Mine in 2007 and Trojan Nickel Mine in 2012. Based on the forecast, a viable project to replace the two mines was needed. Hunters Road Project's Western orebody was identified as a nickel deposit which could sustain Bindura Smelter and Refinery (BSR) at full capacity until 2020 (Anglo American Corporation of South Africa (AACS), 2002). Shangani mine was put on care and maintenance in 2007 followed

by Trojan Nickel Mine in 2008. Trojan Nickel Mine was however reopened in 2012 and has been operational since then. Shangani Mine did not reopen and is going through mine closure processes.

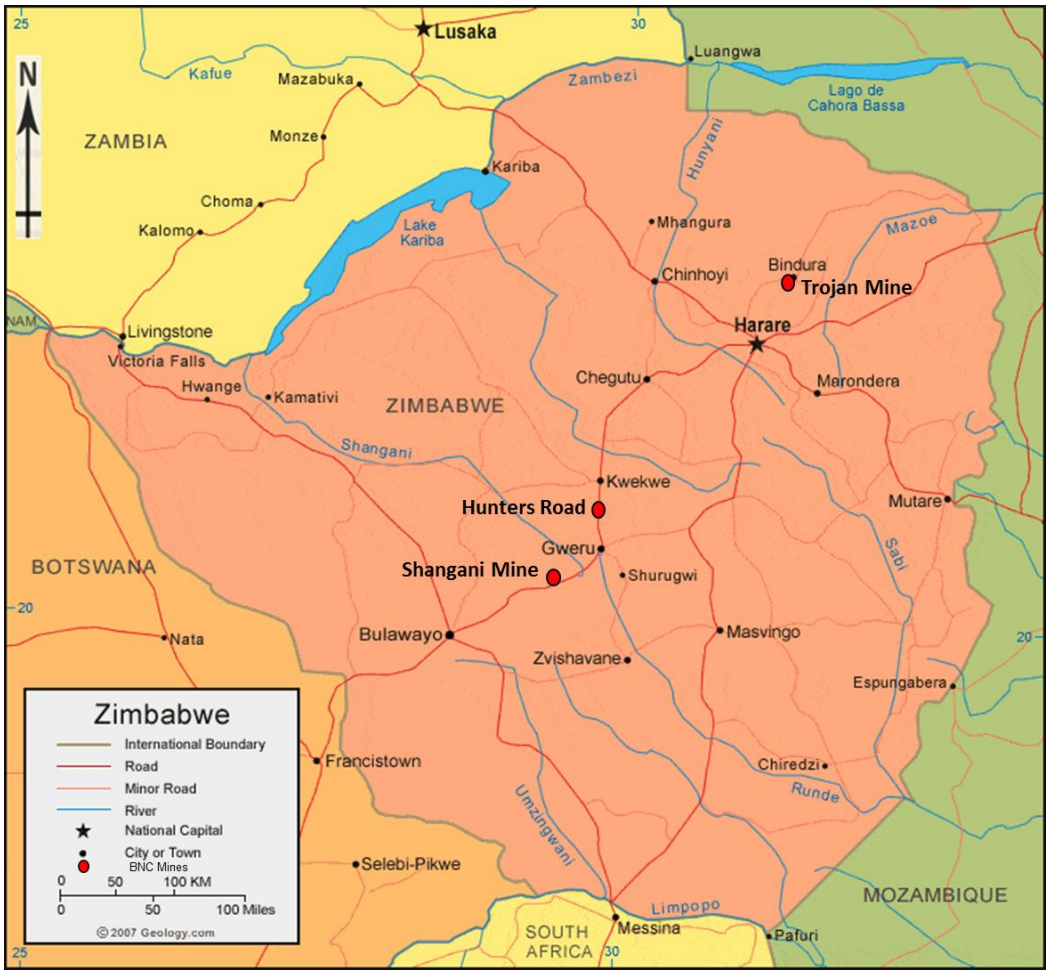

Figure 1: Location map for BNC nickel mines and projects (in red) including Hunters Road nickel project in Zimbabwe.

In the period between 1971 and 2004, exploration and metallurgical test work were carried out at Hunters Road targeting the western area with the aim of increasing geological and metallurgical confidence in the deposit. A total of 173 drill holes were drilled between 1971 and 2002 while 10 additional drill holes were drilled between 2003 and 2004 by Mwana Africa. In May 2006, Mwana Africa, based on Ordinary Kriging (OK) grade interpolation and 0.40%Ni cut-off grade declared an Indicated Resources

estimated at 36.4Mt at an average grade of 0.55%Ni (Bindura Nickel Corporation (BNC), 2006). Similarly, in January 2001, the Mineral Resource Evaluation Department (MinRED), based on 173 drill holes, estimated the same resources on the Western Orebody to be approximately 35.8Mt at an average grade of 0.59%Ni (AACS, 2002). In November 2001, SRK using the same method (OK) estimated 41.3Mt at an average grade of 0.55%Ni. The resource was classified as Inferred due to the fact that indicated portions were very small, isolated and spread across the entire deposit (AACS, 2002).

The results from these three resource statements shows a narrow margin between the resource cut-off grade of 0.40%Ni and an average estimated grade of 0.55% Ni. This margin presents potential risk in that the grades anticipated during mining may not be realised.

Despite such a narrow margin between the resource cut-off grade and the estimated grade, there was no attempt to quantify or assess grade uncertainty for the purpose of optimisation and decision making at that time. However, greater focus was put on understanding metallurgical properties and alteration zones in the deposit. In addition, 2001 estimates were based on a relative density of 2.85t/m^3 while the 2006 estimates were based on a relative density of 2.6 t/m^3. Such significant changes in density presents an additional risk in the estimates. Despite the risky nature of the project, there was no attempt to estimate recoverable resources using a different grade interpolation method suitable for that purpose.

1.4 Problem Statement

The three historical resource estimates highlighted above were all done using OK, which produces a single estimated value and a kriging variance which is independent of the data values. Despite the limitation of OK, the resource estimates obtained may not reflect both local and spatial uncertainty associated with regionalised variables. The fact that OK

standard error is not conditional on the data values implies that it may not provide an accurate measure of uncertainty in grade and tonnage estimates (Yamamoto, 2005; Emery, 2005).

Resource estimates were focussed on quantifying the tonnage and expected grade at the time of reporting rather than quantifying the uncertainty surrounding the estimates. Assessment of the uncertainty associated with resource estimates is fundamental to mine design and evaluation of financial viability of mining operation. Reliance on linear geostatistical methods such as OK alone, which produces smoothed estimates may expose the project to unnecessary risks (Yamamoto, 2005). The smoothing effect of OK will generally result in a grade and tonnage curve which does not match grade tonnage curve of the selective mining units(SMU) at the time of extraction (Rossi, 1999). In order to avoid risks associated with linear geostatistical estimation techniques, indicator kriging and conditional simulation were used to assist in the estimation of recoverable resources assessment of uncertainty associated with nickel grades at Hunters Road.

1.5 Significance of the Work

This research project enables quantification of grade uncertainty surrounding the project and allows for sound decisions to be made based on risk based estimates. Grade uncertainty derived from the research will assist in mine planning and optimisation which is important during feasibility studies and consequently the development of Hunters Road mine. A focus on grade uncertainty will assist in increasing confidence in the resources as well as identifying areas which need further drilling and geological investigation. Economically, the results will assist the company in deciding whether to invest or divest in this project that has been dormant since 2004.

1.6 Research Objectives

The main objectives of the project are:

- To estimate recoverable resources using Indicator Kriging (IK).
- To assess and quantify grade uncertainty associated with the deposit in terms of grade and tonnage estimates.
- To compare historical OK estimates with the current estimates.

1.7 Chapter Summary

This introductory chapter has given context to this research, as well as the background to build a firm foundation for the research. It went on to state the problem and to establish the significance of the study. Finally it articulated the research objectives which provide the study a road map. The next chapter reviews the related literature.

CHAPTER 2: LITERATURE REVIEW

2.1 Introduction

The previous chapter introduced the study. This chapter reviews related literature in order to establish what is already known about the research topic, thereby establishing a knowledge gap that this study attempts to fill. The literature review will focus on linear and non-linear geostatistical methods and conditional simulation which are key themes of the current study.

2.2 Linear Geostatistical Estimation Methods

Geostatistical methods can be classified broadly into two categories namely linear and non-linear geostatistical techniques. Linear geostatistical methods such as Ordinary Kriging (OK) and Simple Kriging (SK) are distinguishable from non-linear geostatistical methods such as indicator kriging (Journel 1982; 1988), multigaussian kriging (Verly, 1983) and uniform conditioning (Rivoirard, 1994) by the way the weights are allocated to the sample. Linear estimation methods assign weights to samples that are independent of the specific sample values at those locations (Vann, et al., 2000). The weights allocated to sample grades depends on the degree of spatial correlation of the underlying phenomena as defined by a variogram and sample configuration (Journel, 1982). In contrast, non-linear estimation methods allocate weights to samples that are a function of the actual grades themselves instead of only depending on the location of data.

The following section will focus on OK which was used in estimating mineral resources at Hunters Road since 1992. OK will be discussed together with SK which is a key estimation method in conditional simulation.

2.2.1 Ordinary Kriging

Ordinary kriging is a non-stationary linear geostatistical estimation technique which corresponds to a non-stationary random function (RF) with a varying mean and a stationary covariance (Rossi and Deutsch, 2014). Unlike SK which uses a constant mean, OK uses an estimated mean which is location dependent. In order to achieve the unbiasedness condition, the sum of weights for OK are maintained at 1. OK equation for an unknown mean can be expressed as follows:

$$Z^*_{OK} = \sum_{i=1}^{n} w_i z(u_i) + [1 - \sum_{i=1}^{n} w_i]$$

$$Z^*_{OK} = \sum_{i=1}^{n} w_i z(u_i) \quad (1)$$

Where $\sum_{i=1}^{n} w_i = 1$ is the unbiasedness condition, Z^*_{OK} is the estimate, $z(u_i)$ are the sample values, w_i represents optimum kriging weights. This is in contrast to SK where the mean is known from sample values and is assumed to be stationary. Due to the use of the local mean of the data, the constraint $\sum_{i=1}^{n} w_i = 1$ falls away. The SK estimate can be obtained using Equation 2 with a constant mean m as shown below.

$$Z^*_{SK} = \sum_{i=1}^{n} w_i . [z(u_i) - m] + m$$

$$Z^*_{SK} = \sum_{i=1}^{n} w_i z(u_i) + [1 - \sum_{i=1}^{n} w_i].m \quad (2)$$

Equation 2 shows that the known mean *m* is subtracted from the sample value and then added back after the residuals have been estimated (Rossi and Deutsch, 2014). Unlike OK which achieves minimum estimation variance by constraining the sum of weights to 1, SK relies on constant mean for the domain under consideration.

The OK method is widely used in resource estimation in the sense that it produces unbiased estimates with minimum estimation variance (Dohm, 2015b). The kriging variance can be expressed mathematically as follows :

$$\sigma^2_{OK} = \sum_{i=1}^{n} w_i \gamma(z_i, T) + \lambda \quad (3)$$

Where $\gamma(z_i, T)$ represents the relationship between the point T and sample (z_i) determined by the semi variogram and λ represents the LaGrange

multiplier. When block support is used, kriging variance can be expressed as follows:

$$\sigma^2_{OK} = \sum_{i=1}^{n} w_i \bar{\gamma}(z_i, A) - \bar{\gamma}(A,A) + \lambda \quad (4)$$

Where $\bar{\gamma}(A, A)$ represents within the block variance, $\bar{\gamma}(z_i, A)$ represents sample to block variance as determined from discretisation points and the semi variogram. The LaGrange multiplier (λ) is used to derive the optimum weights and to minimise the kriging variance (Lloyd and Atkinson, 2001). The SK variance shown in Equation 5 does not have LaGrange multiplier since it relies on a local mean.

$$\sigma^2_{SK} = \bar{C}(A, A) - \sum_{i=1}^{n} w_i \bar{C}(z_i, A) \quad (5)$$

Where $\bar{C}(A, A)$ is within block covariance and $\bar{C}(z_i, A)$ is the sample to block covariance.

However despite producing estimates with minimum estimation variance, OK estimates are known to have a smoothing effect (Yamamoto, 2005). The smoothing effect is when the variance of distribution of block estimates is lower than the variance of the distribution of real block values (Krige, 1996). Due to smoothing effect, OK is unable to reproduce either the histogram of input data or the spatial variability expressed by semi variogram function (Yamamoto, 2005). The smoothed representation of reality has the potential of underestimating real data dispersion or variability associated with regionalised variables thereby creating uncertainty around the estimate.

In support of linear estimation techniques, Krige(1996) argued that smoothing effect is due to two factors namely the estimation technique and the information effect. Smoothing is more pronounced where OK is used with less data and wide spread drilling (Krige, 1997 ; Abzalov, 2006 and De-Vitry, et al. 2007). Furthermore, Krige (1994;1996) argued that the use of SK combined with a change of support from point data to blocks reduced smoothing effect and conditional bias significantly. Although historical

estimates at Hunters Road nickel deposit utilised the change of support from point to block support, the estimation technique chosen is affected by smoothing effect and subsequently conditionaly biased.

In addition, kriging variance (or its square root, the standard error) which is widely considered to be homoscedastic (Journel, 1988; Lloyd and Atkinson ,2001; Emery, 2005) is used as a measure of confidence in the estimate despite the fact that it is independent of the data values. Rossi and Deutsch(2014) argues that kriging variance depends on the covariance hence it can be calculated before any estimation is performed. According to Lloyd and Atkinson (2001) the biggest challenge with the use of OK standard error is the assumption of stationarity and secondly the fact that OK standard error will be the same for a given sample configuration irrespective of the data values locally. The fact that OK standard error is not conditional on the data values, several authors discourage its use in assessing local uncertainty.

Furthermore, linear estimation methods simply give a single estimate of the expected value (an average) (Vann, et al., 2000) instead of the distribution of grades inside the block (risk qualified estimates) (Journel, 1983) . Risk qualified estimates give indications of uncertainity around the grades which is crucial in mine design and optimisation. In addition, OK and other linear estimation methods require determination of the statistical distribution model of the grades or the regionalised variable under consideration. OK and other linear geostatistical estimation such as SK are unstable when the distribution model is strongly skewed (Journel, 1983, Vann, et al., 2000). Some authors recommend capping the data but this may result in elimination of information which may be vital in understanding the variability in grades. Highly variable distributions are characterised by a coefficient of variation greater than 1.0 preferably above 2.0 (Journel, 1983; Rossi and Deutsch, 2014).

Journel (1983) proposed the use of non parametric kriging techniques such as indicator kriging which do not make prior assumptions about the distribution being estimated but rather directly estimate the distribution itself (Rossi and Deutsch, 2014). In addition, Emery (2005) claims that due to the smoothing effect, OK is not suitable to applications that involve probability distributions such as the estimation of recoverable resources based on a cut-off grade as well as the assessment of risk.

Given the limitations and recommendations from Journel (1983) ,the current study aimed at addressing the shortcomings of using OK through the use of indicator kriging and conditional simulation, which are able to produce risk qualified estimates. Previous resource estimates at Hunters Road nickel deposit did not evaluate either local or spatial uncertainity associated with nickel grades. Indiccator kriging and conditional simulation are discussed in detail in the following sections.

2.3 Estimation of Recoverable Resources: Non-Linear Resource Estimation Techniques

One of the key objectives of the study highlighted in Chapter 1 is the estimation of recoverable resources and the assessment of grade uncertainty. The previous section highlighted that linear geostatistical methods produces a single estimate which cannot be used effectively in assessment of grade uncertainty. Non-linear geostatistical methods were proposed in order to estimate the conditional expectation (mean) and the conditional distribution function of grade instead of single estimates (Vann, et al., 2000). The conditional distribution function is represented as a cumulative conditional distribution function (ccdf) which according to Rossi and Deutsch (2014) can be expressed mathematically as shown below:

$$F\ (z, \mathrm{u}\ |(n)) = Prob\ \{Z(\mathrm{u}) \leq z\ |\ (n)\} \qquad (6)$$

Where “|(n)” means conditional to the nearby information used in deriving the ccdf. The ccdf contains vital information about the unknown values and

can be used to obtain E-type (average) estimates and probabilities of grades exceeding specific thresholds. Estimation of recoverable resources relies significantly on the use of ccdf in the estimation of the tonnage and grade of mineral resources above specific cut-off grades. The current study used indicator kriging in the estimation of recoverable resources at Hunters Road nickel project. The following section will focus on indicator kriging which is a non-linear geostatistical estimation method relying on the use of ccdf in estimating recoverable resources (Vann, et al., 2000; Emery, 2005).

2.3.1 Indicator Kriging

Indicator kriging (IK) is one of the non-parametric estimation methods (Journel, 1983) in the sense that it does not make prior assumption about the distribution being estimated (Rossi and Deutsch, 2014). It allows direct estimation of the conditional distribution at an unsampled location (Journel ,1983; Ortiz and Deutsch, 2003). IK approach involves binomial coding of the original variable Z(u) into either 1 or 0 depending on the given threshold values (Basante, et al., 2008). Binary indicator transform of Z(u) can be defined as:

$$I(\mathrm{u}; \mathrm{z}_k) = \begin{cases} 1 & \text{if } \mathrm{Z(u)} \leq \mathrm{z}_k \\ 0, & \text{otherwise} \end{cases} \qquad (7)$$

Indicator kriging involves discretisaton of the continuos variable z with a series of K threshold values z_k, k=1,....,K. According to Rossi and Deutsch (2014), the experimetal cdf of n samples is considered a prior distribution and can be obtained using Equation 6 such that by defination, the expected value for indicator random variable (RV) ($I(\mathrm{u}; \mathrm{z}_k)$ is as follows:

$$E\{I(\mathrm{u};z_k)\} = 1.\mathrm{Prob}\{\mathrm{I}(\mathrm{u}; z_k) = 1\} = \mathrm{Prob}\{\mathrm{Z}(\mathrm{u}) \leq z_k\} \qquad (8)$$

The same relationship applies to conditional expectation such that:

$$E\{I(\mathrm{u};z_k)|\,(n)\} = Prob\{\mathrm{Z}\,(\mathrm{u}) \leq z_k|\,(\mathrm{n})\} = \mathrm{F}\,(\mathrm{u};\,z_k)|\,(\mathrm{n}))$$

The ccdf ($\mathrm{F}\,(\mathrm{u};\,z_k)|(\mathrm{n})$) is built by assembling K indicator kriging estimates such that it represents the probabilistic model of uncertainity around the unsampled value z(u) (Lloyd and Atkinson, 2001; Rossi and Deutsch, 2014). The optimal weights are derived by a kriging systemof equations on the indicator data (Goovaerts, 1997; Rossi and Deutsch, 2014):

$$E\{I(\mathrm{u};\,z_k)|(n)\}^* = [\mathrm{i}\,(\mathrm{u};\,z_k)]^* = \sum_{\alpha=1}^{n} w_\alpha\,(\mathrm{u};\,z_k)\;\mathrm{i}(\mathrm{u}_\alpha;\,z_k) \qquad (9)$$

where * indicates an estimate. The current study used Ordinary Indicator Kriging where the value of indicator transform for each threshold is assumed to be unknown but constant within a local neighborhood (Rossi and Deutsch, 2014) . Ordinary IK equation can be expressed mathematically:

$$\mathrm{i}(\,\mathrm{u}\,;\,z_k) = \sum_{\alpha=1}^{n} w_\alpha\,.\,\mathrm{i}(\mathrm{u}_\alpha\,;\,z_k) + F(z_k)\;[1 - \sum_{\alpha=1}^{n} w_\alpha] \qquad (10)$$

subject to the sum of weights ($\sum_{\alpha=1}^{n} w_\alpha$) being constrained to 1 (Rossi and Deutsch, 2014). The E-type estimate ($m\,(\mathrm{u})^*$) which is the expected value of the ccdf at location u can be written as (Lloyd and Atkinson, 2001; Rossi and Deutsch, 2014):

$$m\,(\mathrm{u})^* = \sum_{k=1}^{k+1} m_k\;[\mathrm{i}(\,\mathrm{u},\,z_k\,|(\mathrm{n})) - \mathrm{i}(\mathrm{u};\,z_{k-1}|(\mathrm{n}))] \qquad (11)$$

where $\mathrm{i}(\mathrm{u}:\,z_k|(\mathrm{n}))$ is the kriged indicator value for threshold k conditioned to nearby information, i(u, z_0)= 0, i(u; z_{k+1}) =1 and m_k is the mean of data falling within the interval ($z_{k-1},\ z_k$) (Rossi and Deutsch, 2014). Goovaerts (1997) suggested that IK conditional variances are good measures of dispersion of the ccdf around its mean.The literature review on OK earlier on indicated that the standard error is not conditional on the data values. According to Lloyd and Atkinson (2001), the dependence of the IK standard error on the data values suggest that it may provide a more accurate guide to assess uncertainty in local estimates.

2.3.2 Multiple Indicator Kriging (MIK) and Median Indicator Kriging(MeIK)

Multiple indicator kriging (MIK) and Median Indicator Kriging (MeIK) are variants of IK which are widely accepable methods for estimating recoverable resources (Vann, et al., 2000; Emery, 2005) and conditional distribution of the grades. MIK involves the kriging of indicators at several cut-off grades (Vann, et al., 2000) such that the ccdf *F*(u, z_k) are dependent on both the location and a number of cut-off grades z_k *, k= 1,….,k* (Rossi and Deutsch, 2014). Application of the method will requre one indicator semi variogram and one kriging system per cut-off grade or threshhold. Lipton et al. (1998) applied MIK in the estimation of a lateritic nickel deposit and found it to be a viable method for estimating recoverable resources. MIK was able to deal with bimodal and strongly skewed population especially in iron ore deposit (Keogh and Moulton (1998). However the calculation of several indicator semi variograms for every cut-off grade makes the process more time consuming than linear geostatistical methods which uses a single semi variogram.

There are situations whereby the spatial continuity of indicator at various cut-off grades can be approximated by a single indicator semi variogram closer to the median (Badel, et al., 2011). Indicator kriging under this assumption is called Median Indicator Kriging (MeIK). Rossi and Deutsch, (2014) refers to it as indicator kriging under the mosaic model. At the median cut-off grade, the indicator data values are evenly distributed. Studies by Hill, Mueller and Bloom(1998) on a gold mine in the Northern territory of Australia revealed that little is lost by using MeIK rather than the full IK. Similarly, Badel, et al.,(2011) working on an iron ore deposit with mixed population found MeIK to be more suitable for minimising the estimation error. More recently, in the thesis of Mudau (2014) which was focussing on the application of linear and non-linear estimation techniques in phosphate project in Democratic Republic of Congo (DRC) found estimates produced by MeIK to be more useful and less smoothed. However, Isaaks and

Srivastava (1989) argued that users of the method have to be cautious of MeIK assumption if there are noticeable differences in the shape of the indicator variogram at various cut-offs. The advantage of MeIK over that MIK is that of time saving in terms of variogram modeling and the actual estimation process. Indicator semi variograms are covered in more detail in Chapter 5. Despite the advantages of MeIK, the current study utilised MIK with cut-off grades defined by deciles of the sample distribution.

2.3.3 Change of Support

Estimation of recoverable resources hinges upon change of support. Vann, et al. (2000) argues that change of support is not inherent in MIK hence is it only applied as a post processing step. In support, Rossi and Deutsch (2014) argues that the ccdf produced by averaging the proportions of point values within the block is not a true block ccdf but rather a composite ccdf $[F_N(\mathrm{u};z\,\mathrm{l}(n)]$*. A composite ccdf is an estimate of point values within the block that do not exceed a given cut-off grade. In contrast, a true block ccdf gives the probability that the average value is not greater than the cut-off grade (Rossi and Deutsch, 2014).

Although there are many approaches to change of support such as the indirect lognormal corrections, the most common approach is the affine correction. The affine correction assumes that the shape of the distribution of samples is similar to that of selective mining unit (SMU) (Vann, et al., 2000; Rossi and Deutsch, 2014). The only change is the reduction in variance as predicted by Krige‘s relationship. Krige relationship states that the variance of blocks in a domain is equal to the variance of samples minus the within- block variance (De-Vitry, et al., 2007). According to Vann, et al. (2000) and Isaaks and Srivastava (1989), the problem with the affine correction is that it does not take into consideration any deskewing of the distribution when moving from sample to block support.

However, due to to the limitation of the software used in the study, change of support was not performed on MIK estimates such that only the composite ccdf is produced.

2.3.4 Order Relations Problem

IK and its variants sometimes suffers from order relations problem (Vann and Guibal, 1998; Ortiz and Deutsch, 2003). This occurs when the proportion above a higher cut-off grade (COG) is estimated to be more than the proportion above a lower COG. This may result in the estimated metal to be higher for a higher cut-off grade than a lower cut-off grade. IK estimated ccdf at each location should be consistent from one COG to another. Vann, et al. (2000) argue that order relations violations are mainly due to methodology problem and can be reduced or eliminated by modifying the methodology. In support, Rossi and Deutsch, (2014) argued that order relations problems are mainly due to inconsistent variograms models and kriging implememtation strategy.

In order to avoid or reduce the effects of order relations problem, some authors encourage the use of the same search volume and number of data for all the cut-off grades or thresholds (Vann, et al., 2000; Rossi and Deutsch, 2014). Furthermore, they suggested that the search volume should be made more istotropic than the anisotropies suggested by indicator semi variograms. In addition, Vann, et al.(2000) suggested the use of MeIK in order to ensure consistency in terms of indicator semi variograms across all the COG. However it is not always the case that all the indicator semi variograms are proportional at all the cut-off grades.

The current study will use the search strategy highlighted by Vann, et al. (2000) and Rossi and Deutsch, (2014) in order to avoid order relations problem. However, where order relations are encountered, they will be

corrected by considering the average of the upward and downward corrections (Deutsch and Journel, 1998).

2.4 Assesment of Spatial Uncertainty : Conditional Simulation.

The previous section focussed on direct estimation of conditional distribution at unsampled location which to a certain extent represents point distribution of uncertainty (Ortiz and Deutsch, 2003). This section will focus on the production of the joint model of uncertainity through the use of conditional simulation. Geostatistical conditional simulation is a Monte Carlo based method used in assessing the impact of spatial heterogeneities (Isaaks, 1991). Unlike estimation, simulations honour data values at their locations, reproduce closely the declustered sample histogram and the semi variogram model (Isaaks, 1991; Goovaerts, 1997; Rossi and Deutsch, 2014). It overcomes the smoothing effect associated with linear geostatistical methods.

Geostatistical simulation approaches build upon kriging and stochastic sampling approach to quantify uncertainity at unsampled locations (Chiles and Delfiner, 2012; Glacken and Trueman, 2014). Many conditional simulation algorithms exist namely Turning Bands(TB), Sequantial Gaussian Simulation (SGS), Continuous Sprectra and Circulant Embedding among others. The availability of these simulation algorithms allows for the intergration of geological uncertainity into mine optimisation studies and financial decision making (Dimitrakopoulos et al. 2002). Of all the simulation methods, SGS is a widely used algorithm for quantifying uncertainty about regionalised variables (Emery and Pelaez, 2011) through the generation of a set of realisations that reproduce input distribution functions, heterogeneity and spatial continuity (Manchuk and Deutsch, 2012). Conditional simulation is about computing conditional distribution of uncertainty given a set of data. According to Prins and Minnit (2016), conditional distribution of uncertainty ($F_{Z_{UL|(n)}}(z)$) is the multivariate

distribution ($F_{Z_{UL}}$) of what is being predicted with z_n data divided by distribution of n data:

$$F_{Z_{UL|(n)}}(z) = F z_{UL},\ z_1,\ldots,\ z_n\ (z_0,\ z_1,\ldots,\ z_n) / (F_{Z_1},\ldots,\ z_n\ (z_0,\ z_1,\ldots,\ z_n)) \quad (12)$$

Simulation therefore samples from the distribution of uncertainity computed using Bayes Law in order to develop a probabilistic model of uncertanity. The current study with second objective being the asessment of grade uncertainity at Hunters Road nickel deposit made use of SGS.

2.4.1 Sequential Gaussian Simulation

SGS is based on the decomposition of the multivariate probability distribution function(pdf) into a series of conditional distributions (Isaaks, 1991). It is based on the factorization of the joint probability *P*, of a set of *m* random variables (RV), *Y* and *n* conditioned data (Isaaks, 1991; Manchuk and Deutsch, 2012a; 2012b):

$$P\{y_{n+1} \leq Y_{n+1},\ldots,y_{n+m} \leq Y_{n+m} | y_1,\ldots y_n\}$$

$$= P\{y_{n+1} \leq Y_{n+1} | y_1,\ldots.y_n\}$$
$$x\ P(\ y_{n+2} \leq Y_{n+2} | y_1,\ldots.y_n, y_{n+1}\}$$
$$x.$$
$$x.P\{y_{n+m} \leq Y_{n+m} | y_1,\ldots.y_n, y_{n+1},\ldots y_{n+m\ -1}\} \quad (13)$$

Accordingly, each component in the decomposition is a conditional cumulative distribution function(ccdf) estimated at each node using SK for a Gaussian random function (RF) (Manchuk and Deutsch, 2012b; Rossi and Deutsch, 2014). Monte Carlo simulation is used to draw randomly from the conditional distribution in order to obtain a simulated value for the node (Rossi and Deutsch, 2014). SGS algorithms are based on a multiGaussian random function (RF) model assumption. Prins and Minnit (2016) postulates that multiGaussian RFmodel has the following five properties:

- It is defined by its mean (μ) and variance (σ^2).

- All lower order distributions are Gaussian
- All conditional expectations (means) are linear functions of the data.
- All conditional variances are homoscedastic.
- The conditional mean (m_c) and and variances (σ^2_{SK}) are given by the normal equations expressed as follows:

$$m_c = \sum_{i=1}^{n} w_i [z(u_i) - u_z(u_0)] \quad (14)$$

$$\sigma^2_{SK} = \sigma^2 - \sum_{i=1}^{n} w_i C_{io} \qquad i = ,\ldots\ldots,n \quad (15)$$

Where C_{io} is is the covariance function. Under multiGaussian RF model, SK is the only method that yields the estimated Gaussian mean and variance (Rossi and Deutsch, 2014) due to strict stationarity.

2.4.1.1 Implementation of SGS

The following general steps are recoomended by Deutsch and Journel (1998) and supported by Rossi and Deutsch (2014) when conducting SGS:

1. Transformation of original data to normal scores (NS) after declustering and despiking in order to obtain Gaussian distribution.
2. Calculation of NS semi variogram models. This step is covered in detail in Chapter 6.
3. Establishment of grid network and coordinate system.
4. Determination of a random path that visits each node on the grid once in order to avoid artifacts.
5. Estimating through simple kriging and a NS semi variogram, the mean Y*(u) and variance (σ^2_{SK}(u) of the ccdf of Gaussian RF Y(u) at location u.
6. Drawing randomly from the conditional distribution in order to obtain a simulated value for the node, Y_s(**u**). A random number between 0 and 1 is generated and a simulated value is obtained by reading the associaed quantile from the estimated ccdf.
7. Incorporation of the simulated value Y_s(**u**) as conditionining data for the nodes to be simulated later.

8. Repeating the process until all the nodes have been simulated.
9. Checking if the histogram of simulated values is Gaussian and whether the simulated values are able to reproduce the NS semi variogram model used in the simulation well.
10. Back transformation of the simulated values in Gaussian space into simulated values in original variable space.

The set of n outcomes, values of all simulated nodes comprises a realisation of the random function $Y(u)$. These equiprobable realisations (Rossi and Deutsch, 2014) provide a visual and quantitative measure of spatial uncertainty (Goovaerts, 1997) which can be used in risk analysis and decision making.

One of the problems in implementing SGS through Equation 13 is the increasing number of conditioning data at each sequential step (Isaaks, 1991). When a set of RV on a grid ($m \geq 10^6$) is considered, probability decomposition in Equation 13 cannot be approximated without restricting the conditioned data to a local neighborhood due to unreasonably large kriging system (Manchuk and Deutsch, 2012b). Under this situation, SGS relies on the screening effect approximations and the moving neighbourhood in determining successive conditional distributions (Emery and Pelaez, 2011; Safikhani, et al., 2016) under a Markov type assumption (Manchuk and Deutsch, 2012b). The Markov assumption in the stochastic process assumes that the conditional probability distribution of a future state of the process depends only upon the present state rather than the sequence of events that preceded it (Ghahramani, 2001). The present state encapsulates all the historical information about the process needed to predict future process.

Reliance on a moving neighbourhood brings into attention the size of the moving neighbourhood, the number of conditioning data and the size of the variogram range (Safikhani et al. 2016). Their studies suggested that the use of such a neighbourhood with less than 50 conditioned data may lead to poor generation of model statistics. Furthermore, Rossi and Deutsch

(2014) suggested that the node spacing in the vertical direction to be the same as the original composite length. This is done in order to ensure the use of all the drill hole samples in conditional simulation. However,an exception is made when the holes are inclined or sub horizontal. In support of conditional simulations, Emery et al. (2006) suggested the use of conditional simulation results in classifying the resources into Measured, Indicated and Inferred categories. The basis for their proposal is that some of the classification systems in use either favour or penalize high grade areas when the grade distribution presents a proportional effect. The current research, did not focus on mineral resource classification.

Simulation techniques have their limitations which are mainly related to time taken to complete multiple realisations (Ortiz and Deutsch, 2003). However, Dimitrakopoulos, et al. (2002) suggested the development of the direct block simulation method based on Generalized Sequential Gaussian Simulation(GSGS) concepts which reduces the time required by estimating directly into blocks. Before revisiting the multiGaussian RF model, one of the critical step is the post processing of SGS output. The next section will focus on the interpretaion of SGS output.

2.4.1.2 Establishing Uncertainty: Post SGS Analysis

Realisations generated through SGS provides a measure of uncertainty about the spatial distribution of a regionalised variable. One of the key validation methods is to ensure that the histograms and experimental variograms can be acceptably reproduced for the realisations (Prins and Minnit, 2016). In addition, visual assessment of realisations for trends and similarities can be done. Srivastava (1994) in Goovaerts (1997) developed an algorithm which produces animated displays of realisations allowing one to distinguish areas that remain stable over all realisations (low uncertainty) from those with high fluctuations (high uncertainity). Further analysis of realisations is done through post processing using various transfer functions that yield the following:

- Conditional E-type mean
- Conditional E-type variance
- Probability maps (P10, P50 and P90).
- Probability of exceeding a fixed threshold, the average value above that threshold, and the average value below that threshold.

(Goovaerts, 1997; Deutsch and Journel, 1998; Prins and Minnit, 2016)

The E-type estimates are obtained from point by point averaging of the realisations (Statios, n.d.). A probability map is a quantile map showing the probability of exceeding given thresholds such as P10 and P90. A P10 probability map is a 0.1 quantile representing the probability of 10% of the data being below the mean (Prins and Minnit, 2016). Accordingly at every grid node on the P10 map there is a 90% probability that the true value is higher than the value on the map. The same principle applies to P90 map whereby every single grid node has a 90% probability that the true value is lower than the value on the map.

The current study used Datamine Studio RM SGS algorithm which was able to produce E-type estimates and probability maps as described above. In addition, node and block confidence were calculated based on several cut-off grades. The steps involved and results of the process are covered in detail in Chapter 8.

2.5 Normal Score Transformation

The univariate distribution of a RV is not always Gaussian but is rather transfromed to a Gaussian RV through the normal score transformation (Manchuk and Deutsch, 2012b). A standard Gaussian distribution has a mean ($\mu_y = 0$) and standard deviation ($\sigma_y = 1$). In order to transform sample data from original values (z) to Gaussian space (y), a quantile to quantile transformation using the cdf of each distribution is performed with the preservation of rank (Rossi and Deutsch, 2014). The normal score transformation process is illustrated in Figure 2.

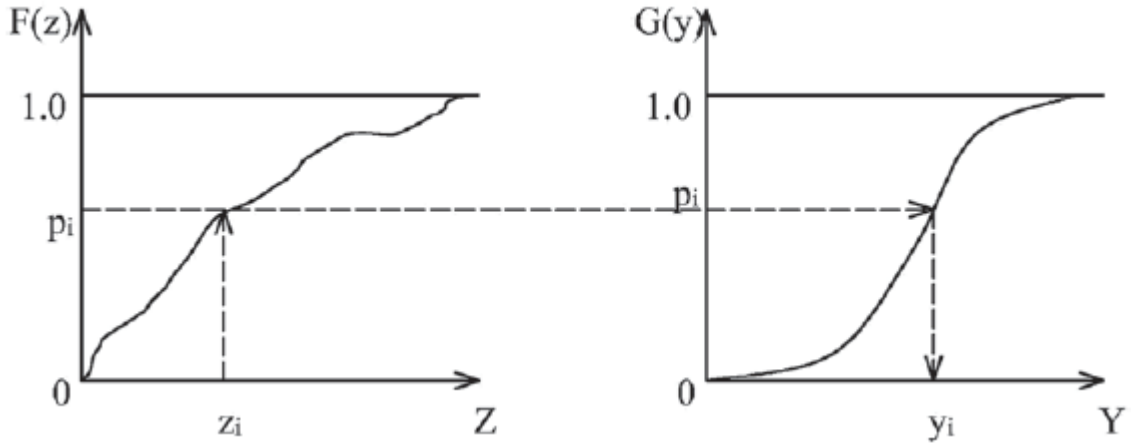

Figure 2: Quantile to quantile transformation using cumulative distribution function (Source: Rossi and Deutsch, 2014, p. 22)

The NS transformation is achieved through a quantile to quantile transformation which is mathematically expressed by the following formula:

$$y = G^{-1}(F(z)) \ , \forall \ z \quad \text{where} \quad y = ((z - m_z)/ \sigma_z) \tag{16}$$

Where m_z represents the mean , σ_z standard deviation and *z* original values of the variable.Back transformation from normal scores to original values (z) is achieved mathematically through the following formula:

$$z = F^{-1}(G(y)) \quad \forall \ y \quad \text{where } z = y. \sigma_z + m_z \tag{17}$$

The NS transform ensures that the univariate marginal distributions are all Gaussian while higher order spatial and multiple variable distributions are not necessary Gaussian (Manchuk and Deutsch, 2012b). In support of NS transformation, Ortiz and Deutsch (2003) argue that the proportional effect which is more expressed in positively skewed distribution is eliminated or filtered through the change in the anamorphosis function. However, the proportional effect is reintroduced back during back transformation process to the orginal units (Manchuk, et al., 2007). Conditional simulation techniques such as Sequential Gaussian simulation relies on the use of NS data in modelling uncertainty associated with regionalised variables. The NS transformation and associated statistics are covered in more detail in

Chapter 4. The second stage of SGS steps which involves calculation of NS semi variograms is covered in detain in Chapter 5.

In concluding the literature review chapter, the current study will use MIK in the estimation of recoverable resources based on a 0.40%Ni cut-off grade. Due to the limitation assocaited with the production of a block ccdf using indicator kriging, only an E-type estimate is going to be produced through MIK. The second objective of the study will be addressed through the use of SGS as described earlier on. SGS will assist in the assessment of grade uncertainity at Hunters Road based on 100 simulated realisations. The literature review section highlighted key points that should be taken into consideration when conducting the study. Several authors supported the use of MIK and SGS in the estimation of recoverable resources and the assessment of uncertainty associated with regionalised variables. Their support for the methodology applied set the basis for their use in the current study. The basis for comparing the OK based estimates and IK based estimates has been set and due to differences in approach, highligted under linear and non-linear geostatistical methods.

CHAPTER 3: HUNTERS ROAD GEOLOGICAL SETTING

3.1 Introduction

The previous chapter focussed on the literature review thereby setting a theoretical basis for the study. This chapter will cover regional and local geology of Hunters Road nickel project, concluding with the determination of geological domains. An understanding of regional and local geology is a very important tool in both implicit and explicit modelling of mineralisation and in defining geological domains. The choice of estimation and simulation method hinges upon accurate definition of geological domains.

3.2 Regional Geology

The Hunters Road deposit lies on the western limb of the north trending anticlinal structure located on the eastern flank of the synclinal Gweru-Midlands South greenstone belt (Prendergast, 2001). According to Harrison (1970) and Cheshire, et al. (1980), regional stratigraphy comprises of a Late Archean sequence of felsic to intermediate lavas and volcaniclastic rocks of the Kwekwe Felsitic Formations (KKFF) which are considered to be Lower Bulawayan aged rocks. These Lower Bulawayan aged rocks are overlain by banded iron formations (BIF) and felsic volcaniclastic rocks of the Redcliff Jaspilite Formation (RJF). The BIF unit is associated with a number of argillaceous units and is overlain by a thin sequence of komatiitic lavas (komatiitic basalts) of the Fife Scott Ultramafic Formation (FSUF) and mafic lavas (massive basalts) of the Ingwenya Mafic Formation (IMF). A 100-300m peridotite sill was emplaced within the felsic rocks concordantly beneath the RJF (Prendergast, 2001). A geological map showing regional setting of Hunters Road deposit is shown in Figure 3.

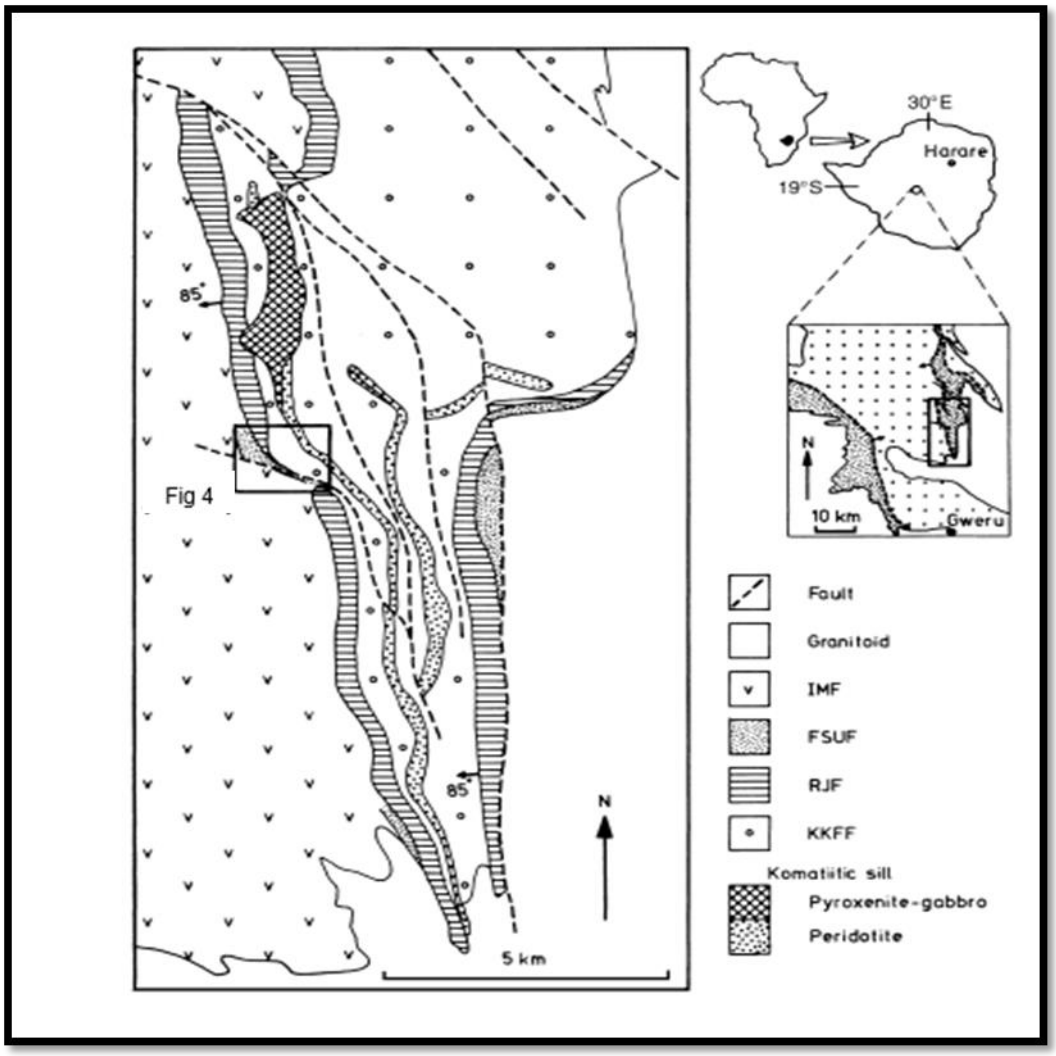

Figure 3: Regional setting of Hunters Road nickel deposit (extracted from Prendergast, 2001)

The regional sequence on the western limb shows a north-northwest strike with a steep westerly dip. The RJF forms a conspicuous ridge with the FSUF largely hidden beneath the BIF, except at Hunters Road (see Figure 4). Prendergast (2001) suggested that nickel mineralisation at Hunters Road occur at the base of the FSUF in a thin komatiite unit called the Main Flow. Other authors such as Tinofirei (1996) suggested that the mineralised serpentinite strikes east-west following fault zones.

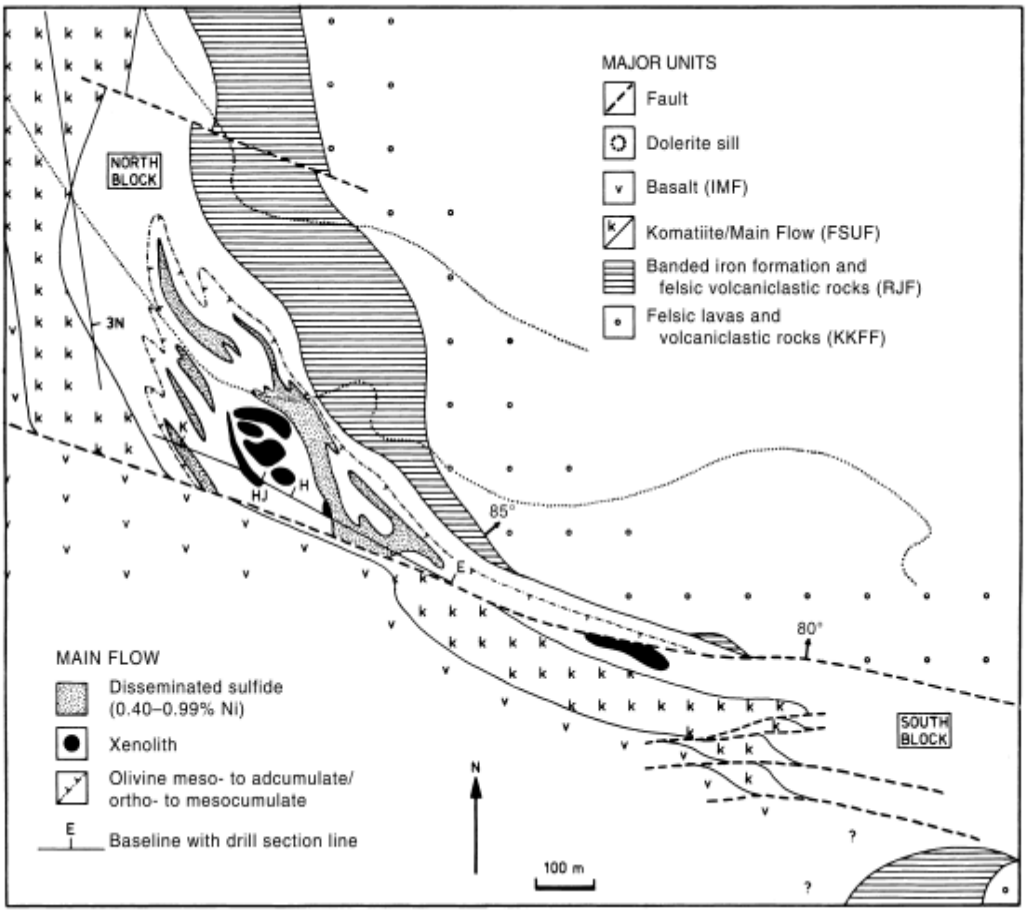

Figure 4: Local geology for Hunters Road nickel deposit extracted from Prendergast (2001).

3.2.1 Local Geology

Locally, the Hunters Road nickel deposit lies in a sheared serpentinised Archaean ultramafic sequence which intruded into a series of metamorphosed felsic to intermediate volcanic rocks of KKFF (Cheshire, et al., 1980). The serpentinites (Main Flow unit) is bounded by basalts on the footwall and by BIF and felsic volcaniclastic rocks of RJF and KKFF (see Figure 4). There are also a number of intrusives, especially dolerite sills and quartz porphyries

Tinofirei (1996) observed pillowed lavas in the footwall which suggested a southerly younging direction. Based on the pillowed lavas, he suggested that the Hunters Road serpentinite or Main Flow unit is overturned. One of the noticeable features in the Mass Flow unit are numerous xenoliths that are dominated by BIF and felsic rock and they transgress both the intrusive serpentinised dunites and extrusive basalts. One of the megaxenoliths which measures up to 200m, is comonly referred to as the Rietfontein megaxenolith.

Major oblique strike faults exist in the area and have caused duplication and truncation of the regional sequence (Prendergast, 2001). The most conspicuous fault is the east-south east (ESE) trending sinistral Hunters Road fault, which caused an approximately 1.5km displacement of the Main Flow unit and the RJF(Prendergast, 2001; SRK Consulting Zimbabwe, 2002). There are different views regarding the emplacement of the ultramafic body with Tinofirei (1996) suggesting that it was emplaced parallel to an easterly strike along a fault zone or rift. He argues that the east trend of the serpentinite was created by later sinistral faulting given the fact that the dunite is less brittle than the surrounding rocks hence it may have been dragged along the fault.

On the contrary, Dirks (2001) based on the dip of the nickel bearing unit being 70^0 N, argued that the WNW trending porphyry dykes intruded parallel to the existing shears that truncated the ultramafic body. Based on that observation, he proposed two scenarios for the formation of the ultramafic body:

1. Late intrusion of the ultramafic body and related dykes parallel to the NNE trending brittle – ductile shear steeply dipping at 70^0. BIF and other xenolith being fault blocks found along the shear, were incorporated within the ultramafic body (Main Flow unit)
2. Early intrusion of the ultramafic body parallel to the strike of the BIF unit and subsequent sinistral shearing offset the BIF unit. The

ultramafic unit enveloped the BIF and other xenoliths at this stage. The shear zone controlled the later emplacement of both dolerites which are unrelated to the ultramafic body and quartz porphyries.

3.2.2 Nickel Mineralisation

Mineralised serpentinite has a total strike length of about 1800m and varies in width from 50 to 100m. One of the noticeable features of the deposit is the change in the strike from NNW to WNW (see Figure 5) within the 1800m strike length. The dip of mineralised serpentinite is approximately 76^0 to either north or east depending on the strike as discussed above. According to Tinofirei (1996) and SRK Consulting Zimbabwe (2002) the highly mineralised zone and also widest point of mineralisation occur where the strike direction of the deposit changes from NNW to WNW. This area is where the Western Orebody of Hunters Road nickel deposit is located. The area is marked West Pit Area in Figure 5.

Furthermore, studies by Winter (1994) on two drill holes revealed that pentlandite and violarite are the nickel rich sulphides while the lowest nickel concentration occurred in serpentinite, chromite and magnetite. Sulphide mineralisation is fine grained, interstitial and cocumulus to olivine and weakly disseminated (Prendergast, 2001). Winter (1994) observed that in DH119, the pentladite increased with an assocciated decrease in violarite with depth. The xenoliths are largely barren zones within the mineralised zone. One of the concerns raised by Winter (1994) is the presence of tochilinite (5wt%Ni) which is a yellow–brown coloured mineral with very poor flotation properties.

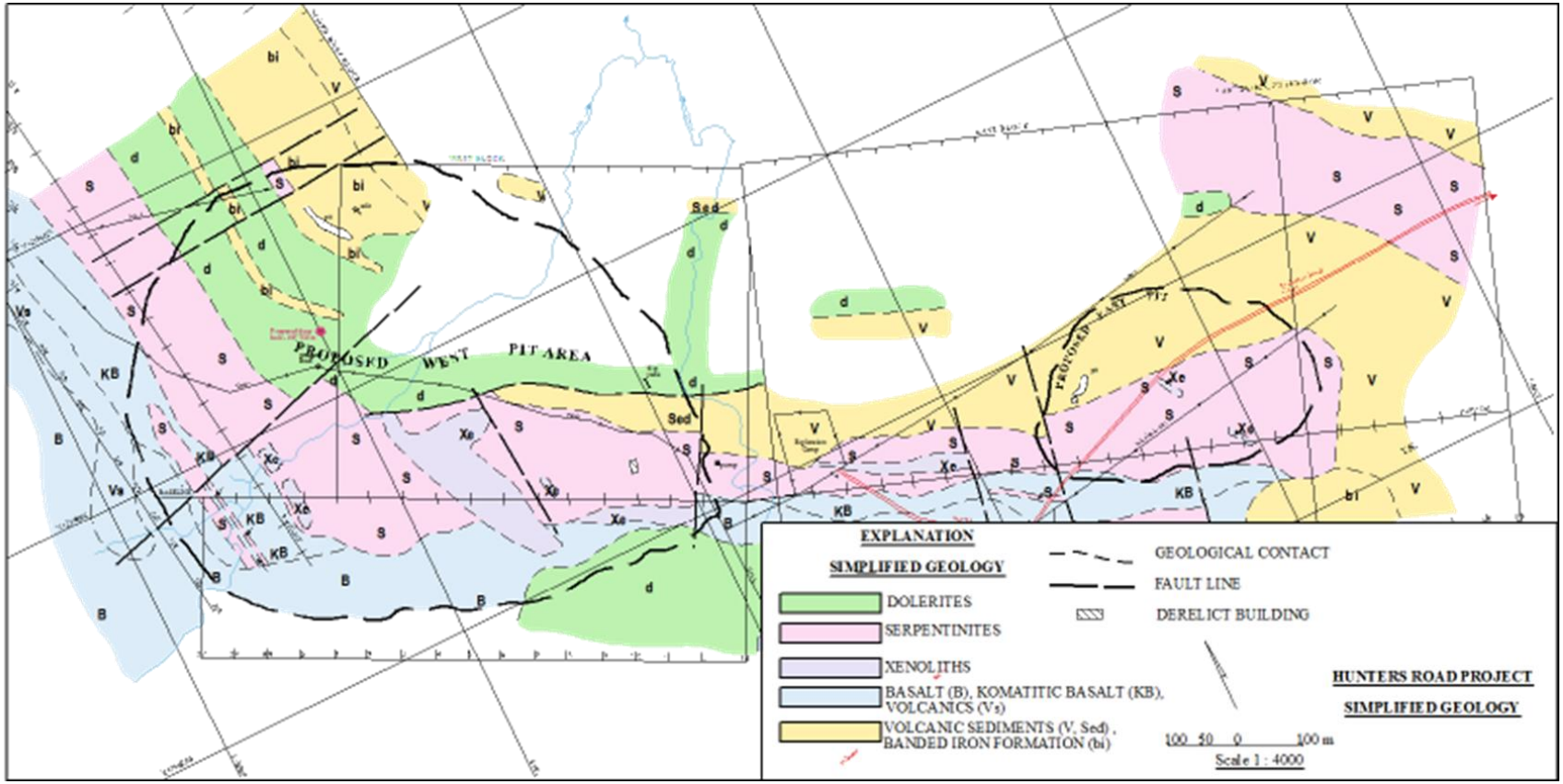

Figure 5: Geological map showing the location of the Western orebody (Proposed West Pit Area) of Hunters Road nickel deposit.

NB: The East Pit Area and its orebody which is the Eastern orebody do not form part of the research report

3.2.3 Geozones

Earlier sections of this chapter focused on describing both local and regional geology of the Hunters Road nickel deposit, closing in on the Western orebody (area marked West Pit Area in Figure 5). This section will focus on defining geozones or domains within the Western orebody based on explicit modelling of the orebodies. Duke and Hanna (2014) described geological domains as zones that are geologically and statistically homogeneous.

Explicit modelling of the orebody using an indicator cut-off grade of 0.40%Ni resulted in identification of two orebodies within the Western orebody. The two geological domains are known as the Eastern and Western domains and are shown in Figure 6. The two domains appear to be separated by NE trending zenolith domain which disapppears with depth. The orebody wireframes which were modelled in May 2006 were based on the assumption that the two orebodies do not merge at depth. This was a departure from previous orebody modelling which used a soft boundary with the two domains merging below 1080m above sea level. The current study adopted the May 2006 wireframes as a true reflection of the Hunters Road orebodies.

The choice of using 0.40%Ni cut-off grade dates back to March 1996 when MinRED delineated resource boundary using a 0.40%Ni and the peripheral low grade material using a 0.28%Ni cut-off. In 1992, MinRED had conducted resource estimations using a low cut-off grade of 0.28%Ni with an open pit mining method in mind. However, the financial analysis conducted that time showed a low return on investment, resulting in an underground mining focus. Since grades were increasing with depth, additional drilling was conducted and a high cut-off grade of 0.40Ni% was adopted for delineation of the resources in 1996. Since then, a 0.40%Ni cut-off grade has been used in delineating and reporting Mineral Resources at Hunters Road Nickel Project.

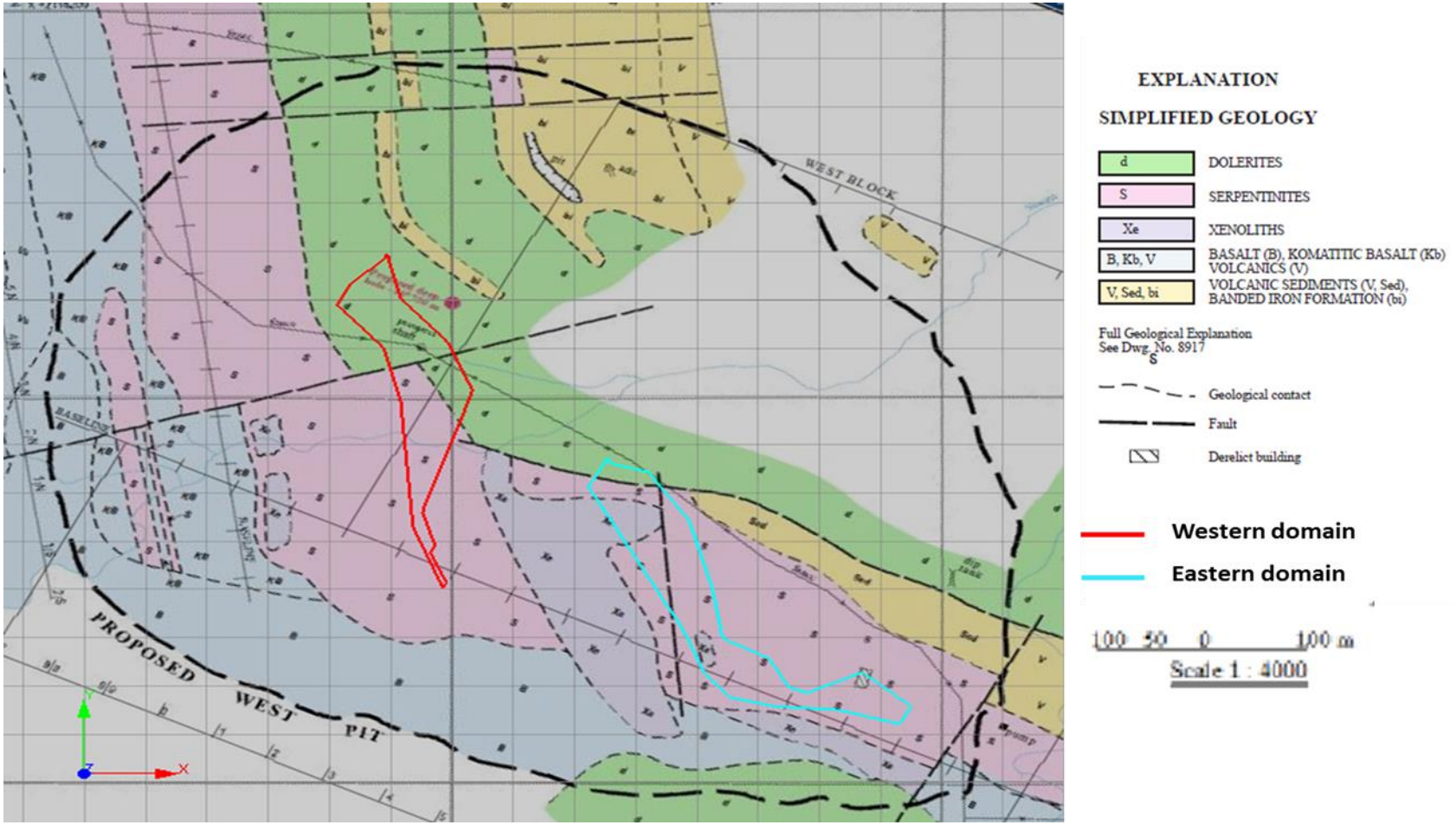

Figure 6 : Geological map showing the Eastern and Western domains of the Western Orebody of Hunters Road nickel deposit.

3.3 Chapter Summary

This section covered both the regional and local geology of Hunters Road and concluded by defining geological domains of interest. Hunters Road nickel deposit has two main orebodies namely the Western and Eastern orebodies. The current study focusses on the Western orebody which has two domains namely the Eastern and Western domains which were defined based on 0.40% Ni cut-off grade. The next chapter will focus on validation of historical data as well as the statistical analysis of the sample data, a key component of Exploratory Data Analysis (EDA).

CHAPTER 4: EXPLORATORY DATA ANALYSIS (EDA)

4.1 Introduction

The introductory chapters focused on giving a detailed description of the problem under investigation as well as giving background information regarding the geology of the target area and exploration work conducted. Given the fact that the research relied on drill hole information gathered between 1971 and 2004, it is important to validate the information before using it in resource estimation and conditional simulation. In addition, solid wireframes, representing the orebodies date back to May 2006 when mineral resources estimates were declared. This section start by looking at drill hole information validation followed by orebody wireframe validation, compositing and statistical analyses of each geological domain. The main purpose of this section is to assess the integrity of the information used in resource estimation

4.2 Validation of Historical Data.

Validation of primary data such as assays, survey data and geological observations is one of the critical stages in mineral resource estimation. Dohm (2015) argues that the foundation of all resource estimation is the data used hence the integrity of the data used is very important. The intergrity of the data used is highly dependent on the quality of sampling as well as the assay procedures used during exploration and other phases of mine development (Roden and Smith, 2014). The last point highlights the importance of quality assurance and quality control of assay data, popularly known as QAQC. Through proper QAQC procedures, both sampling and assay errors are minimised thereby enabling attainment of both sample accuracy (absence of systematic bias) and reproducibility (precision). QAQC and related issues will be looked at in the following sections of the report.

The Hunters Road primary data has been stored in separate Excel files as listed below:

- Collar file: containing the drill hole collar coordinates.
- Survey file: Containing the azimuth and dip direction information of drill holes.
- Assay file: containing the assay information for all the boreholes.
- Geology file: containing the lithology information.

In addition, physical logs and other geological and meturgical reports were made available and have been kept for future use. The only problem is that electronic information has not been stored in a safe and secured database. Some of the information such as orebody wireframes are very difficult to locate as they have been saved in different Datamine Project files depending on the person doing the evaluation. This problem has since been rectified by putting all the information relevant to this project in one project file on the local serve with user restrictions.

The drill hole validation process considered the following key issues:

- Whether the drill hole had four sets of information that is the collar, survey, assay and lithology information.
- Duplication of information especially sampling interval.
- Checked for consistence in ‘from’ and ‘to’ values of sampling and lithological interval.
- Data capturing mistakes from physical logs to Excel worksheet.
- Outliers in terms of both coordinates and assay values.

4.2.1 Summary of Findings

The collar file for Hunters Road nickel project, initially had a total of 243 holes. After comparing the physical logs and other Excel files, the number of drilled holes were reduced to 189 initially and then to 172. The reduction from 189 to 172 drill holes was mainly driven by unavailability of either collar, geology, assay and survey data. A list of holes that were removed from the database of 189 drill holes is given in Table 1 accompanied by an

explanation for their removal. In addition, a map showing the location of at least 12 boreholes that had problems is shown in Figure 7.

Table 1: A summary of drill holes that were excluded from the database used in the current research.

DRILL HOLE ID	COMMENT
DH006, DH019 & DH142	Had geology information but did not have collar, survey and assay information.
DH062 and DH063	Had collar and survey information. Geology and assay information was not found.
DH061	Had collar but no survey, assay and geology information
DH0N/1 and DH0N/2	Does not have assay and geology information
DH100N/1, DH100N/2 & DH100N/3	Despite having the collar and survey information, the holes do not have assay and geology information. Physical logs of these holes were not found.
DH100W/1 and DH100W/2	Despite having the collar and survey information, the holes did not have assay and geology information. Physical logs of these holes were not found.
DH150N/1, DH150N/2 & DH150N/3	No geological and assay information. Physical logs were not found at the time of reporting
DH150W/1 and DH150W/2	No geological and assay information. Physical logs were not found at the time of reporting

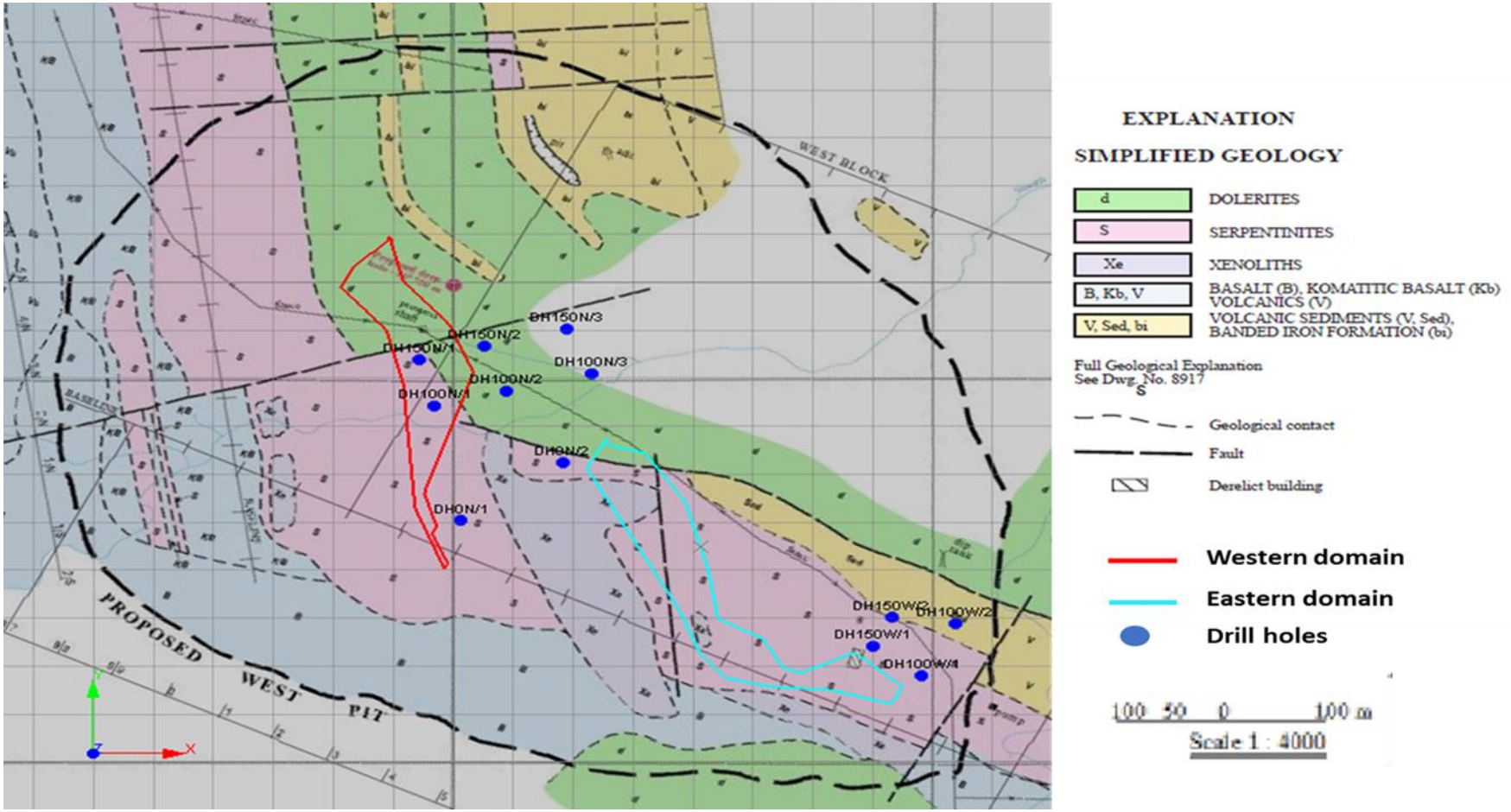

Figure 7: Geological map showing the location of boreholes with validation problems.

Further analysis of the remaining 172 boreholes revealed that a total of fifteen (15) boreholes did not have assay results due to the fact that they did not intersect nickel mineralisation. A map showing the location of these boreholes in relation to the two mineralised domains is shown on Figure 8. Most of these holes with the exception of DH137 plotted outside the mineralised domain.

In order to identify any boreholes that may be lying outside the project area, a plot of borehole collars was done and is shown in Figure 9. The map shows that the drilled area covers a south easterly trending zone covering a strike length of approximately 1.8km. The boreholes were drilled covering both the Western orebody and the Eastern orebody. However, intensive drilling was done on the Western Orebody which is the main focus of the current study. Given the fact that not all drill holes are targeting the orebody understudy, the author had to select boreholes that were drilled targeting the Western orebody. The procedure and process of constraining the boreholes to the current domains will be dealt with in the following sections.

Borehole validation, as highlighted earlier on, involved checking sample runs with the aim of identifying sample duplicates as well as holes with sample run problems. A total of 30 boreholes had sample run problems with either sample overlap, missing sample runs or typing errors. These boreholes were corrected based on the available sample records and log sheets.

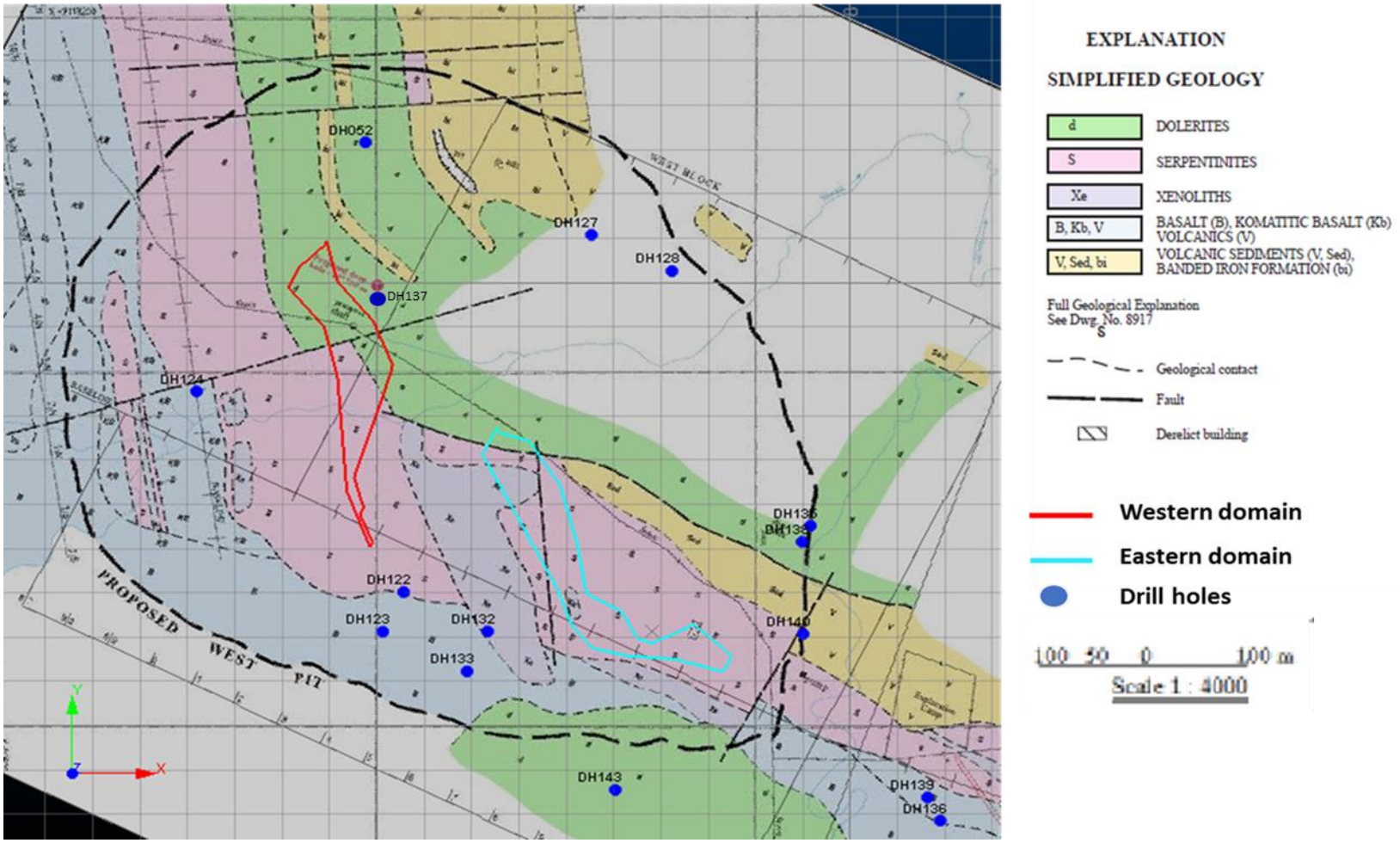

Figure 8: Map showing the location of the 14 holes which did not intersect nickel mineralisation.

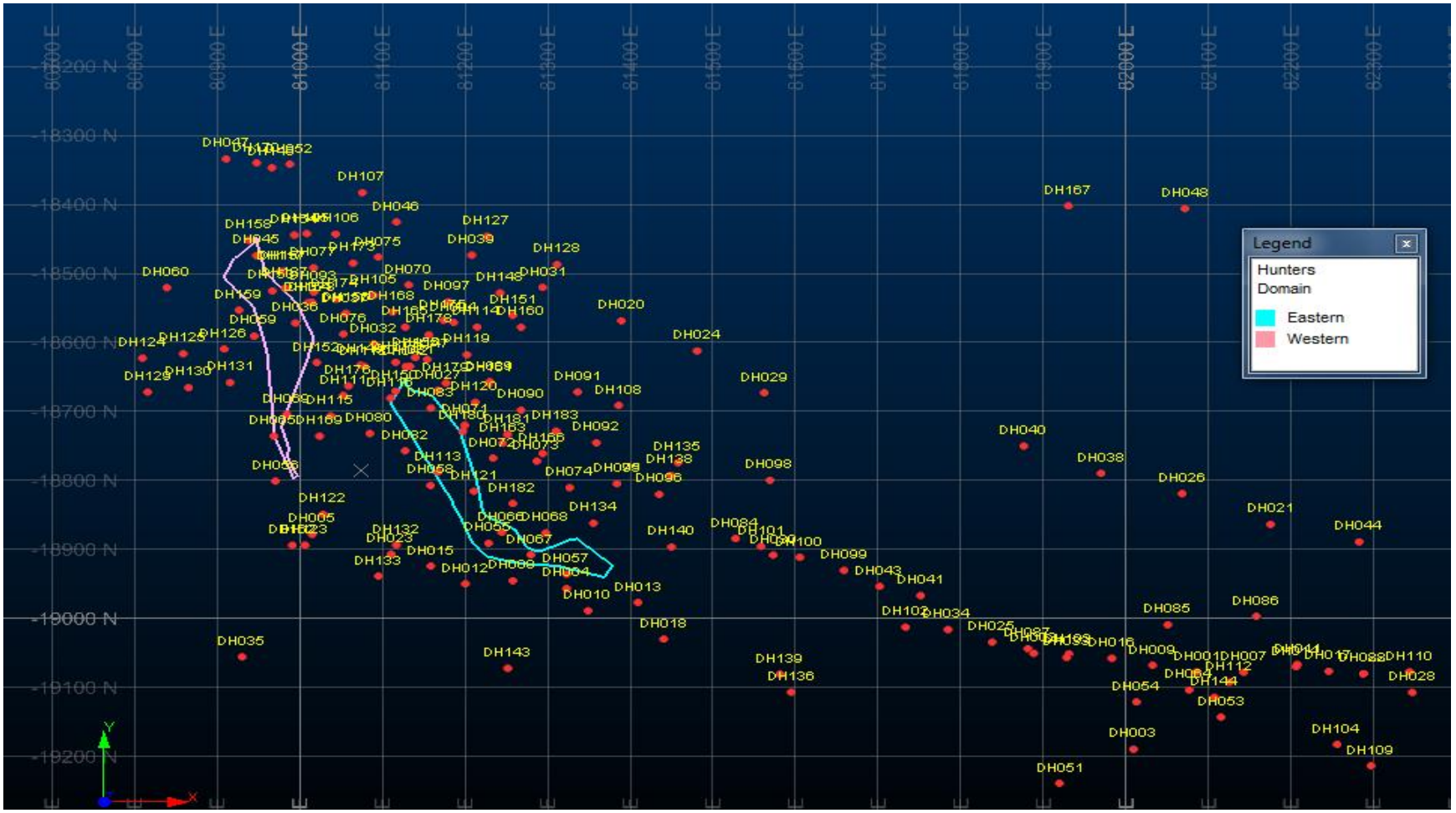

Figure 9 : Map showing geographical location of the 172 boreholes used in the current study.

After correcting sample run problems as well as geology information, the primary data files were imported into Datamine Studio RM were they were desurveyed and validated. No errors were found and the database was deemed to be clean for further use in the study.

4.3 Orebody Wireframe Validation

Orebody wireframes for the two domains shown in Figure 10 were generated in 2006. The two wireframes where validated focussing on the following issues:

- Open edges: these are edges of triangles which are not shared between two faces.
- Crossovers or intersections: check for non-adjoining wireframe faces that intersect each other.
- Shared edges: Check of wireframe edges shared by more than 2 faces.
- Duplicate faces.

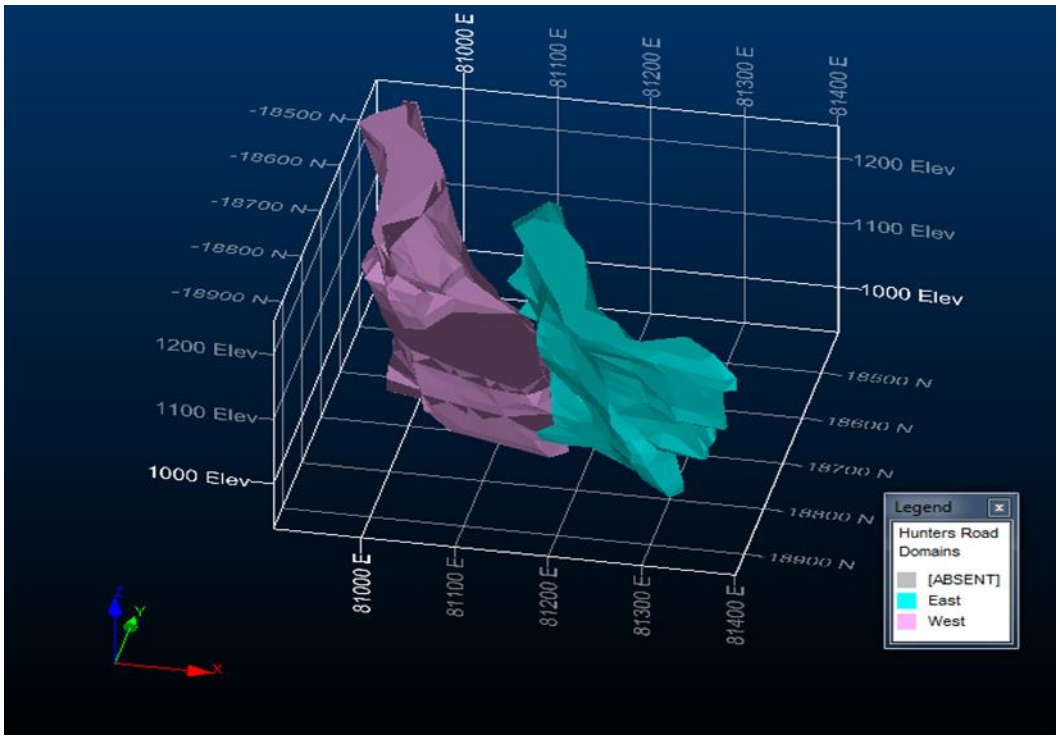

Figure 10: 3D image of the Eastern and Western domain of the Western orebody

The orebody wireframes were found to be clean with no issues as far as the four highlighted issues were concerned. The second stage of wireframe validation was to check if the wireframe boundary honour the drill hole data used in constructing the orebody model based on 0.40%Ni cut-off grade. Several sections or slices oblique to the two mineralised domains were done as part of orebody boundary analysis. In many cases, a wireframe boundary defined by 0.40%Ni COG was very difficult to delineate, resulting in either incorporation of material below the COG or exclusion of some mineralised zones that were above the COG. A slice of the orebody showing grades from drill holes against the orebody wireframe is shown in Figure 11.

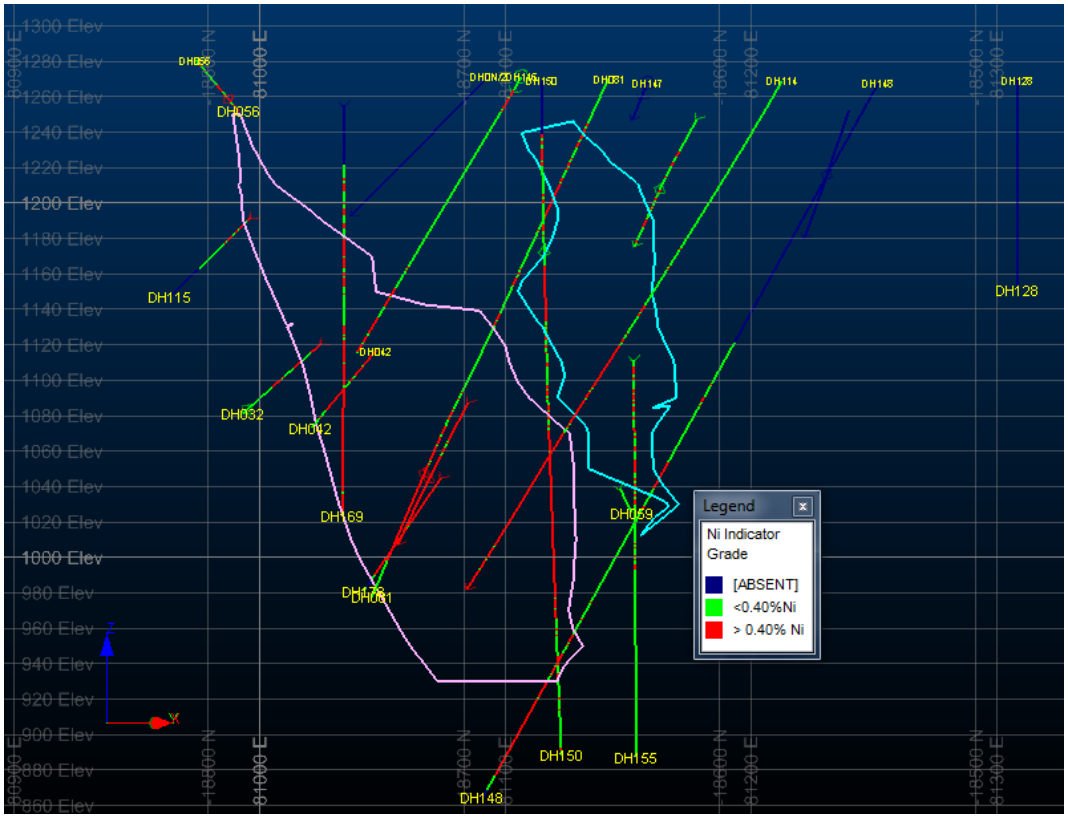

Figure 11 : A section showing orebody outlines and drill hole intersections based on indicator grades.

If a lower geological COG was applied, the orebody boundary could have been defined more accurately. The sections also review that the orebody wireframes leaves out approximately 30m of oxidised zone above the mineralised domains.

The absence of a geological model showing different lithological units as highlighted in the geology literature section earlier on made it very difficult to justify the split in the orebody. A few sections that have been observed by the author in the absence of a geological model revealed that below 1240m ASL, the separation in orebodies may be due to the applied cut-off grade rather than the presence of the Rietfontein xenolith (see Figure 6).

Based on these few observations, the hard boundary approach used in coming up with the wireframe may not be appropriate for this deposit. There is need to use both geology and a lower cut-off grade in defining the mineralised domains.

4.4 QAQC

The Hunters Road nickel exploration covers a period starting from 1971 up to 2004 with 183 drill holes. QAQC data obtained from historical reports covers a period from October 1991 up to December 1993. The most recent QAQC data obtained relates to core drilling and geochemical studies targeting 10 holes with a total of 2850m, drilled between 2003 and 2004. According to BNC (2006) quartz blanks, base metal certified reference material (CRM) namely GBM300-4 (low grade 4103ppm), GBM999-1 (high grade 11728ppm) and GBM998-8C (medium grade 8118ppm) were inserted after every fifty (50) (4m composite samples). Repeats and duplicates were also inserted following the same insertion rate highlighted above.

Sample preparation was conducted by Inner Core Exploration Services at the Institute of Mining and Research (IMR) at the University of Zimbabwe. Geochemical analysis was carried out in Canada by ACME Analytical laboratories. Unfortunately the raw data for QAQC was not available in a form which would allow generation of control charts. Analyses of the printed control charts of CRM revealed that the results met the required standard of being within 3 standard deviation of the mean value. Results for duplicates

and repeats were not available while those of quartz blanks revealed that there was no sample contamination. Based on the analyses of the 2003 QAQC data, the author can attest that the results of the 2003-2004 campaign achieved acceptable levels of accuracy but cannot attest to precision.

QAQC data covering 1992 and 1993 was based mainly on three local standards (M78, MZH62 and TN67) with a recommended value and four other standards (HR3, standard 1, 2 and 3) with unknown assay value. Two laboratories namely the Institute of Mining Research and Geomet were used. Analyses of the blanks using control charts are shown in Appendix 1 Figure A1 shows that there was either contamination of samples or the blank which was chosen had nickel mineralisation as high as 0.03%Ni. Analysis of standards HR3, M78, TN67 and MZH62 using control charts in Appendix1 Figures A2 to A5, in the absence of standard deviation showed mixed results in terms of accuracy. Standard TN67 and M78 showed a bias towards high values while MZH62 and HR3 produced reasonable levels of accuracy. Given the high bias and high levels of contamination or poor choice of blank sample, the QAQC for the exploration campaign did not achieve acceptable levels of accuracy. The absence of repeats and duplicates also makes it very difficult to comment on precision.

4.5 Relative Density

Historical estimates from 1992 up to 2001 used an average relative density of 2.85t/m^3 based on an assumption that the relative density at Hunters Road is similar to other operating BNC mines at that time. In 2002 during prefeasibility studies, Peacock, Simpson & Associates laboratories measured relative densities on archived core segments that were from ore zones and obtained 2.60 t/m^3. However, it was felt that the relative density was significantly lower than the expected 2.85 t/m^3, perhaps because it had been determined from deteriorated core samples. A follow up relative density measurements on fresh cores were conducted by Dr Gwavava in

March 2004 based on 576 samples and obtained an average density of 2.65 t/m^3. Based on the 2002 and 2004 outcome, BNC settled for an in-situ density of 2.60t/m^3 for the Western orebody ore.

The current study verified the relative density information and has found it in order although there are reservations regarding the size of the samples and the method used for sample selection. Every sample that was submitted for assaying between 2002 and 2004 should have been analysed for density. A relative density of 2.60t/m3 which was also used by BNC in May 2006 resource estimates, was chosen for comparison purposes.

4.6 Statistical Analysis of the Data

4.6.1 Compositing and Declustering

A precursor to any resource evaluation activity is statistical analysis of the sample values in order to infer knowledge about the grade distribution of the deposit. Boreholes lying inside the two domains were selected separately and composited to 2m in order to achieve the same support. The 2m compositing length was derived from an assessment of raw sample intervals which were predominantly 1m. In addition to compositing, data declustering was performed. Data declustering is the process of adjusting the full data set by removing or weighting data points in densely sampled areas in order to give a more representative and evenly spaced samples (Journel, 1983; Rossi and Deutsch, 2014). There are a number of declustering techniques such as the polygonal method, nearest neighbour and cell declustring among others. Cell declustring was used in this study by defining a 25m x 25m x 10m grid similar to block dimensions. The technique assigns a weight to every sample based on the number of samples in the grid cell as follows:

- Dividing the volume of interest into regular grid with cell size *L* (25m x 25m x 10m)
- Counting the number of occupied cells L_0 and the number of data in each occupied cell n_{l_0}, l_0=1,….,L_0.

- Calculating declustering weights using the following formula for each block or cell.

$$W_i(c) = 1/(n_I \times L_0) \quad (17)$$

Where n_I is the number of samples in a block or cell, L_o is the number of occupied blocks.

Statistical analysis of cell declustering of 2m composite samples for the two domains are shown in Table 2. Declustering statistics shows that the two domains have the same mean of 0.56%Ni and they all drop by 1.82% to 0.55%Ni after declustering. While the means are similar, the Eastern domain which has less samples is highly variable compared to the Western domain with a higher number of samples. However, percentile-percentile (PP) plot (see Figure 12) of the cumulative probability of the Eastern domain samples against cumulative probability of the Western domain samples showed that the two data sets are from a population with the same distribution.

Table 2: Declustering statistics for the Eastern and Western domains.

Domain	Eastern		Western	
Domain Code	1		2	
Declustering	NO	YES	NO	YES
Number of samples	1680	1680	2772	2772
Minimum(%Ni)	0	0	0	0
Maximum(%Ni)	3.70	3.70	5.44	5.44
Mean(%Ni)	0.56	0.55	0.56	0.55
Variance	0.13	0.13	0.09	0.09
Skewness	3.41	3.49	3.73	3.86

The PP plot and QQ plot shown in Figure12 shows that the two distributions have the same shape. While the PP plot and the QQ plot data lie within the 45 degree line, the tail behaviour of QQ plot shows that the Eastern domain

grades are higher than the Western domain, especially above 1%Ni. The same trend is observed on the lower tail where the lower values (below 0.20%Ni) are more on the Eastern domain than the Western domain. The two graphs support earlier observation that the two domains appear to be separated on the basis of geological COG of 0.40%Ni and there is no structural or lithological break observed at depth. While these two domains will be treated separately in resource estimation, there is a high probability that they will be mined as one orebody.

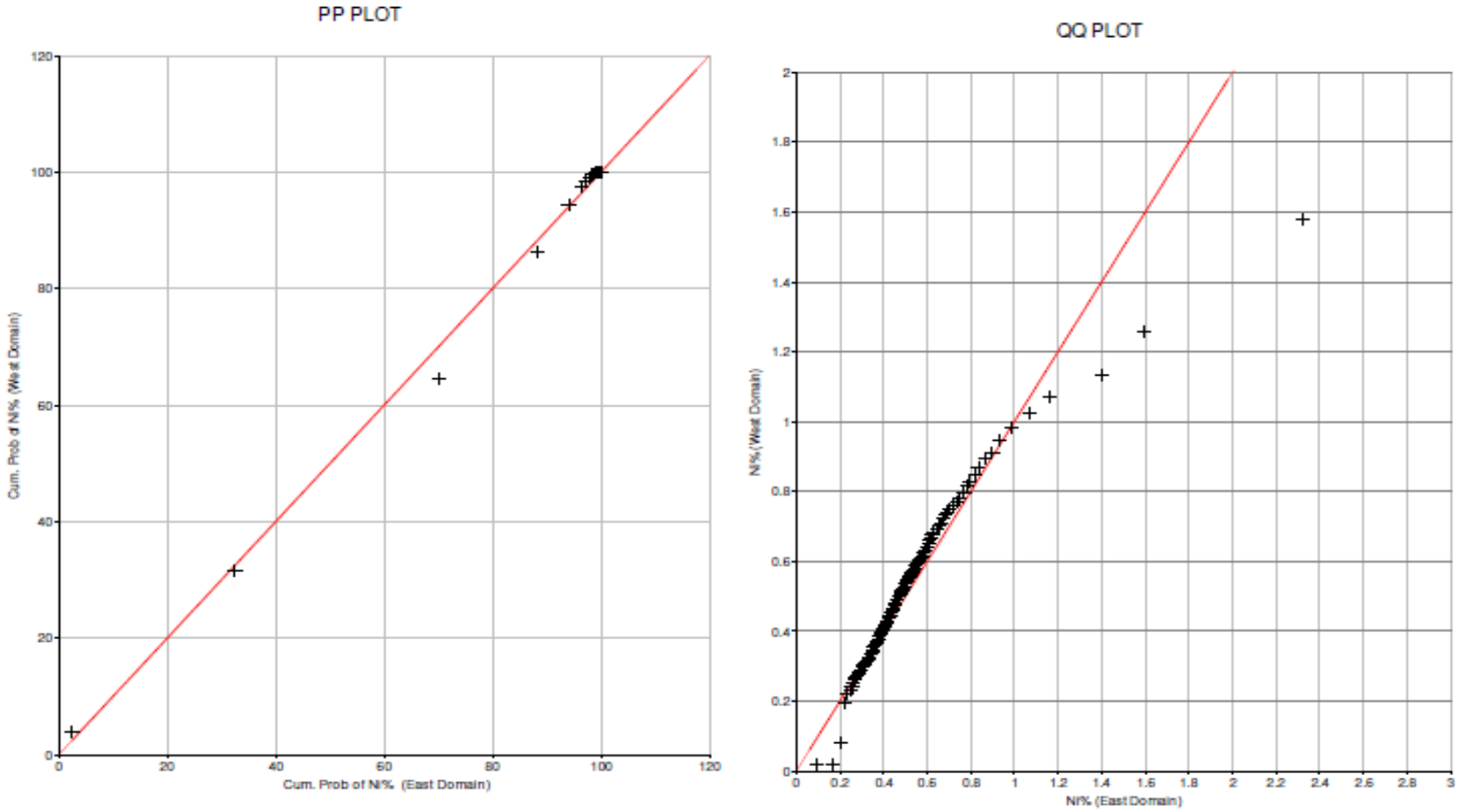

Figure 12: PP and QQ plot of eastern and western domain of the Western orebody of Hunters Road nickel deposit.

4.6.2 Descriptive Statistics

In order to have full understanding of statistical behaviour of sampling data of the two domains, descriptive statistics of 2m composites before cell declustering was performed on the data. A histogram and cumulative frequency distribution curve were used in analysing sample data. The graphs for the Eastern and Western domains are shown in Figures 13 and 15 respectively accompanied by key statistical parameters.

Statistical analysis of declustered data for the two domains revealed a positively skewed distribution with a skewness of 3.41 and 3.73 for the Eastern and Western domains respectively. The coefficient of variation (COV) is higher for the Eastern domain (0.63) than the Western domain (0.54). The analysis shows that, although the Western domain is skewed than the Eastern domain, the latter is highly variable. The variability in Eastern domain may have been due to the lower number of samples (1680) compared to 2772 samples for the Western domain. Analysis of the drill hole locations showed a more intensive exploration drilling on the Western domain than the Eastern domain.

Although the two distributions are highly skewed, a COV less than 2 is not considered to be highly variable (Journel, 1983; Rossi and Deutsch, 2014). Given low COV, there is a possibility that MIK E-type estimate will be comparable to the OK estimates.

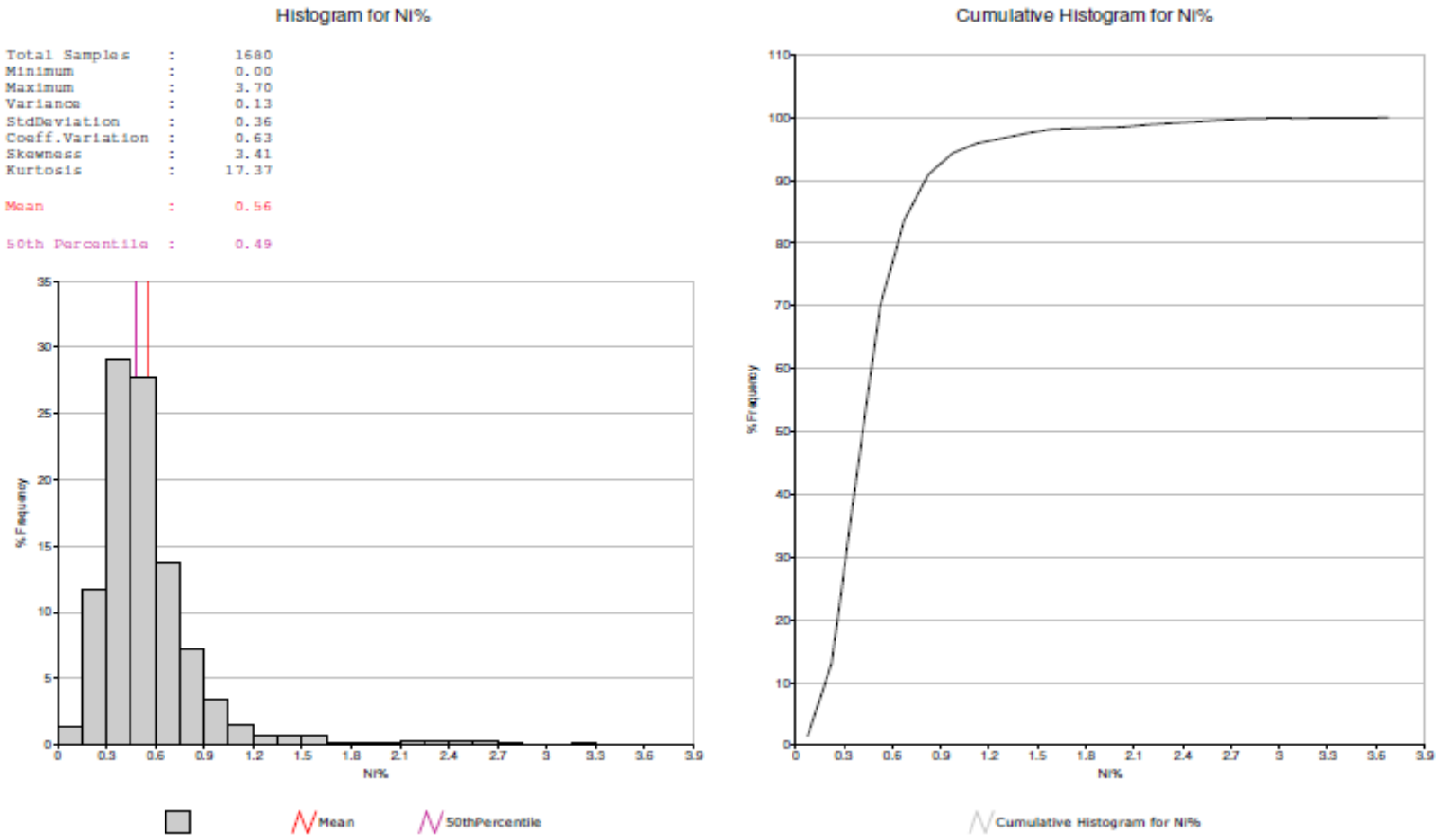

Figure 13: Histogram and cumulative frequency curve for the Eastern domain before declustering.

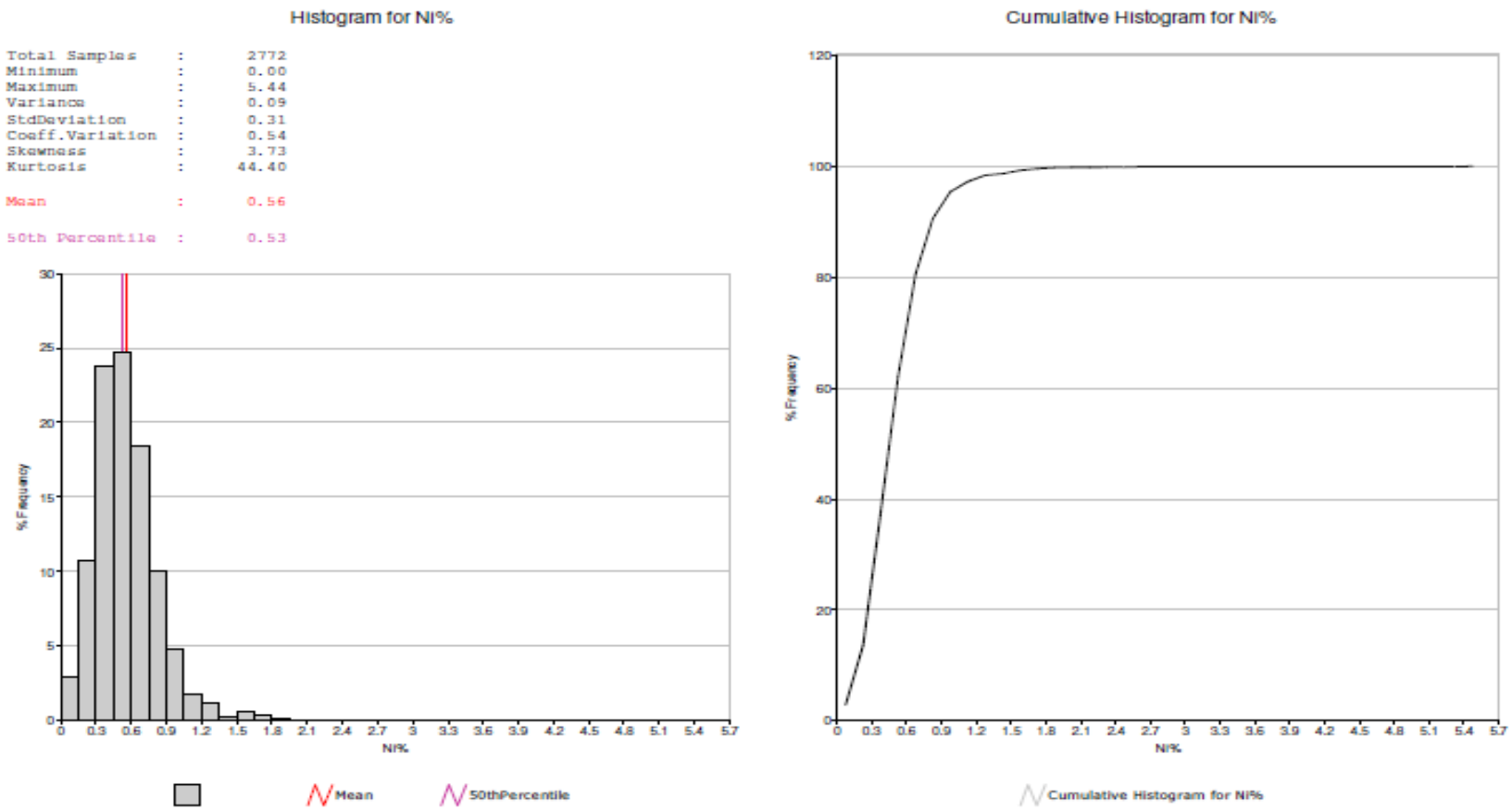

Figure 14: Histogram and cumulative frequency curve for the Western domain before declustering.

4.7 Normal Score Statistical Analysis

The NS transformation of 1680 samples in the Eastern domain and 2772 samples in the Western domain of the Western orebody resulted in normally distributed data with a mean of zero (0) and standard deviation of 1. The highly positively skewed distribution was transformed to a normal distribution in Gaussian space with zero skewness. A summary of the descriptive statistics before and after transformation as well as a histogram for the Eastern and Western domains are shown in Figures 15 and 16 respectively.

NS transformation of original nickel values of the Eastern and Western domain resulted in a Gaussian distribution. NS values follows cumulative distribution function of standard Gaussian G(y) with mean ($m_y = 0$) and variance ($s^2_y = 1$). Since NS transformation confirmed a Gaussian distribution, SGS and its associated process can be performed using NS data.

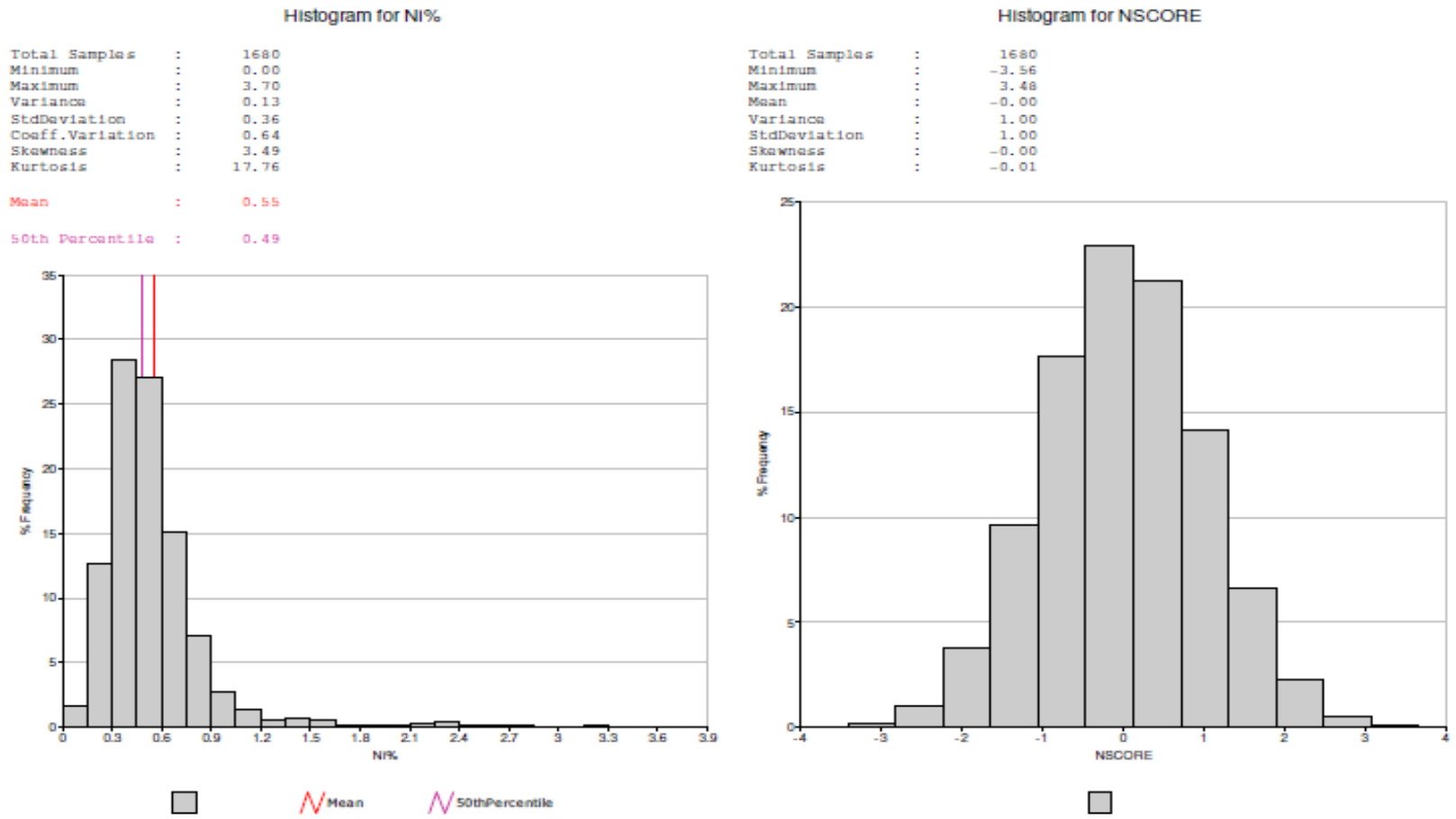

Figure 15: Histogram and descriptive statistics before and after NS transformation for the Eastern domain samples.

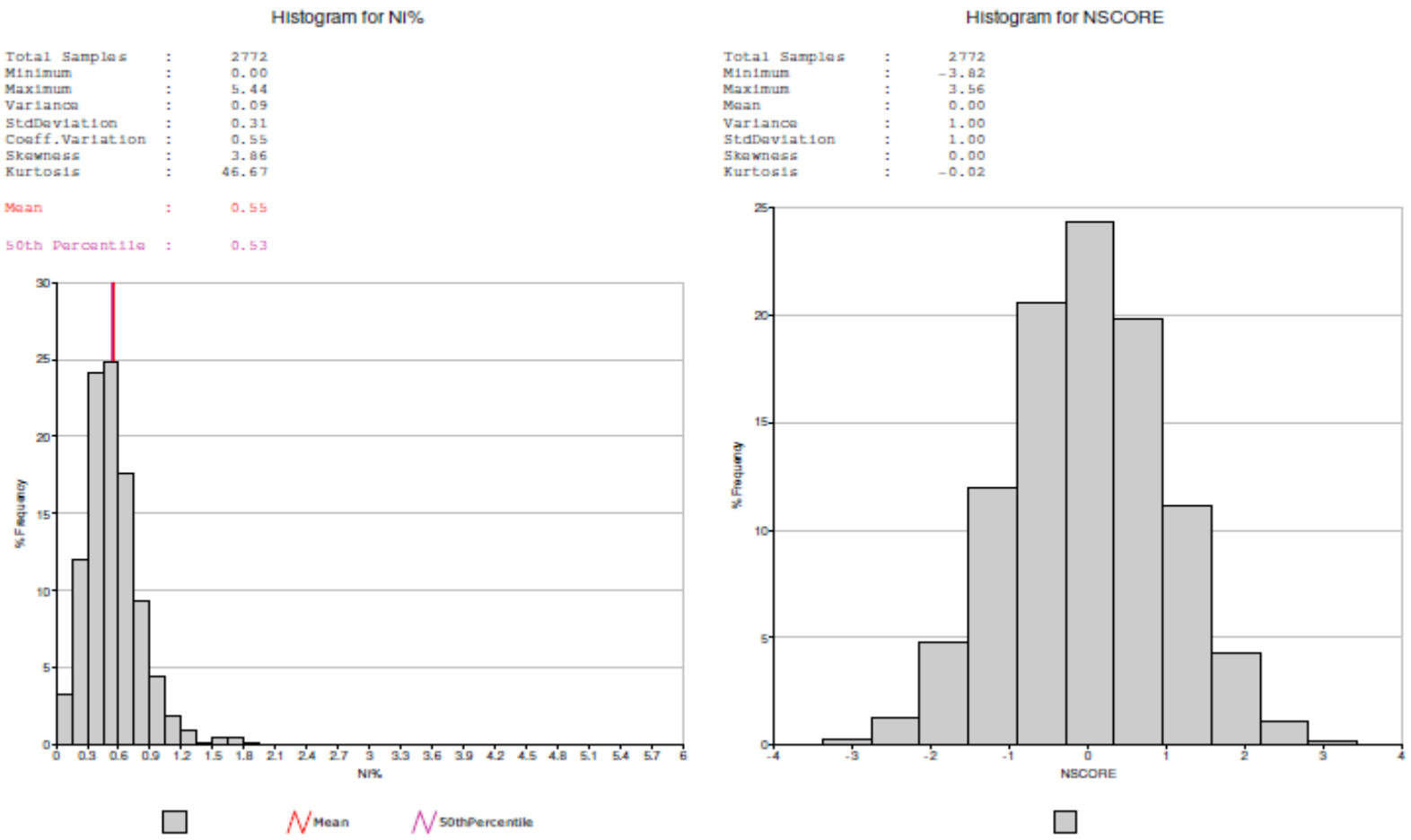

Figure 16: Histogram and descriptive statistics before and after NS transformation for the Western domain samples.

4.8 Summary of Findings

This chapter centred on exploratory data analysis with a focus on validation of historical information and descriptive statistics. Key findings of the data validation exercise were that out of the 189 drill holes, 172 drill holes were found to be clean. QAQC data was only available for drill holes drilled between 1992-1993 and 2003-2004. The rest of the drill holes drilled since 1971 did not have QAQC data. QAQC results for 2003-2004 met acceptable levels of accuracy at that time while QAQC results for 1992-1993 do not meet required levels of accuracy and precision. The absence of a reliable and secured electronic database for the Hunters Road data is a cause for concern given the amount of drilling done on the project.

Orebody wireframes showed a split of the Western orebody into two separate domains separated on surface by xenoliths. These orebody wireframes did not have open edges and cross overs hence they were found to be acceptable for use in resource estimation and conditional simulation. However, boundary analysis of the orebody wireframes revealed some inconsistencies in the use of a 0.40%Ni COG in defining orebody outlines. There was no geological model to assist in the interpretation of the domains defined using grade indicator.

Statistical analysis of the two domains showed a positively skewed distribution with the Western domain being more skewed than the Eastern domain. The Eastern domain with a COV of 0.63 is highly variant than the Western domain with COV of 0.54. Given the low COV, it is more likely that MIK E-type estimates will be similar to OK estimates. Statistical analysis of the declustered data supported the notion that the two domains are from the same distribution. A mean of 0.55%Ni was obtained for both the Eastern and Western domain, with the latter being less variable. NS transformation of sample data based on 2m composites resulted in a standard Gaussian distribution with a mean of 0 and standard deviation of 1 for both domains. The next chapter focusses on the modelling spatial variability.

CHAPTER 5: VARIOGRAPHY

5.1 Introduction

The previous chapter looked at the exploratory data analysis (EDA) which focussed on data validation and descriptive statistics. Key findings from the statistical analyses of the two domains were that the population distribution is positively skewed with skewness greater than 3. In addition, QQ and PP plots of the two domains of the declustered data revealed that the two distributions are the same with differences in variability. The fact that the two domains exhibit strongly skewed sample distributions meant that the use of linear geostatistical estimation method such as OK which assumes stationarity can be risky. While OK has been successful in producing unbiased estimates with minimum estimation variance, the problem arise when dealing with skewed distributions with extreme values or outliers. In many cases, mineral resource estimators are forced to trim off the outliers by applying a top cap. Journel (1983) argued against trimming of outliers as the trimmed data may be carrying valuable information about the deposit. Instead of applying a top cap, the use of non-parametric method such as Indicator Kriging (IK) was proposed.

The main purpose of this chapter is to investigate spatial continuity of nickel grades through the use of indicator semi variogram and normal scores semi variogram. In coming up with the theory of regionalised variable, Matheron (1971) argued that there is some degree of spatial autocorrelation that exist between location and any regionalised variable such as nickel grades. The degree of spatial autocorrelation can be observed on a semi variogram which shows two contradictory aspects namely the random aspect commonly known as the nugget effect and the structured aspect which is the correlated component. The chapter will start by looking at indicator variogram followed by NS variogram for the two domains.

5.2 Indicator Variography

Variography examines the spatial continuity or variability of mineralisation in relation to spatial dispersion. A variogram is the average squared difference of data pairs separated by a specific lag distance and can be expressed mathematically as follows:

$$2\gamma\,(h) = \left(\sum_{i=1}^{N(h)}[\,z\,(u_i) - z\,(u_i+h]^{2}\right)/\,N(h) \qquad (18)$$

The semi variogram is therefore one half of the variance of the average squared differences and can be expressed mathematically as:

$$\gamma(h) = \left(\sum_{i=1}^{N(h)}[\,z(u_i)-z(u_i+h]^{2}\right)/(2N(h)) \qquad (19)$$

Where γ (h) represents the semi variogram, $N\,(h)$ represents the number of pairs, h represents lag distance and u_i and u_i+h represents sample values spatially separated by a lag distance h. The semi variogram used in the current study were indicator semi variograms.

The indicator approach involves binominal coding of a regionalised variable such as nickel grades into either 1 and 0, depending on it being above or below a given threshold (cut-off grade) (Basante, et al., 2008). For a given cut-off (z_c), the indicator random function I(x,z) is defined at every location x as the binary function that assumes a value of 1 or 0 under the following conditions:

I (x, zc) = 0 if Z(x) $\leq z_c$

I (x, zc) = 1 if Z(x) > z_c

An indicator semi variogram is therefore a variogram of the indicators defined using specific threshohd or cut-off. In this study, the first stage involved identification of cut-off grades to be used in creating indicator variograms. MIK uses multiple cut-off grades and these were determined

using deciles of sample values for the two domains. A summary of the cut-off grades used in creating indicators for MIK is shown in Table 3.

Table 3: A summary of the cut off grades used in calculating indicator variograms for the Eastern and Western domains.

	Domain	
	Eastern	Western
Percentile (%)	(%Ni)	(%Ni)
10	0.28	0.28
20	0.34	0.34
30	0.40	0.40
40	0.44	0.47
50	0.49	0.53
60	0.54	0.59
70	0.6	0.66
80	0.7	0.75
90	0.87	0.89

A total of fifty four (54) experimental variograms were calculated honouring the three principal directions. The first variogram calculated in each case was a downhole experimental semi variogram to determine the nugget effect or the random component of the semi variogram. The nugget effect reflects the difference between samples which are very close together but not on the same position (Clark and Harper, 2007). The difference in samples very close together as expressed by the nugget effect may be either due to inherent variability of mineralisation or sampling and analytical errors.

Downhole semi variograms were followed by directional experimental variograms at each specific cut off grade honoring the azimuth and dip direction in the rotated XY plane. The rotation was done to enable calculation of experimental variograms following the dipping plane. The following parameters were key in the calculation of the experimental variogram:

- lag distance (15m)

- the number of lags (At least 15)
- angle of tolerance (22.5^0)
- Cylindrical search radius (30m)
- Cut-off grade for the indicator variogram (9 cut-off grades were used)
- Horizontal and vertical increments of dip and azimuth

Rossi and Deutsch (2014) argued that lag and angles of tolerence should be small enough to define good directional continuity and the maximum lag distance should be less than half of the domain size. After calculating experimental indicator variograms, fitting of variogram models were done defining the nugget effect (C_0) component, correlated component (C_1-C_n) depending on the number of structures and the range (a). The fitted indicator variogram models will be discussed separately under each domain in the next section.

5.2.1 Indicator Variograms for Eastern Domain

A total of 24 indicator semi variograms were calculated, three(3) per COG as highlighted in Table 3. A summary of the indicator semi variogram parameters for the Eastern domain are shown in Table 4. In addition, the indicator semi variogram with a fitted model for 0.49%Ni COG is shown in Figure 17. This variogram is the median indicator semi variogram for the Eastern domain. All other indicator semi variograms for the Eastern domain are shown in Figure A6 to A12 in Appendix 2.

The nugget effect is relatively low ranging from 32% to 42% of the variance. The indicator semi variograms display geometric anisotropy implying that the ranges are different in the three principal directions as shown in Figure 17 for example. The maximum range of grade continuity obtained was 67m at a COG of 0.49%Ni along the WNW direction. The two anisotropic directions of grade continuity were the WNW and the ENE directions. In

general, the spatial continuity displayed by the indicator variograms conform to the geological interpretations.

Table 4: The double structured spherical models for the indicator semi variograms of the Eastern Domain at various cut-offs.

COG(%Ni)	0.28	0.34	0.40	0.44	0.49	0.54	0.60	0.70	0.87
1st Rotation angle	199	149	139	224	214	179	214	214	145
Rotation AXIS	Z	Z	Z	Z	Z	Z	Z	Z	Z
NUGGET (C_0)	**0.34**	**0.36**	**0.38**	**0.33**	**0.41**	**0.42**	**0.35**	**0.33**	**0.38**
1st Structure	SPH	SPH	SPH	SPH	SPH	SPH	SPH	SPH	SPH
ST1Range X	17.10	9.10	10.40	30.00	21.50	2.70	16.60	17.00	6.83
ST1Range Y	6.10	26.50	25.30	16.30	4.60	4.30	10.60	11.30	4.72
ST1Range Z	6.10	7.50	9.30	8.20	6.10	8.50	6.10	6.10	4.84
1st Sill (C_1)	**0.24**	**0.02**	**0.18**	**0.33**	**0.01**	**0.34**	**0.15**	**0.05**	**0.18**
2nd Structure (ST2)	SPH	SPH	SPH	SPH	SPH	SPH	SPH	SPH	SPH
ST2Range X	53.10	22.40	33.90	67.20	67.50	31.20	54.20	39.90	36.59
ST2Range Y	17.70	54.40	59.90	38.40	39.80	45.50	34.90	31.40	18.81
ST2Range Z	40.20	36.10	30.00	27.60	31.80	28.10	28.00	27.80	31.94
2nd Sill (C_2)	**0.42**	**0.62**	**0.44**	**0.34**	**0.58**	**0.25**	**0.49**	**0.61**	**0.44**

NB: SPH represents spherical semi variogram model. ST# = Structure Number # where # = 1 or 2 for the 1st and 2nd modelled structures.

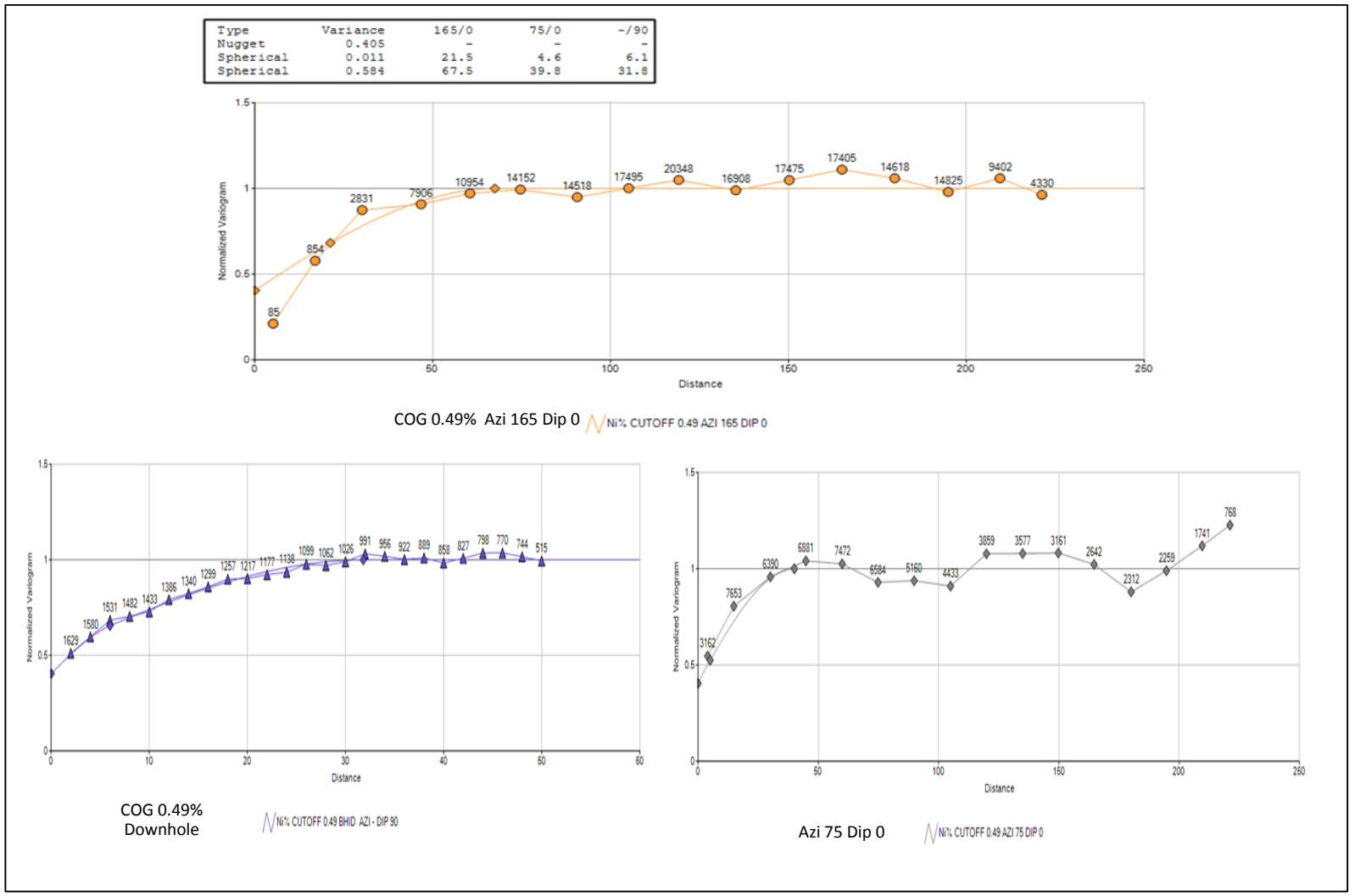

Figure 17: Indicator semi variogram for the Eastern Domain using a 0.49%Ni COG.

5.2.2 Indicator Variogram for Western Domain

The Western domain indicator semi variograms, just like for the Eastern domain, display geometric anisotropy with a much lower nugget effect. The nugget effect ranged between 27% and 39% of the variance (total sill). The well-defined structure of the downhole indicator variograms are a function of the intense drilling that has been carried out on this portion of the Western orebody as shown by the number of samples. The maximum range of grade continuity was 64.71m at a COG of 0.47%Ni towards the WNW direction. The indicator semi variogram showing the direction of maximum continuity at 0.53% Ni COG is shown in Figure 18. The variogram is the median variogram for the Western domain. The rest of the indicator semi variograms at the various cut-off are shown in Appendix 3 in Figure A13 to A20.

Two principal directions of grade continuity were deduced from the indicator variograms namely the WNW and NNW. These directions conform to geological interpretation of mineralisation discussed under the local geology and mineralisation section of the report (Chapter 3). All the indicator variograms are double structured spherical models and are shown in Table 5.

Table 5: The double structured spherical models for the indicator semi variograms of the Western Domain at various cut-offs.

COG (%Ni)	0.28	0.34	0.4	0.47	0.53	0.59	0.66	0.75	0.89
1st Rotation angle	150	150	135	130	135	110	110	110	115
Rotation axis	Z	Z	Z	Z	Z	Z	Z	Z	Z
Nugget (C_0)	**0.27**	**0.29**	**0.34**	**0.38**	**0.34**	**0.37**	**0.39**	**0.35**	**0.36**
1st Structure (ST1)	SPH	SPH	SPH	SPH	SPH	SPH	SPH	SPH	SPH
ST1Range X	15.22	4.55	12.33	19.10	22.93	15.50	7.20	15.20	6.60
ST1 Range Y	29.89	23.30	24.13	17.80	37.36	11.3	10.20	10.80	9.20
ST1 Range Z	6.05	6.25	8.02	6.88	6.73	5.90	6.10	6.60	4.20
1st Sill (C_1)	**0.44**	**0.1**	**0.16**	**0.11**	**0.47**	**0.29**	**0.17**	**0.26**	**0.31**
2nd Structure(ST2)	SPH	SPH	SPH	SPH	SPH	SPH	SPH	SPH	SPH
ST2 Range X	31.05	29.28	28.65	44.7	36.85	43.4	30.00	32.20	44.30
ST2 Range Y	62.02	55.3	59.55	64.24	64.71	31.4	28.30	27.20	25.80
ST2 Range z	38.59	39.95	30.10	32.08	30.12	28.00	26.90	27.90	32.10
2nd Sill (C_2)	**0.29**	**0.61**	**0.5**	**0.51**	**0.19**	**0.34**	**0.44**	**0.39**	**0.33**

NB: SPH represents spherical semi variogram model. ST# = Structure Number # where # = 1 or 2 for the 1st and 2nd modelled structures.

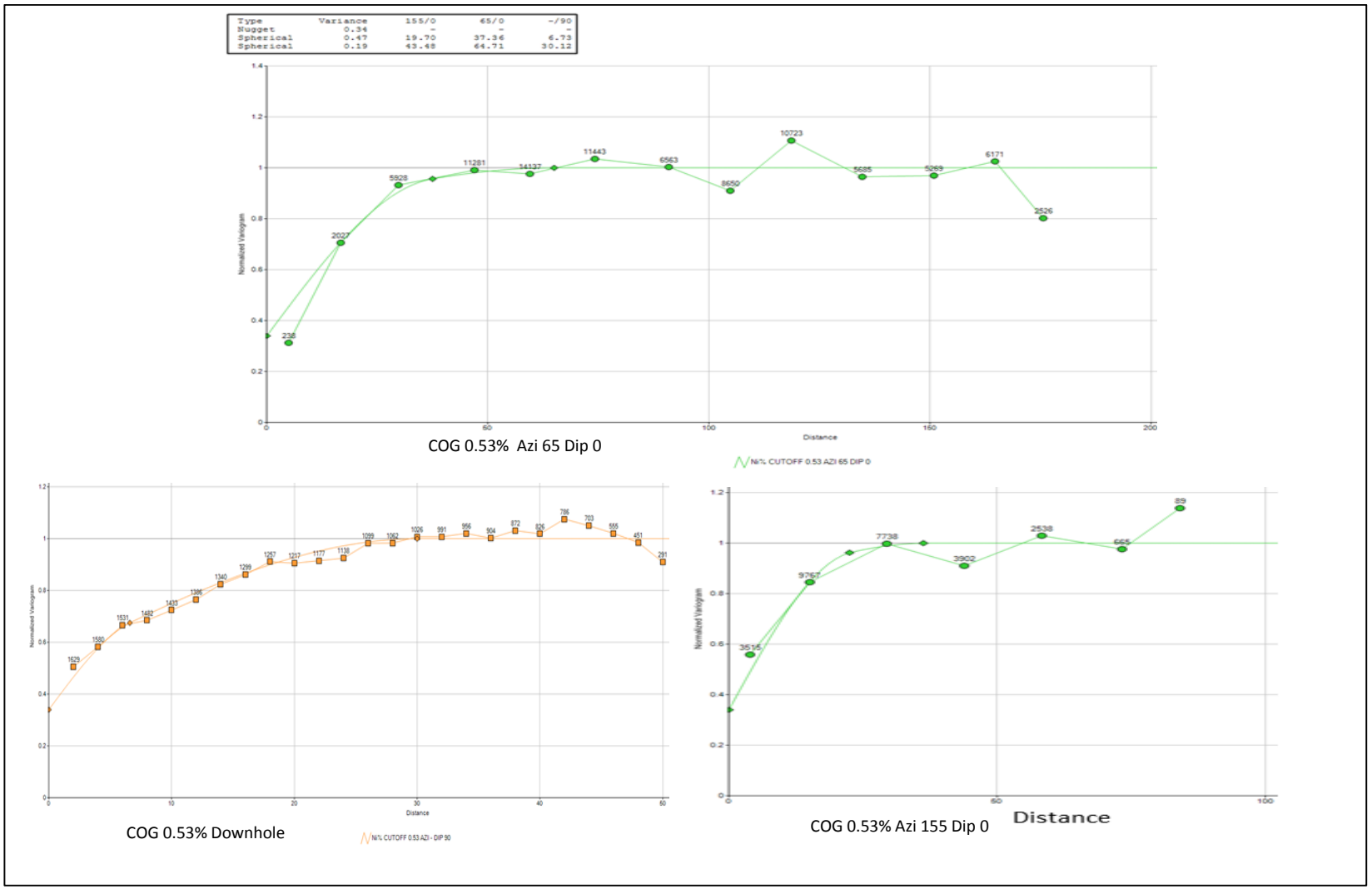

Figure 18: A plot of indicator semi variogram model for the Western Domain using a COG of 0.53%Ni.

5.2.3 Cross Validation of Indicator Semi Variogram Models

Datamine Studio RM module allows for the cross validation of the semi variogram models together with the search volume parameter file. Cross validation is run through point estimation by removing each point in turn from the data file and estimating its value from the remaining data. The main disadvantage of point estimation according to Rossi and Deutsch (2014), is that it does not allow for definite conclusion about the final estimation parameters since it is more focussed on point support instead of block support. When running cross validation, discretisation points are set to 1 x 1 x 1 implying that it is a point estimation rather than block estimation. Despite its weakness, cross validation accompanied by a good kriging neighbourhood analysis offers the best tool for checking the performance of the variogram and the search parameters employed.

All of the 18 semi variograms were cross validated individually after fitting the model and later on they were cross validated together in a single run. A summary of cross validation statistics for the Eastern and Western domains, together with a scatter plot of actual versus estimated is shown in Figure 19. The Eastern domain's estimated mean without declustering at 0.56%Ni is similar to actual sample mean. The Western domain scatter plot shows a slightly higher estimated grade at 0.57%Ni against the actual value of 0.56%Ni.

The scatterplot of the Western domain estimates versus actual shows a symmetrical cloud around the 45^0 line with a narrow spread than the Eastern domain. Despite the spread around the 45^0 line not being perfect, the correlation coefficient at 0.81 and 0.80 for the Eastern and Western domains respectively. They indicate a strong correlation between the estimated values and sample values. The kriging neighbourhood was increased in order to address the possibilities of under estimation of grades.

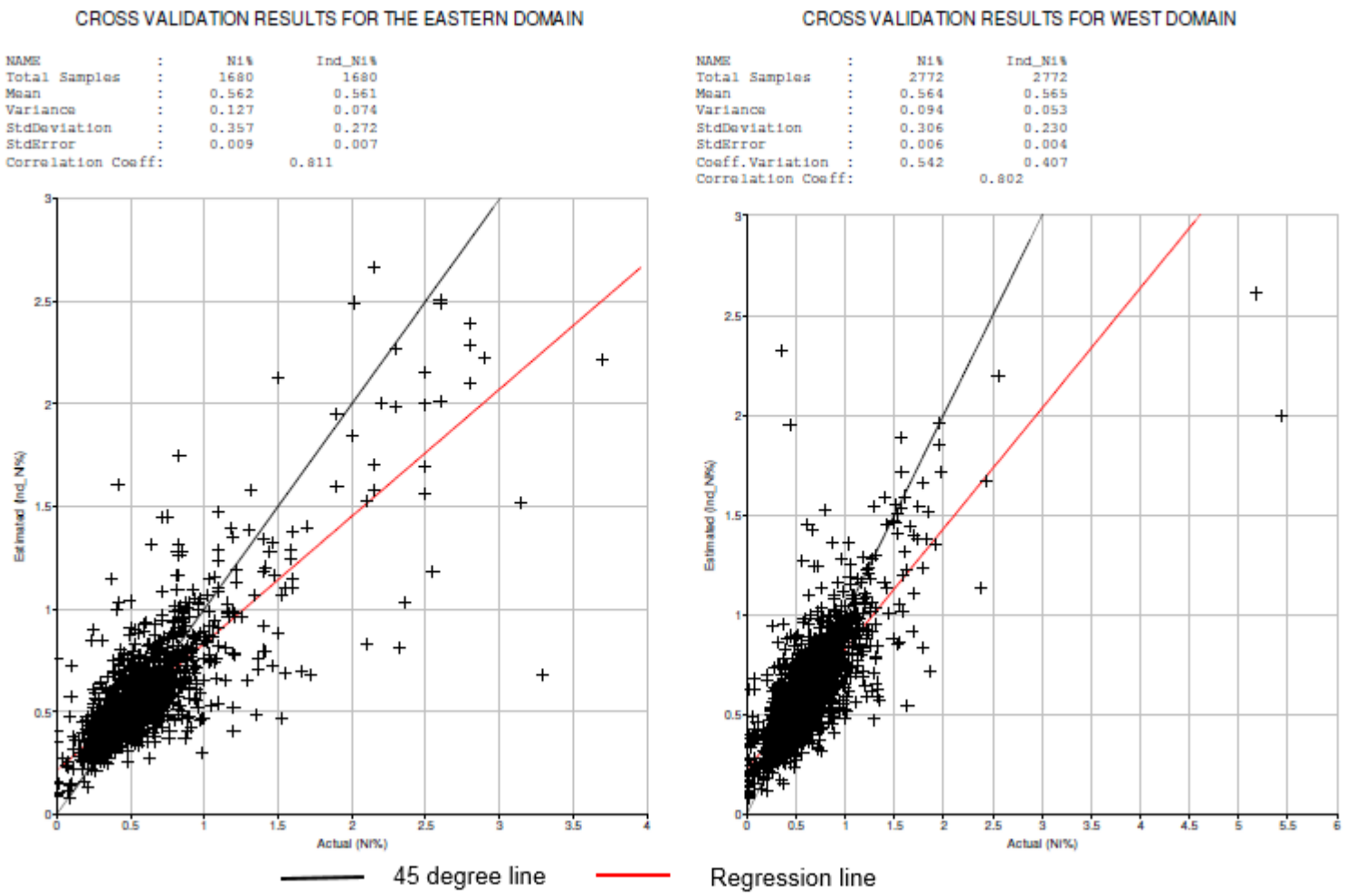

Figure 19: Scatter plot of actual versus estimated grades for the Eastern and Western domains.

An isotropic search volume was used in cross validation exercise following the recommendation by Vann, et al. (2000) and Rossi and Deutsch (2014) regarding order relations problem. A search radius of 40m with a minimum of 12 samples and a maximum of 30 samples was chosen based on the validation exercise. The choice of the kriging neighbourhood could have been improved through 'Quantified Kriging Neighbourhood Analysis (QKNA) (Vann, et al., 2003). However, QKNA was not carried out due to unavailability of the algorithm in the software used in the study. Based on cross validation results, the indicator semi variogram models represent the spatial variability expected in the Eastern and Western domains of the Hunters Road nickel deposit. The choosen kriging neigbourhood is appropriate for the current study.

5.3 Normal Scores Semi Variogram Models

One of the key prerequisites for conditional simulation method such as SGS is obtaining a Gaussian semi variogram model for the transformed regionalised variable. The same process followed when calculating indicator semi variograms was used in calculating NS variograms. The only difference was that there were no COG involved hence only one NS semi variogram per domain was calculated. Unlike the indicator semi variograms, the nugget effects were 10% and 17% of the total variance for the Western and Eastern domains respectively. The reduction in the nugget effect may be attributed to the removal of the proportional effect through the NS transformation. While IK account for proportional effect, there are shortcomings such as uncontrolled variations between cut-off grades (or classes) (Manchuk, et al., 2007), which may result in higher nugget effects. The Eastern domain NS semi variogram was fitted with two (2) spherical model structures with a total sill of 1 as shown in Figure 20.

The Western domain NS semi variogram was fitted using three (3) spherical model structures bringing the total sill to 0.96 (see Figure 21). The Western domain NS semi variogram was scaled off to 1 and the final parameters of the variogram models for the two domains are shown in Table 6.

The maximum range was 46m in the east-west direction of the rotated plane of the Eastern domain and 76m towards SSW direction for the Western domain. The two directions conform to the two directions suggested in Chapter 3. The directions obtained from NS variograms are similar to indicator variograms which revealed a WNW and NNW directions. These directions literally refer to north-south and east-west trends. Based on the assessment of geological interpretations, the NS semi variogram findings are consistent with geological interpretations of mineralisation in Chapter 3.

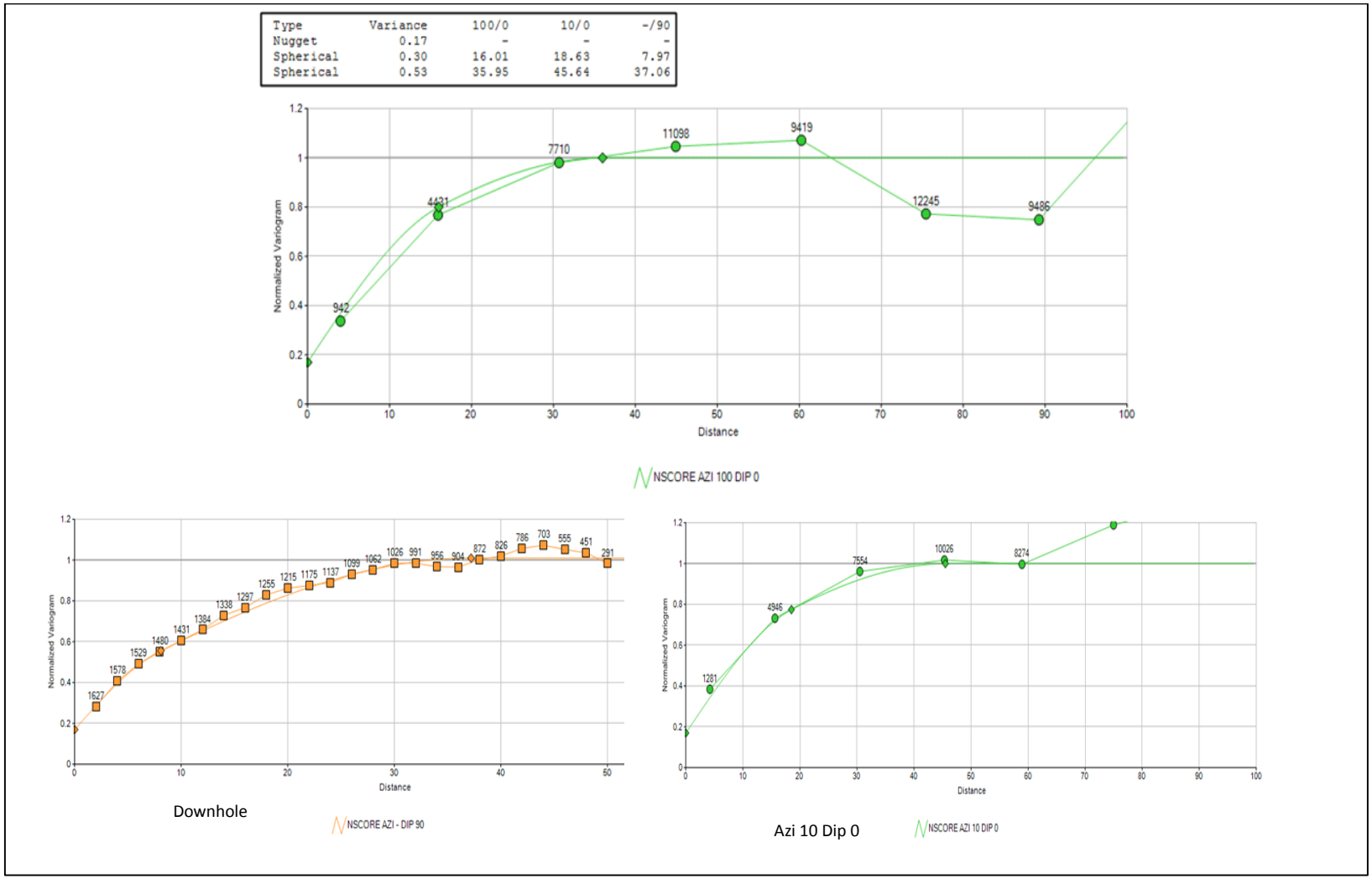

Figure 20: NS variogram for the Eastern domain showing directional variogram and downhole variogram.

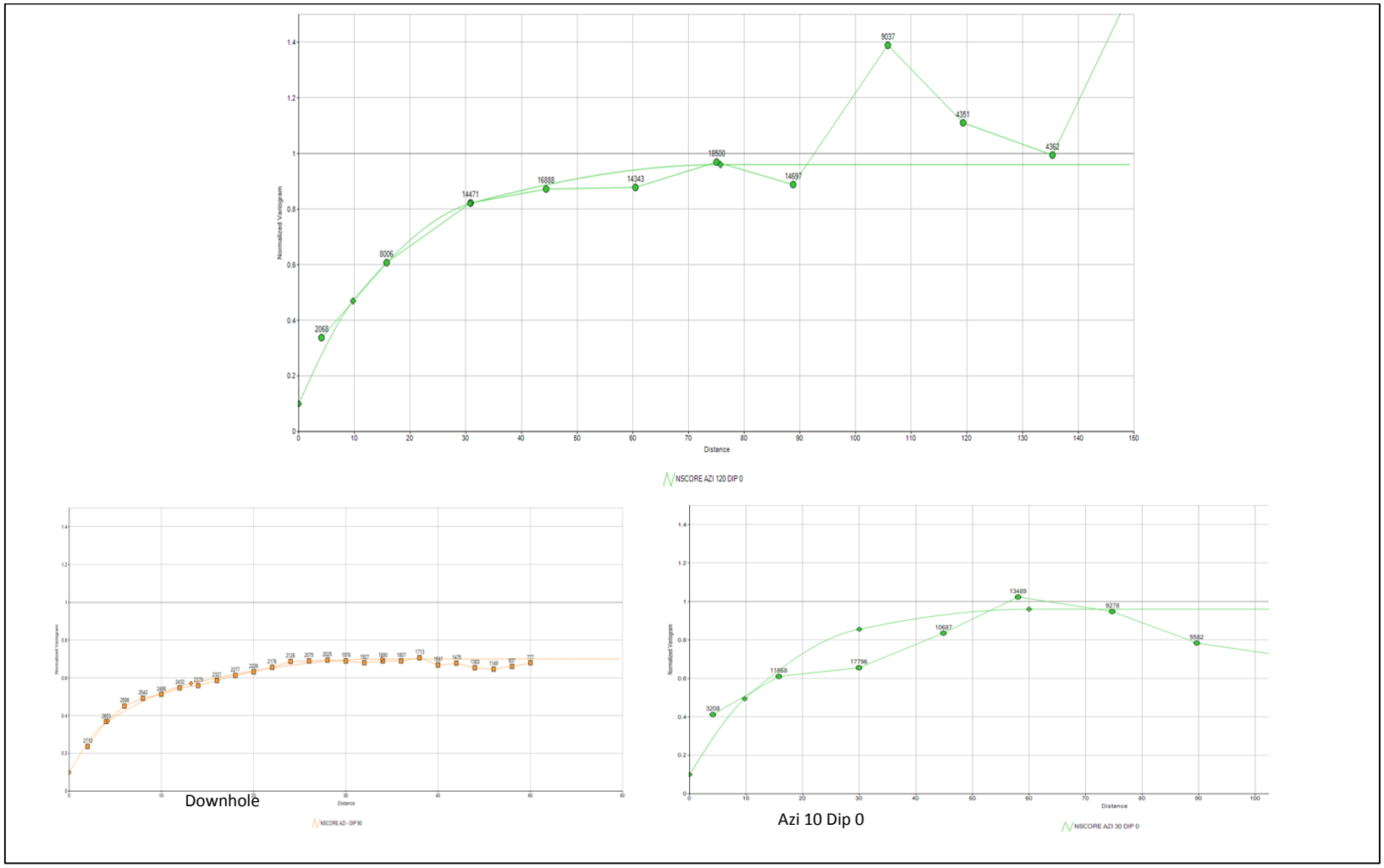

Figure 21: NS variogram for the Western domain showing directional variogram and downhole variogram.

Table 6 : NS semi variogram parameters for the Eastern and Western domain

DOMAIN	EASTERN	WESTERN
DOMAIN CODE	1	2
VREFNUM	1	22
VDESC	10/100	120/30
1st rotation angle	89.85	100
2nd rotation angle	-1.73	0
3rd rotation angle	-9.85	0
Rotation axis1	Z	Z
Rotation axis2	Y	Y
Rotation axis3	X	X
Nugget (C_0)	0.17	0.10
1st Structure (STI)	Spherical	Spherical
ST1 Range X	16.01	10.1
ST1 Range Y	18.63	9.8
ST1 Range Z	7.97	4.2
1st Sill (C_1)	0.30	0.13
2nd Structure (ST2)	Spherical	Spherical
ST2 Range X	35.95	31.1
ST2 Range Y	45.64	29.7
ST2 Range Z	37.06	13.3
2nd Sill (C_2)	0.53	0.43
3rd Structure (ST3)	NA	Spherical
ST3 Range X	0	75.7
ST3 Range Y	0	60.3
ST3 Range Z	0	33.8
3rd Sill (C_3)	0	0.34

5.3.1 Cross validation of NS semi variogram

Cross validation of NS semi variogram using OK was conducted with the aim of checking the performance of the chosen variogram and search parameters. While the results were very close to the actual estimates, the inability to use declustering weights affected to a large extent reproduction of the actual values for both domains. OK because of its smoothing effect resulted in reduced variance and standard deviation. Two graphs showing a plot of the actual versus estimate are shown in Figure 22 for both Eastern and Western domain.

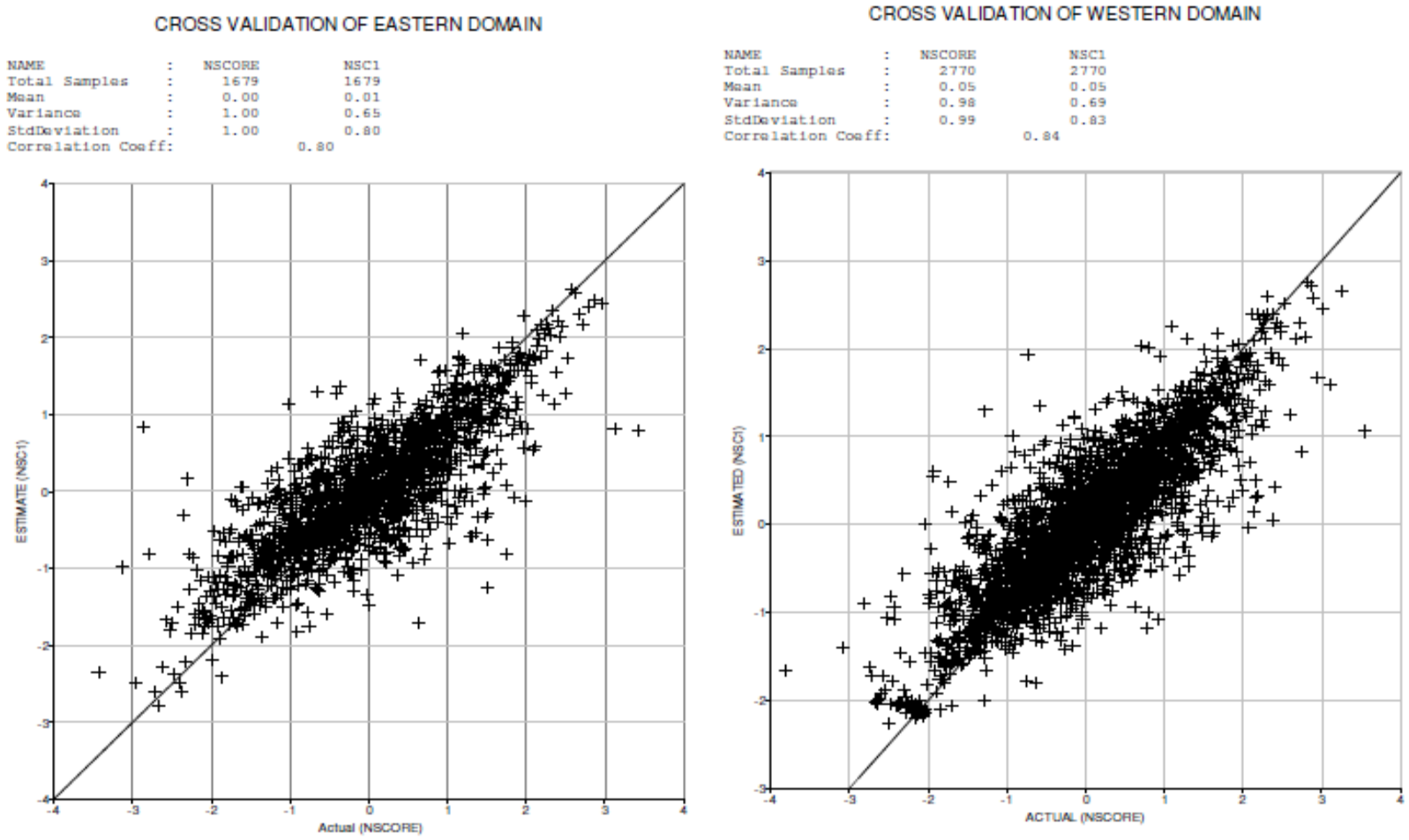

Figure 22: Cross validation results for NS variogram for the Eastern and Western domain.

In the cross validation, the search volume was defined honouring anisotropy shown by NS variogram in Table 6 under 2nd structure (ST2) parameters. The scatter plot in Figure 22 shows a symmetrical cloud around the 45 degree line indicative of unbiased results. Descriptive statistics of scatter plot that showed a similar mean for the actual and estimated value for the Western domain. However the Eastern domain estimated mean at 0.01 was slightly higher than the actual mean of 0. Failure to use declustering weights during validation, may have resulted in some of the noticeable differences.

Regression analysis of the two data sets shows a correlation coefficient of 0.80 and 0.84 for Eastern and Western domains respectively. The correlation coefficient supports a strong relationship between the estimated value and the actual value derived from composite samples. Based on the scatter plot and descriptive statistics, the chosen kriging neighbourhood and NS semi variogram are suitable for use in SGS.

5.4 Summary of the Findings

A summary of the findings from variography analysis are listed below:

- Median indicator variogram (COG 0.49%Ni and 0.53%Ni for Eastern and Western domains respectively) had the longest range in all the domains
- The indicator variograms for the Western Domain had higher nugget effects (27% to 39%) of the sill than for the Eastern Domain where the nugget effects were between 32% and 42% of the total sill.
- Indicator semi variogram confirmed the existence of anisotropy in the mineralisation which are consistent with geological interpretation of a NNW and WNW along and across the strike of nickel mineralisation.
- Cross validation of indicator semi variograms using point validation was able to acceptably reproduce statistics of the input sample values with

correlation coefficient of 0.81 and 0.80 for the Eastern and Western domains respectively.

- NS semi variograms showed two directions namely E and SSW which are consistent with geological interpretation of mineralisation for the two domains mineralisation structures in the NS direction and EW direction. NS variogram had a lower nugget effect due to the elimination of proportional effect.
- Cross validation statistics for NS semi variogram showed a closer reproduction of the input sample values for the Western domain than the Eastern domain. Correlation coefficient was slightly higher for Western domain at 0.84 compared to 0.80 for the Eastern domain. Regression analysis results and descriptive statistics are in support of the chosen kriging neighbourhood.

CHAPTER 6: RESOURCE ESTIMATION

6.1 Introduction

The previous chapter focussed on understanding the spatial distribution of nickel grades using grade indicators and normal scores transformation. This chapter will focus on estimation of the recoverable resource using MIK which is a non parametric method capable of producing risk qualified estimates without relying on a particular distribution (Journel , 1983; Badel, et al., 2011). The chapter will start by a brief discussion of the estimation parameters, search volume and block dimensions. The chapter also gives a summary of the recoverable mineral resources estimated using MIK as well as cross validation results of the block model.

6.2 Indicator Kriging Estimation Parameters.

Indicator kriging is the kriging of indicator transformed values using indicator semi variogram derived in Chapter 5. In this study, nine (9) cut-off grades were defined for each domain by setting the cut-offs at deciles of sample distribution. Analysis of the indicator variograms reviewed that the maximum range of grade continuity were obtained when the cut-off grade was equal to the median of the sample grade distribution namely 0.49%Ni and 0.53%Ni for the Eastern and Western domains respectively. This finding supports Journel (1983)‘s finding that the best experimental indicator variogram correspond to the cut-off grade closer to the median. Despite this observation, a multiple indicator kriging (MIK) approach was chosen instead of the median indicator (MeIK) approach. This was mainly driven by the fact that different directions of grade continuity was observed during variography with two principal directions WNW and NNW prevailing.

6.2.1 Multiple Indicator Kriging Search Volume Parameters

In order to avoid order relations problems dicussed in detail in Chapter 2, an isotropic search volume with a radius of 40m was used. The rotation angles suggested in the analysis were not considered in this case given the observed changes in anisotropy directions for the various cut-off grades. A minimum of 12 samples were required for grade estimation throughout the three dynamic search volumes. In addition, the number of samples from one borehole was restricted to four (4). A summary of search parameters used in the current estimation is shown in Table 7. Dynamic search volume was also used by multiplying the original search volume by a factor of 1.5 and 3 reaspectively.

The use of the dynamic search volume approach assists in the classifiction of the mineral resource based on the search volume. For instance, block grades estimated using the first search volume defined by 40m radius can be classified as Measured Resources while those in the second and third search volume can be classified as Indicated and Inferred Resources respectively. Although the purpose of the current study is not classification of the resources, MIK estimation results were also reported honoring dynamic search volumes.

Table 7: Search volume parameters for MIK for Eastern and Western domains.

Domain	Eastern	Western	Comments
No COG	9	9	9 COG for each domain stated separately in the search volume parameter file
Search method	Ellipsoid	Ellipsoid	Search volume method
SDIST1	40	40	
SDIST2	40	40	
SDIST3	40	40	
1st rotation angle	0	0	No rotation was done
2nd rotation angle	0	0	No rotation
3rd rotation angle	0	0	No rotation
1st rotation axis	3	3	Rotation about the Z axis
2nd rotation axis	2	2	Rotation about the Y axis
3rd rotation axis	1	1	Rotation about the Z axis
MINNUM1	12	12	Minimum number of samples in SVOL1
MAXNUM1	30	30	Minimum number of samples in SVOL1
SVOLFAC2	1.5	1.5	2nd Search volume multiplying factor
MINNUM2	12	12	
MAXNUM2	30	30	
SVOLFAC3	3	3	3rd search volume multiplying factor
MINNUM3	12	12	
MAXNUM3	30	30	
MAXKEY	4	4	Maximum number of samples per borehole.

NB: COG category represents the number of cut off grades listed in Table 3.

6.2.2 Block Size Dimensions

One of the critical factors in resource estimation is determination of block size. Whilst Vann, et al. (2003) recommends that a Quantified Kriging Neighbourhood Analysis (QKNA) be carried out as a key step in determining block dimensions as well as the search volume. In this research, block dimensions of 25m x 25m x 10m in the XYZ plane were choosen by taking cognisance of the mining method proposed and drill hole spacing. The proposed mining method for the deposit is open pit with 10m benches. The choosen block sizes were similar to the ones used in the previous estimates and are representative of the selective mining unit (SMU).

The final block model contained proportion of the subcell above each cut-off grade (PRAB1…PRABn) and the corresponding grade above each cut-off grade (GRAB1…GRABn). GRAB is calculated from the PRAB and the average grade between each pair of cut-off. One of the major drawbacks of MIK highlighted by Journel (1988) and Vann, et al.(2000) is the order relation problem. Order relations problems were resolved by using an algorithm derived from GSLIB (Deutsch and Journel, 1998) which considers an average of an upward and downward correction.

6.2.3 Mineral Resource Estimates

MIK was carried out using variogram parameters shown in Tables 4 and 5, and search volume parameters in Table 7. An image of the block model produced through MIK is shown in Figure 23. A summary of Mineral Resource estimates without a cut-off grade applied to the block model results is shown in Table 8. Mineral Resource estimates based on 0.40%Ni COG are shown in Table 9.

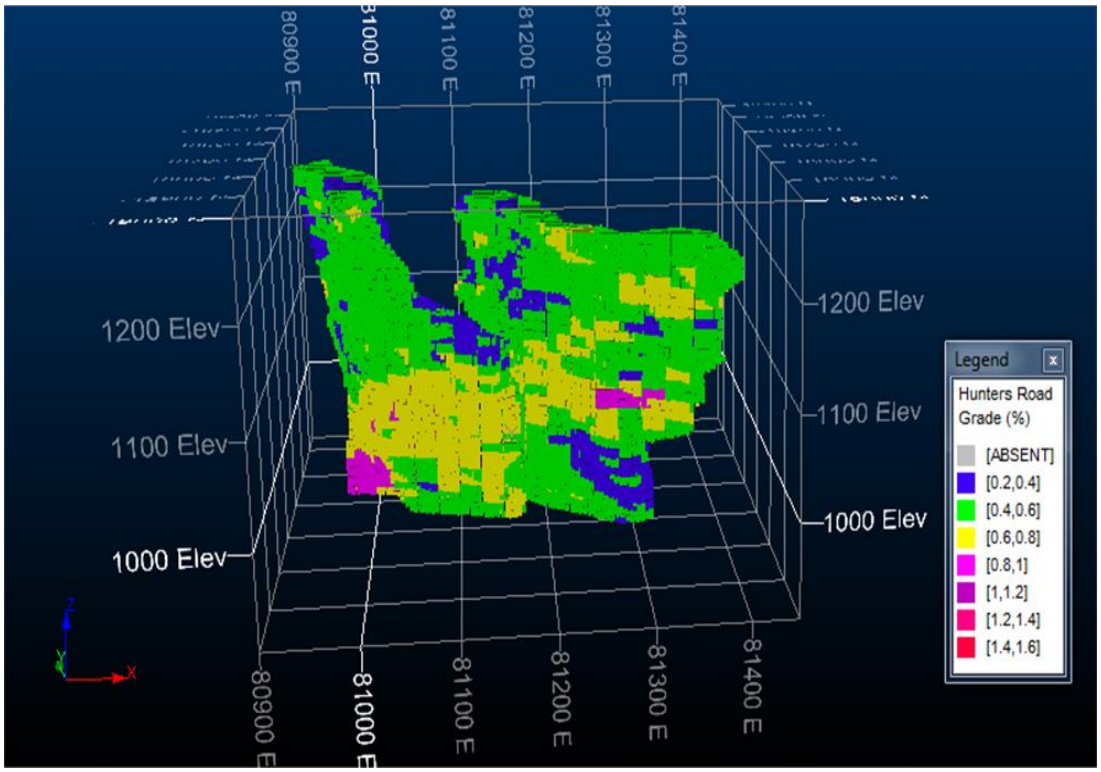

Figure 23: Block model for the Eastern and Western domain showing grades determining through MIK.

The block model image shows most of the grades being between 0.40%Ni and 0.60%Ni. There is quite a considerable number of portions with grades above 0.60%Ni. The blue portions indicate zones that have grades lower than the 0.40%Ni cut-off grade.

Table 8: Mineral Resource MIK Estimates for Eastern and Western domains without COG.

Domain	Volume (m^3)	Tonnes (Mt)	Relative density (t/m^3)	Grade (%Ni)	Metal Content (t)
Eastern	5,269,562.84	13.7	2.60	0.52	71,861.50
Western	8,752,192.05	22.76	2.60	0.55	126,074.32
Total	14,021,754.89	36.46	2.60	0.54	197,935.82

Table 9 : Mineral Resource MIK Estimates for the Eastern and Western domain based on a 0.40%Ni COG.

Domain	Volume (m^3)	Tonnes (Mt)	Relative density (t/m^3)	Grade (%Ni)	Metal content (t)
Eastern	4,678,385.56	12.16	2.60	0.54	66,286.36
Western	7,745,648.33	20.14	2.60	0.58	116,847.83
Total	12,424,033.89	32.30	2.60	0.57	183,134.20

In addition, the estimation method used the dynamic search radius by multiplying the initial search radius by a factor of 1.5 and 3 to define SVOL2 and SVOL3 respectively. The Mineral Resource split based on the dynamic search volume parameter (SVOL1, SVOL2 and SVOL3) is summarised in Tables 10 and 11 for the Eastern and Western domains respectively. The dynamic search volume factors used were defined based on the analysis of the nugget effect and the range of indicator semi variogram. The chosen factors were supported by cross validation results in Chapter 6. In order to show the variation in grade and tonnage as the COG changes, grade tonnage curves for the Eastern and Western domains are shown in Figures 24 and 25 respectively.

Table 10: Mineral Resource MIK Estimates for the Eastern domain per search volume (SVOL) based on 0.40% Ni COG.

SVOL	Volume (m^3)	Tonnes (Mt)	Relative Density (t/m^3)	Grade (%Ni)	Metal content (t)
1	2,061,379.01	5.36	2.60	0.55	29,489.73
2	1,970,335.10	5.12	2.60	0.54	27,733.23
3	646,671.45	1.68	2.60	0.54	9,063.41
Total	4,678,385.56	12.16	2.60	0.54	66,286.37

SVOL 1= Measured, SVOL 2 = Indicated, SVOL 3= Inferred

Table 11: Mineral Resource MIK Estimates for the Western domain per search volume (SVOL) based on 0.40% Ni COG.

SVOL	Volume (m^3)	Tonnes (Mt)	Relative density (t/m^3)	Grade (%Ni)	Metal content (t)
1	4,282,340.86	11.13	2.60	0.59	65,758.47
2	3,301,564.92	8.58	2.60	0.57	48,799.57
3	161,742.55	0.42	2.60	0.54	2,289.79
Total	7,745,648.33	20.14	2.60	0.58	116,847.83

SVOL 1= Measured, SVOL 2 = Indicated, SVOL 3= Inferred

In order to present the variation in grade, tonnage and contained metal per cut off, a summary of resources per cut-off grade for the Eastern and Western domains are shown in Table12 and 13 respectively.

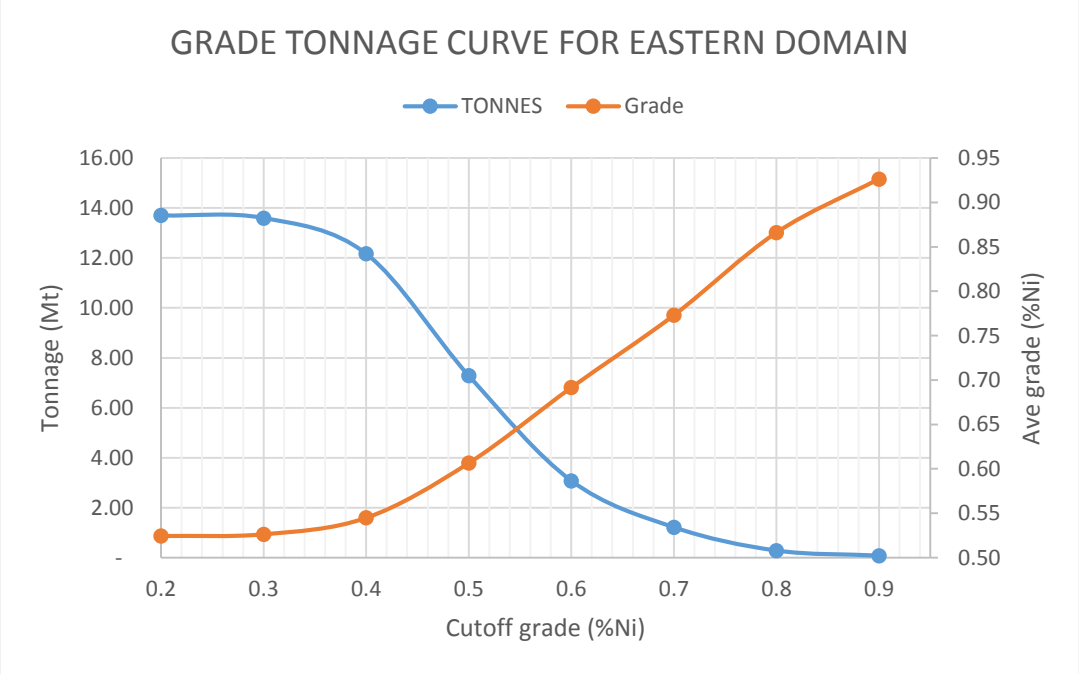

Figure 24: MIK Grade Tonnage curve for the Eastern Domain - Block size 25m x 25m x 10m)

Table 12: MIK Grade, Tonnage and Metal content for the Eastern domain at various cut-off grades (Block size 25m x 25m x 10m).

Cut-off (%Ni)	Average Grade (%Ni)	Volume (m^3)	Tonnes (Mt)	Relative Density (t/m^3)	Metal Content(t)
0.20	0.52	5,269,562.84	13.70	2.60	71,861.44
0.30	0.53	5,229,739.35	13.60	2.60	71,576.58
0.40	0.54	4,678,385.56	12.16	2.60	66,286.40
0.50	0.61	2,801,149.42	7.28	2.60	44,176.28
0.60	0.69	1,183,731.79	3.08	2.60	21,284.90
0.70	0.77	467,306.24	1.21	2.60	9,391.56
0.80	0.87	108,485.22	0.28	2.60	2,442.63
0.90	0.93	30,351.14	78,91	2.60	731.04

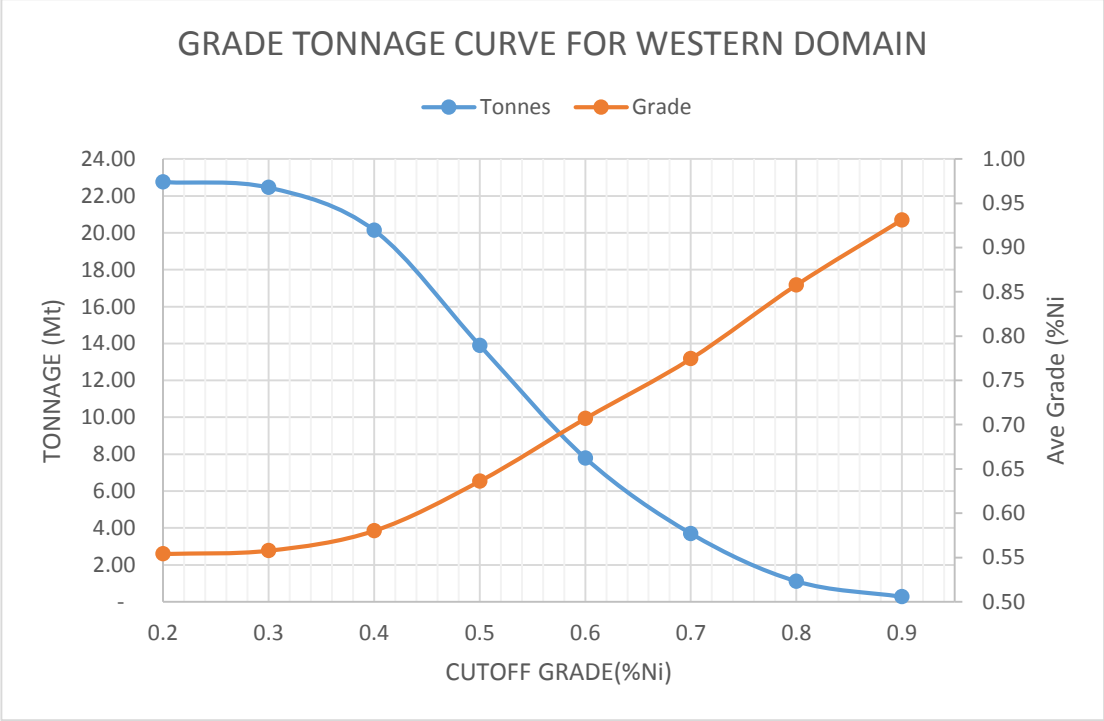

Figure 25: MIK Grade Tonnage curve for the Western Domain - Block size 25m x 25m x 10m)

Table 13 : Grade, Tonnage and Metal content for the Western domain at various cut-off grade.

Cut-off (%Ni)	Average Grade (%Ni)	Volume (m^3)	Tonnes (Mt)	Relative Density (t/m^3)	Metal Content(t)
0.2	0.55	8,752,192.05	22.76	2.60	126,074.31
0.3	0.56	8,637,140.01	22.46	2.60	125,256.88
0.4	0.58	7,745,648.33	20.14	2.60	116,847.88
0.5	0.64	5,346,224.34	13.90	2.60	88,438.94
0.6	0.71	2,996,983.91	7.79	2.60	55,087.52
0.7	0.77	1,422,711.79	3.70	2.60	28,646.89
0.8	0.86	427,728.63	1.11	2.60	9,538.14
0.9	0.93	103,516.11	0.27	2.60	2,506.29

6.2.4 Cross Validation of the Block Model

Validation of block model results is a key processes to be conducted in order to check whether the resource model reflects the input drilling and sampling information. The current study used two validation methods for the block model namely:

- Visual assessment of plots of sections showing drill hole sample information and block model grades.
- Swath plot in the three principal directions(X, Y and Z) comparing grade trends of samples and block grades.

The analysis of sectional plots of block grades and sample values showed similarity between the grade trends shown in the block model and those of drill whole samples. According to Glacken and Trueman (2014), grade patterns in the sample data should be similar to those exhibited by the block model. However, the grade magnitudes differs due to the support effect. One of the sectional plots showing block grades and drill hole sample grades for the Western and Eastern domains is shown in Figure 26.

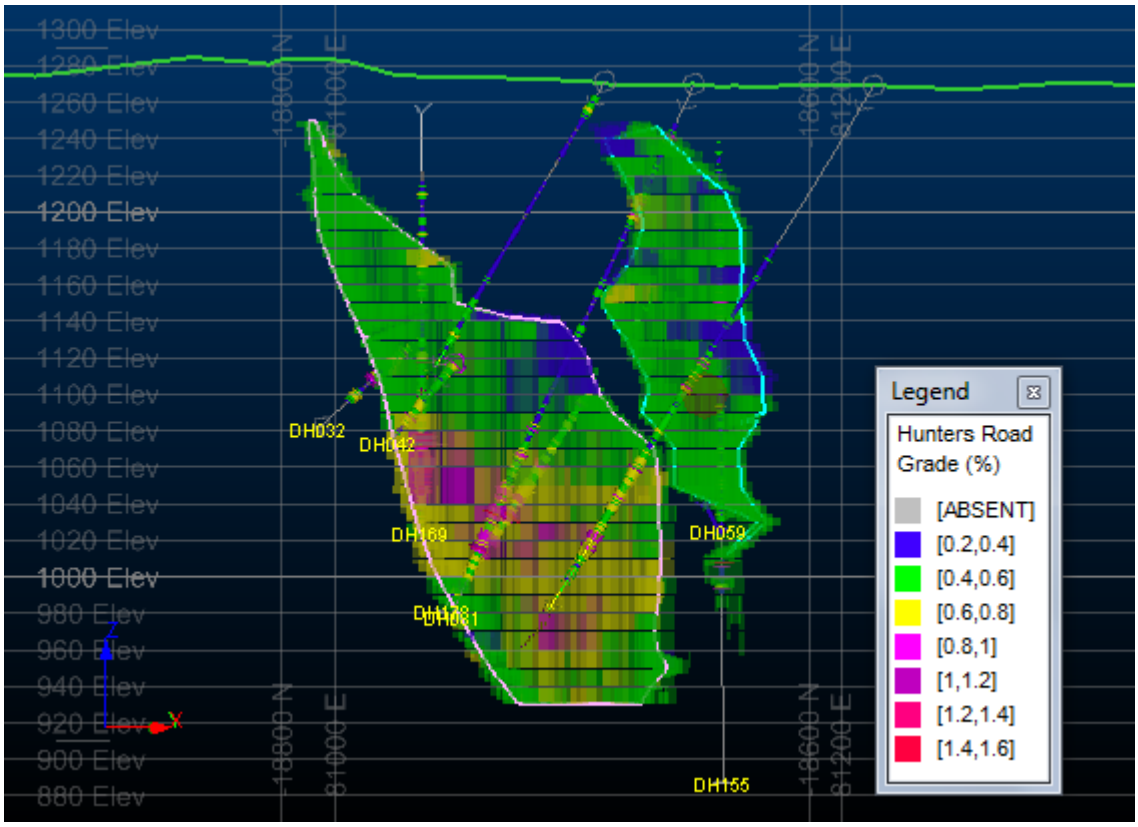

Figure 26: A sectional plot of block grades and drill hole sample grades for the Western and Eastern domain.

The sectional plot in Figure 26 above shows similarity between sample grades and estimated block grades. Higher grade zones in borehole samples corresponds to higher grade zones in the block model. The same relationship applies to the low and medium grade zones. They were no inconsistencies or any evident errors observed through visual assessment of the block model.

In addition to sectional plots of block grades and sample values, swath plots in three principal directions were plotted separately for the two domains. The Swath plots for the Eastern and Western domains are shown in Figures 27 and 28 respectively.

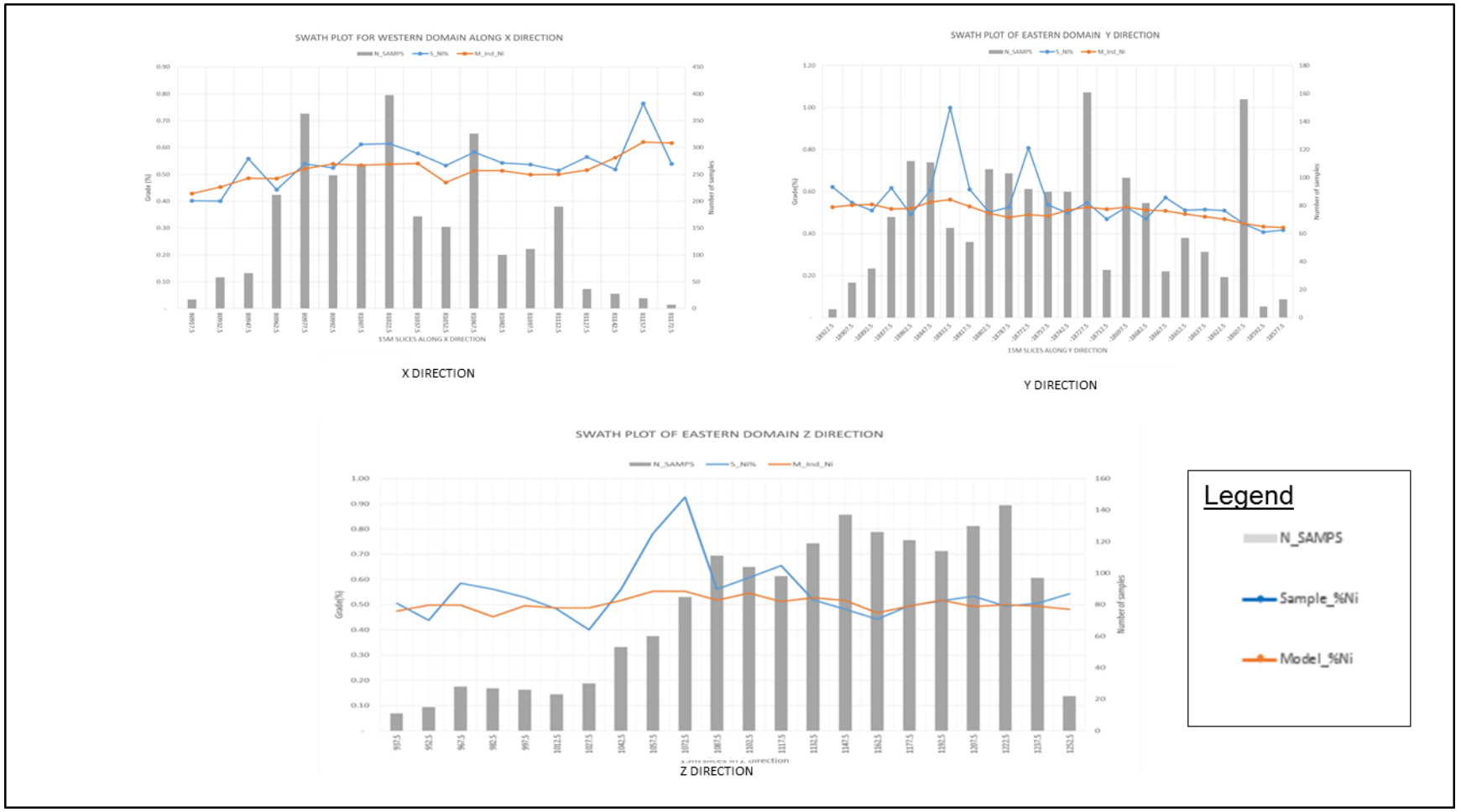

Figure 27: SWATH plot of sample values versus estimated values along the three principal direction for the Eastern domain.



Figure 28: SWATH plot of sample values versus estimated values along the three principal direction for the Western domain.

The grade trends in the Eastern domain (Figure 27) shows a similar trend between the block grades and sample composite grades in all the three principal directions . However, the variability in drill hole sample values is higher than MIK produced block grades. Similarly, the Western domain grade trends (Figure 28) shows a similar trend between the MIK estimated grades and composite sample grades with the latter being highly variable. The difference between the two values may be attributed to a change from point support to block support

The Swath plots show similar trends between the estimated grades and the sample composite grades used in the estimation. Visual assessment of block model showed that there were no inconsistencies observed such that the estimated grade in the block model can be explained by the composite samples surrounding the block.

6.3 Comparison of MIK Estimates and Historical OK Estimates.

One of the key advantages of MIK is the production of risk quantified estimates through the use of ccdf. Results of MIK based estimation indicated that after applying a 0.40%Ni cut-off grade on the blocks, the combined Mineral Resources for the Western orebody is 32.30Mt at a grade of 0.57%Ni resulting in 183.13kt of contained nickel. Resource estimates reported as of May 2006 based on a 0.40%Ni cut-off grade indicated a 36.44Mt at a grade of 0.55%Ni resulting in 199.80kt of contained nickel. The reported resource tonnage is similar to the one obtained when either no cut-off grade is applied or when a 0.20%Ni cut-off grade is applied. The estimated Mineral Resource tonnage without applying cut-off grade was 36.46Mt at a grade of 0.54%Ni resulting in 197.94kt of contained nickel metal. While the resource tonnages are similar, the estimated grade as of May 2006 is 2% lower than the MIK estimate without COG.

A summary of historical estimates from 1992 to 2006 is shown in Table 14. In order to compare the estimated resource tonnage, an in-situ density of 2.60t/m^3 was applied across all resource estimates which had a historical in-situ density of 2.85t/m^3.

Table 14: A summary of Hunters Road Western orebody nickel resource estimates

Date	Estimated by	COG (%Ni)	SG (t/m^3)	Tonnage (Mt)	Grade (%Ni)	Tonnes (Mt) corrected using 2.60 (t/m^3) SG
Jan-17	Author	0.4	2.60	32.3	0.57	32.30
May-06	BNC	0.4	2.60	36.44	0.55	36.44
Jan-01	AACS	0.4	2.85	35.78	0.59	32.64
Nov-01	SRK	0.4	2.85	41.27	0.55	37.65
Apr-96	MinRED	0.4	2.85	34.84	0.56	31.79
Aug-92	MinRED	0.28	2.85	53.61	0.49	48.91

NB: SG represents specific gravity

Analysis of historical estimates shown raised the issue of application of cut-off grade. In most of the estimates, a cut-off grade of 0.40%Ni was applied to drill hole intersection in defining mineralised envelope. However, the author was able to verify that the April 1996 resource estimate with a resource tonnage of 31.79Mt at a grade of 0.56%Ni (2% below MIK estimate) was based on application of 0.40%Ni COG on block grades. The same applies to SRK resource estimate of 37.65Mt at a grade of 0.55%Ni. At a grade of 0.55%Ni, SRK grade estimate is 4% lower than MIK grade estimate.

The AACS (2001) grade estimate of 0.59%Ni is 4% higher than the MIK estimate of 0.57%Ni. However, they highlighted that there is 95% confidence that the estimated block grade will be within 21% of the true value. The

resource tonnage after adjusting the in-situ density is 1% higher than the reported tonnage using MIK. In order to get a better understanding of the differences in grades between the estimates, the following section focused on the analysis of the reported grades per domain.

6.3.1 Analysis of Mineral Resources per Domain

Analysis of historical estimates per domain or zone focussed on the May 2006 estimates and January 2001 AACS estimates. A summary of Mineral Resources for the two domains after applying a cut-off grade of 0.40%Ni on the block estimates appears in Table 9. In addition, a breakdown of the Mineral Resources below and above 0.40%Ni cut-off grade for the Eastern and Western domains based on MIK are shown in Tables 15 and 16 respectively.

Table 15: A summary of Mineral Resources Estimates above and below 0.40% cut-off grade for the Eastern Domain

Grade category	Volume (m^3)	Tonnes (Mt)	Relative Density (t/m^3)	Grade (%Ni)
Below 0.40%	591,177.28	1.54	2.60	0.36
Above 0.40%	4,678,385.56	12.16	2.60	0.54
Total	5,269,562.84	13.70	2.60	0.52

Table 16: A summary of Mineral Resources Estimates above and below 0.40% cut-off grade for the Western Domain

Grade category	Volume (m^3)	Tonnes (Mt)	Relative density (t/m^3)	Grade (%Ni)
Below 0.40%	1,006,543.72	2.62	2.60	0.35
Above 0.40%	7,745,648.33	20.14	2.60	0.58
Total	8,752,192.05	22.76	2.60	0.55

BNC‘s May 2006 mineral resource estimate shown in table 17 for the Western orebody shows a very low resource tonnage for the Eastern domain (7.09Mt at 0.50%Ni) compared to the MIK estimates of 12.16Mt at a grade of 0.54%Ni (see Table 15). However, the BNC estimate of grade and resource tonnage is similar to AACS January 2001 estimate of 7.75Mt at a grade of 0.51%Ni. There is a 6% increase in grade and a 72% increase in resource tonnage compared to the May 2006 resource estimates.

Table 17: Hunters Road West orebody resource summary as at May 2006(BNC estimate)

Orebody	Tonnage (Mt)	Grade (%Ni)	Metal Content(t)
West Zone	29.35	0.56	164,363
East Zone	7.09	0.50	35,433
Total	36.44	0.55	199,796

The difference in resource tonnages for the two domains between the current MIK estimate and AACS estimate can be attributed to the use of a hard boundary based on a cut-off grade of 0.40%Ni. Under this scenario, the two domains or zones did not merge into a single zone below 1080m above sea level. In contrast, AACS’s 2001 resource model was based on the two major domains merging to form a richer zone below 1080m ASL. The merged zone is what is referred to in Table 18 as the Bottom Zone in AACS resource estimates.

Table 18: A summary of AACS January 2001 resource estimates for the two domains at 0.40% Ni cut-off grade.

SG of 2.85t/m^3					SG of 2.60t/m^3		
Interval m.A.S.L	Source	Tonnage (Mt)	Grade (%Ni)	Metal Content (t)	Tonnage (Mt)	Grade (%Ni)	Metal Content (t)
1250 to 1080	East Zone	8.50	0.55	46,569	7.75	0.55	42,484
1250 to 1080	West Zone	8.98	0.51	45,369	8.20	0.51	41,389
1080 to 930	Bottom Zone	18.29	0.65	118,539	16.69	0.65	108,141
1250 to 930	Total	35.78	0.59	210,357	32.64	0.59	191,905

Current resource estimates based on MIK used the same orebody wireframes used by BNC in May 2006. Based on these wireframes, the two orebodies do not merge below 1080m ASL. However despite acknowledging the use of hard boundary, BNC estimates may have merged the Eastern domain into Western domain below 1080m ASL resulting in a higher resource tonnage for the latter. BNC separated the two domains but the actual estimation macro could have used a soft boundary similar to AACS but then wrongly apportioned the resource.

Given the difference in the approaches and procedural flaws associated with the May 2006 estimates, it is very difficut to compare the resource estimates per domain. In order to compare the MIK estimate to the AACS estimates which has shown some consistencies in terms of methodolody, a split of the MIK estimate based on the stated elevations is shown in Table 19 and 20 for the Eastern and Western domains respectively. In addition, a summary of MIK estimates per 10m bench is shown on Table A1 and A2 in Appendix 4.

Table 19: MIK Mineral Resource Estimates for the Eastern domain split by elevation interval.

Interval m.A.S.L	Grade Range	Volume (m^3)	Tonnes (Mt)	Relative density (t/m^3)	Grade (%Ni)
1250-1080	Above 0.40%	333,484.97	7.65	2.60	0.53
	Below 0.40%	2,943,295.51	0.87	2.60	0.37
	Total	3,276,780.48	8.52	2.60	0.52
1080-930	Above 0.40%	1,735,090.05	4.51	2.60	0.56
	Below 0.40%	257,692.31	0.67	2.60	0.35
	Total	1,992,782.36	5,18	2.60	0.54
	Grand Total	5,269,562.84	13.70	2.60	0.52

After splitting the resource tonnage by elevation, the Eastern domain resource at 7.65Mt is comparable to AACS and BNC's 2001 and 2006 estimate respectively. However, the MIK grade at 0.53%Ni is 6% higher than BNC estimate and 4% higher than AACS 2001 estimate.

MIK estimates of the Western domain split by elevation shows 8.16Mt at an avarage grade of 0.51%Ni which is similar to AACS 2001 estimate of 8.20Mt at a grade of 0.51%Ni. Resource estimates by AACS in January 2001 showed 16.69Mt resource tonnage at a grade of 0.65%Ni for the Bottom zone, which is a zone created by merging the Eastern and Western domains below 1080m ASL. The current estimates resulted in 16.49Mt at an average grade of 0.61%Ni for areas below 1080m ASL for the two domains. While there is no significant difference in the resource tonnage, the estimated grade is 7% lower than AACS estimated grade of 0.65%Ni. BNC resource estimate is not comparable by elevation and it has a higher tonnage of 29.35Mt, at a comparatively lower grade of 0.56%Ni for the Western domain.

Table 20: MIK Mineral Resource Estimates for the Western domain split by elevation interval and 0.40% COG.

Interval m.A.S.L	Grade Range	Volume (m^3)	Tonnes (Mt)	Relative Density (t/m^3)	Grade (%Ni)
1250-1080	Above 0.40%	3,138,089.46	8.16	2.60	0.51
	Below 0.40%	750,985.08	1.95	2.60	0.35
	Total	3,889,074.54	10.11	2.60	0.48
1080-930	Above 0.40%	4,607,558.87	11.98	2.60	0.63
	Below 0.40%	255,558.63	0.66	2.60	0.35
	Total	4,863,117.51	12.64	2.60	0.61
ALL	Grand Total	8,752,192.05	22.76	2.6	0.55

In general, the Western domain has higher grades than the Eastern domain. In summary, there are inconsistencies observed in BNC estimates dated May 2006. This inconsistencies emanate from the methodology used in the estimation which resulted in a higher resource tonnage for the Western domain and significantly lower tonnage for the Eastern domain. The resource grades based on a 0.40%Ni cut-off grade are significanlty suppressed for BNC estimate. There is a close similarity between AACS's January 2001 and current MIK based estimate after splitting the resources by elevation ranges.

Overally, MIK estimated grade of 0.57%Ni is 4% higher than BNC estimate (0.55%Ni), 2% higher than MinRED 's April 1996 grade estimate of 0.56%Ni and 4% lower than AACS 's January 2001 estimate of 0.59%Ni. The resource tonnage for these three estimates are very similar, ranging between 31.79Mt and 32.64Mt. Based on the analysis, there is a higher probability that BNC estimates reported resources falling within the mineralised envelope defined by 0.40%Ni borehole intersections rather than applying the same cut off grade on the block estimates. Incorporation of material below cut off grade of 0.40%Ni

may have resulted in OK estimated grade being 4% lower than MIK estimated grade for the Western orebody as a whole.

6.4 Summary of the Findings

The Mineral Resource E-type estimates for the Western orebody using MIK as the grade interpolation method was 32.3Mt at an average grade of 0.57%Ni with 183kt of contained metal at 0.40%Ni cut-off grade. An estimated 36.5Mt at a grade of 0.54%Ni equivalent to 198kt of contained nickel was obtained through MIK without applying a 0.40% Ni cut-off grade on the block estimates. At 183kt, the contained metal estimated through MIK was 8% below BNC 2006 estimate, 5% below AACS 2001 estimate and 3% higher than MinRED 1996 estimate.

The Eastern domain has an estimated recoverable resources of 12.2Mt at a grade of 0.54%Ni resulting in 66kt of contained nickel based on a 0.40%Ni cut-off grade. The Western domain mineral resources were estimated to be 20.14Mt at an average grade of 0.58%Ni resulting in 116.8kt of contained nickel at 0.40%Ni cut-off grade. The Western domain has higher nickel grades and resource tonnage than the Eastern domain. Cross validation results of the block model showed similar trends between the block grades and sample grades with the latter showing higher variability.

A comparison between historical estimates based on OK and the current estimates based on MIK showed close similarity between to AACS's January 2001 estimates after splitting the resources by elevation ranges. Overall ,MIK estimated grade of 0.57%Ni is 4% higher than BNC estimate (0.55%Ni), 2% higher than MinRED 's April 1996 grade estimate of 0.56%Ni and 4% lower than AACS 's January 2001 estimate of 0.59%Ni. The resource tonnage for these three estimates are highly comparable ranging between 31.79Mt and

32.64Mt. The MIK estimate of contained metal at 183kt was lower than both BNC 2006 estimate (199.80kt) and AACS 2001 estimate(192.56kt), but 3% higher than MinRED 1996 estimate(178kt).It is important to note that the reported historical tonnages and metal content were after correcting the relative density to 2.60t/m^3 following the reduction in density.The May 2006 estimates by BNC which are the most recent estimates have inconsistencies which makes them unrealiable. The next chapter focuses on conditional simulation.

CHAPTER 7: CONDITIONAL SIMULATION

7.1 Introduction

The previous chapter focussed on the estimation of recoverable resources through Multiple Indicator Kriging (MIK). The main purpose of this chapter is the assessment of spatial uncertainty associated with the nickel grades of the Western orebody of Hunters Road nickel prospect. The previous chapter, through the use of MIK, allowed for the estimation of local uncertainty resulting in the production of risk quantified estimates of both grade and tonnage. Linear geostatistical estimation techniques have been lauded for production of unbiased estimates of the average, however it suffers greatly from the smoothing effect (Vann, et al., 2000; Yamamoto, 2005).

Unlike estimation, simulation allows for the generation of several possible realisations of a regionalised variable which captures original variability observed in the data. In assessment of spatial uncertainty, conditional simulation honours local data and spatial variability (Rossi and Deutsch, 2014). The current study used Sequential Gaussian Simulation (SGS) in the assessment of uncertainty associated with nickel grades at Hunters Road nickel project in Zimbabwe.

7.2 SGS Steps in Datamine Studio RM

The following steps were followed in SGS using Datamine Studio RM module:

1. Data declustering which was covered in detail in Chapter 4.
2. Normal score (NS) transformation of sample grades for the two domains (Chapter 4).
3. Construction of NS semi variograms and fitting of the models. This was covered in detail under variography in Chapter 5.

4. Running of SGS using SGSIM process in Datamine Studio RM. The SGSIM process is able to do both NS transformation and back transformation in one step. However, the NS transformations were done separately using NSCORE process. Separation of the stages allowed detailed EDA (Chapter 4).to be done prior to simulation.
5. The SGSIM process input parameters allows the use of a prototype model file to define a regular grid of simulated points. The parameter was used since there were two specific domains to be simulated. The prototype was used to define the domains using a 25m x 25m x 10m block sizes in the XYZ direction. Simulation points were set at 5 x 5 x 5 due to the limitation in terms of size and speed of processing. A total of 100 realisations were used per each domain.
6. The output file from SGSIM contained both simulated points file and block model file with 100 simulations or realisations.
7. The first stage of running SGSIM did not include back transformation to original values. This was however done in order to check if the output in Gaussian space honoured the histogram and variogram used in the simulation.
8. After the validation process, SGSIM was run continuously with back transformation.
9. The point file containing simulated points created in SGSIM was input into the CSMODEL process which created block models that include statistical parameters and grade tonnage resources tables from simulated point data. There are two key output files from CSMODEL, namely SIMMOD (containing simulated grade values for each cell and each realisation) and STATMOD (which is the block model containing statistical parameters).
10. The STAMOD file was loaded into CELLCONF process which calculated the 90% confidence level for the parent cells in the block model, based on the results created using SGSIM. SIMMOD created by

CSMODEL process was loaded into MODCONF in order to calculate confidence levels for the block model grades at various cut-off grades.

The last two process provided a good measure of confidence at individual cell level as well as at block model level. Two types of estimates were given by MODCONF namely E-Type 1 (E1) and E-Type 2 (E2) estimates. E1 refers to the average of all simulations within a cell while E2 refers to the average of all simulations in the entire block model. For a cut-off grade of 0%Ni, E1 and E2 are expected to be the same while for cut-off grades above 0%Ni, the E2 will be greater than E1 (Datamine Studio RM,nd).

7.2.1 SGSIM Results

7.2.1.1 SGSIM Validation of Input Histogram (NS)

The results section of SGSIM starts by looking at conditional simulation validation results. Due to space and speed constraints, 25 simulations out of 100 were selected for both histogram and variogram validation. The first stage involved comparison of NS histogram of samples with those ones generated by 25 simulations. The results of Eastern and Western domains are shown in Figures 29 and 30. In both cases, the results of SGS reproduced the input sample distributions. SIMNUM 0 represents original sample distribution in normal scores space while SIMNUM 1 to 25 represents distribution obtained from each simulation. A summary of statistical parameters of the 25 chosen realisations and input sample used in the validation process are shown in Table 14 in for Normal Scores.

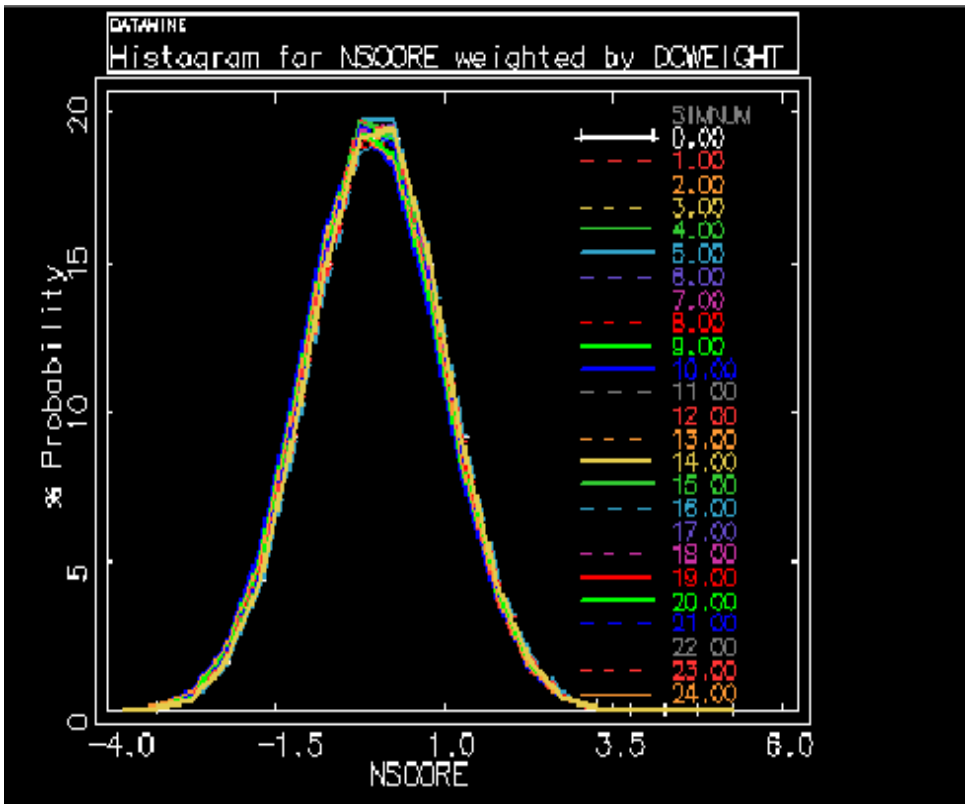

Figure 29: NS histogram showing a comparison of sample and 25 simulation realisation distribution for the Eastern domain.

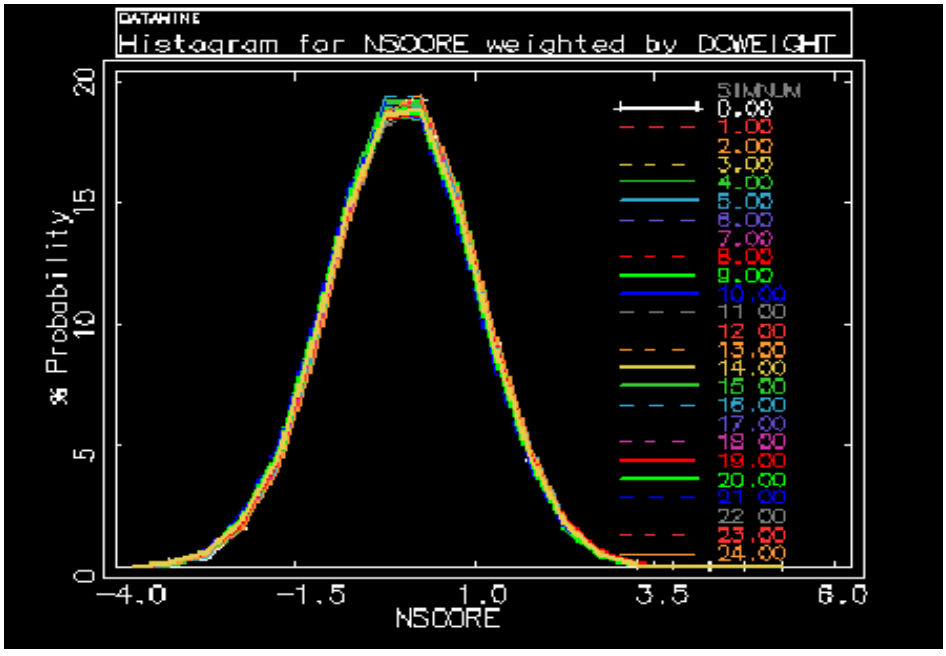

Figure 30 : NS histogram showing a comparison of sample and 25 simulation realisations distribution for the Western domain.

Table 21: Statistical summary of 25 simulations and the samples used in the simulation in NS space

DOMAIN	Eastern		Western	
DATA	**Samples**	**SIM_all**	**Samples**	**SIM_all**
Number of samples	1,678.	4,584,375	2,772	6,637,500
Mean	0.00	-0.02	0.00	0.01
Variance	0.99	1.00	1.00	1.01
Standard Deviation	0.99	1.00	1.00	1.00
Skewness	0.00	0.00	0.00	0.00

The results in Table 21 show good reproduction of sample distribution in NS. There are however slight deviations in terms of the mean and variance but these deviations are minor and acceptable.

7.2.2 SGSIM Validation of Input Variogram (NS)

The second stage involved generation of semi variogram from the 25 simulated points. In each case, two sets of semi variograms were generated, namely the downhole variogram and the directional variogram. The two sets of variograms for the Eastern domain are shown in Figures 31 and 32 which indicate the downhole and directional variogram. In both cases, the input semi variogram had a 0.17 nugget effect, 37m ranges in downhole direction and 45m range in the direction of maximum continuity.

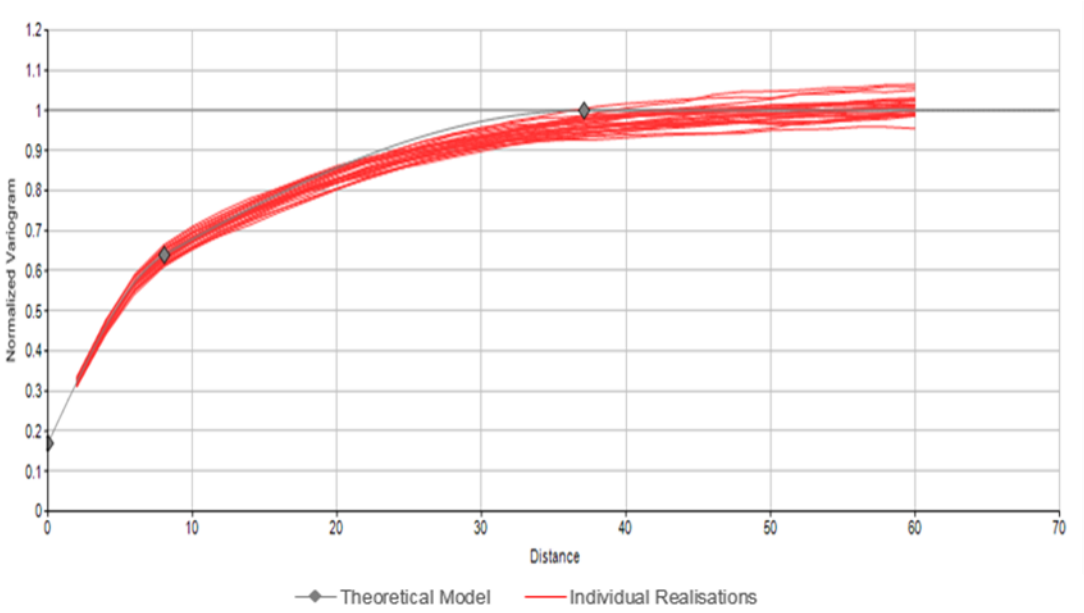

Figure 31: Eastern Domain downhole and directional semi variogram generated from 25 realisations (downhole variogram).

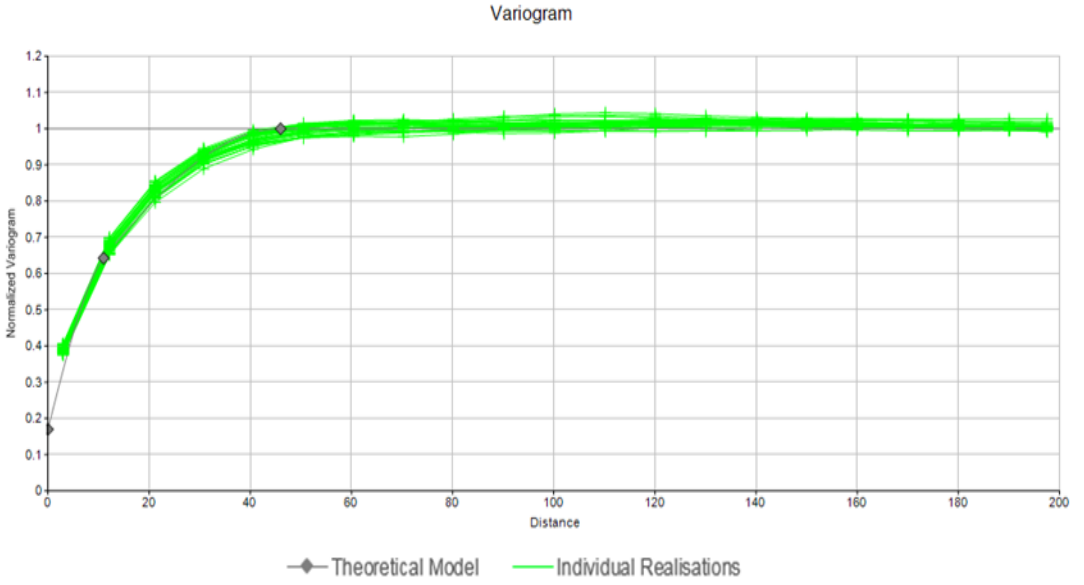

Figure 32: Directional variogram for the 25 simulations of Eastern Domain

The Western Domain downhole variogram fitted model (see Figure 33) does not reach the sill, but it replicates the input semi variogram shown in Figure 21. The variability is higher due to the adjustments done on the input file to get a

sill of 1. The three spherical structures observed in the input variogram can also be observed on the directional variogram with a maximum range of 76m. A nugget effect of 0.10 obtained from the input downhole variogram is observed in the downhole variogram obtained from simulations. The directional semi variogram in Figure 34 deviates slightly from the input semi variogram at shorter ranges with simulations being more variable. However, the input semi variogram is reproduced quite well after 20m.

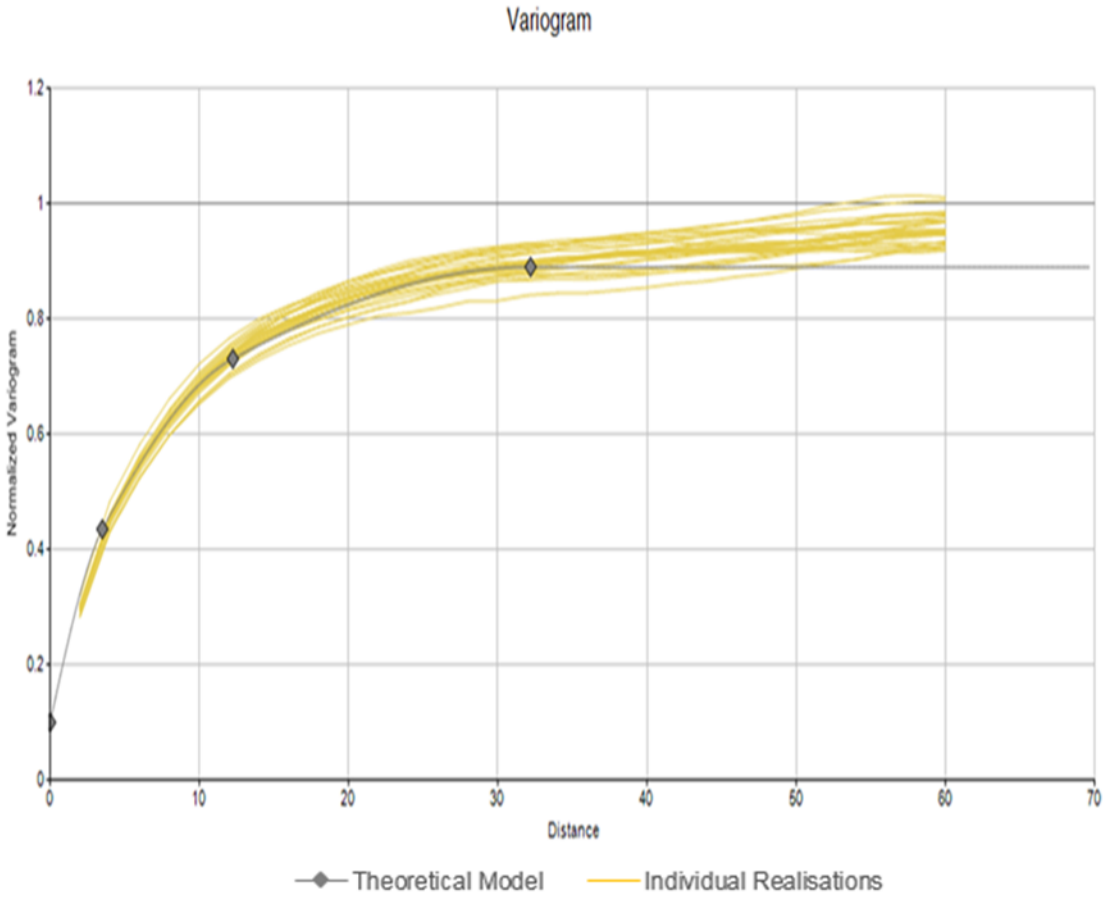

Figure 33 : Western Domain downhole and directional semi variogram generated from 25 realisations.

By comparing the input variogram model and those reproduced from the SGS simulations, the results honour the variability observed in the input information.

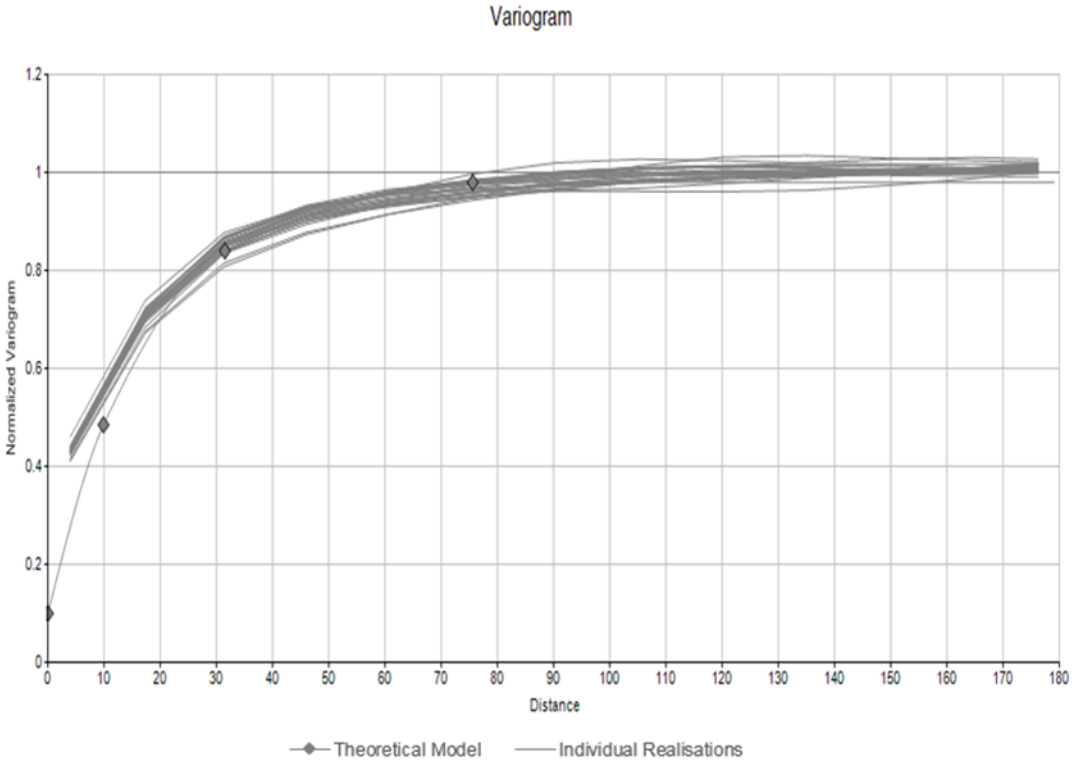

Figure 34: Directional variogram for the 25 simulations of Western Domain

7.2.2.1 SGSIM: CSMODEL Results

CSMODEL process in SGSIM was used to create a block model from simulated points. In this study, a total of 100 realisations were used for each domain with approximately 18.3 and 26.6 million simulated points for the Eastern and Western domains respectively. The output of this process is a block model containing simulated grade, which is the average of simulated nodes lying within a block. The second output file is the STATMOD file which shows the mean, variance, percentiles and other statistical parameters defined by averaging the simulated nodes within the block. The blocks in this study were 25m x 25m x 10m similar to block dimensions used in MIK. The statistical output of the 100 simulations for Eastern and Western domains are shown in Table 22. SIM_all represents statistical parameters from all the simulations.

Table 22: Statistical parameters for simulated points of 100 realisations.

Domain	EASTERN		WESTERN	
Data	**Samples**	**SIM_all**	**Samples**	**SIM_all**
Number of samples	1,680	18,337,500	2,771	26,550,000
Minimum(%Ni)	0	0	0	0
Maximum(%Ni)	3.7	3.7	5.44	5.44
Mean (%Ni)	0.55	0.55	0.55	0.56
Variance	0.13	0.12	0.08	0.09
Standard deviation(%Ni)	0.36	0.35	0.29	0.30
Skewness	3.49	3.39	2.72	2.75

The Eastern domain mean sample at 0.55%Ni is similar to the one produced through SGSIM while the Western domain sample mean was slightly lower than simulated mean. Simulation results for the Eastern domain were less variable than the sample variance while the Western domain had more variability in the simulated points than the input samples.

In addition to statistical analysis of the output from SGSIM, probability maps, namely the P10, P50 and P90 were analysed on plan and in 3D. According to Prins and Minnit (2016), a lower quantile map such as P10 shows that there is a 90% chance that the true value is higher than the value on the map. Due to this relationship, lower quantile maps are identify areas with higher grades while the higher quantile map such as the P90 identifies low grade areas. This is due to the fact that at every single grid point on the P90 map, there is a 90% chance that the true value is lower than the value on the map. The P50 map is a map of medians, meaning that that there is a 50% chance of the true value being over or below the value on the map. P10 probability map and block model are shown in Figure 35 while P50 probability map and block model are shown in Figure 36.

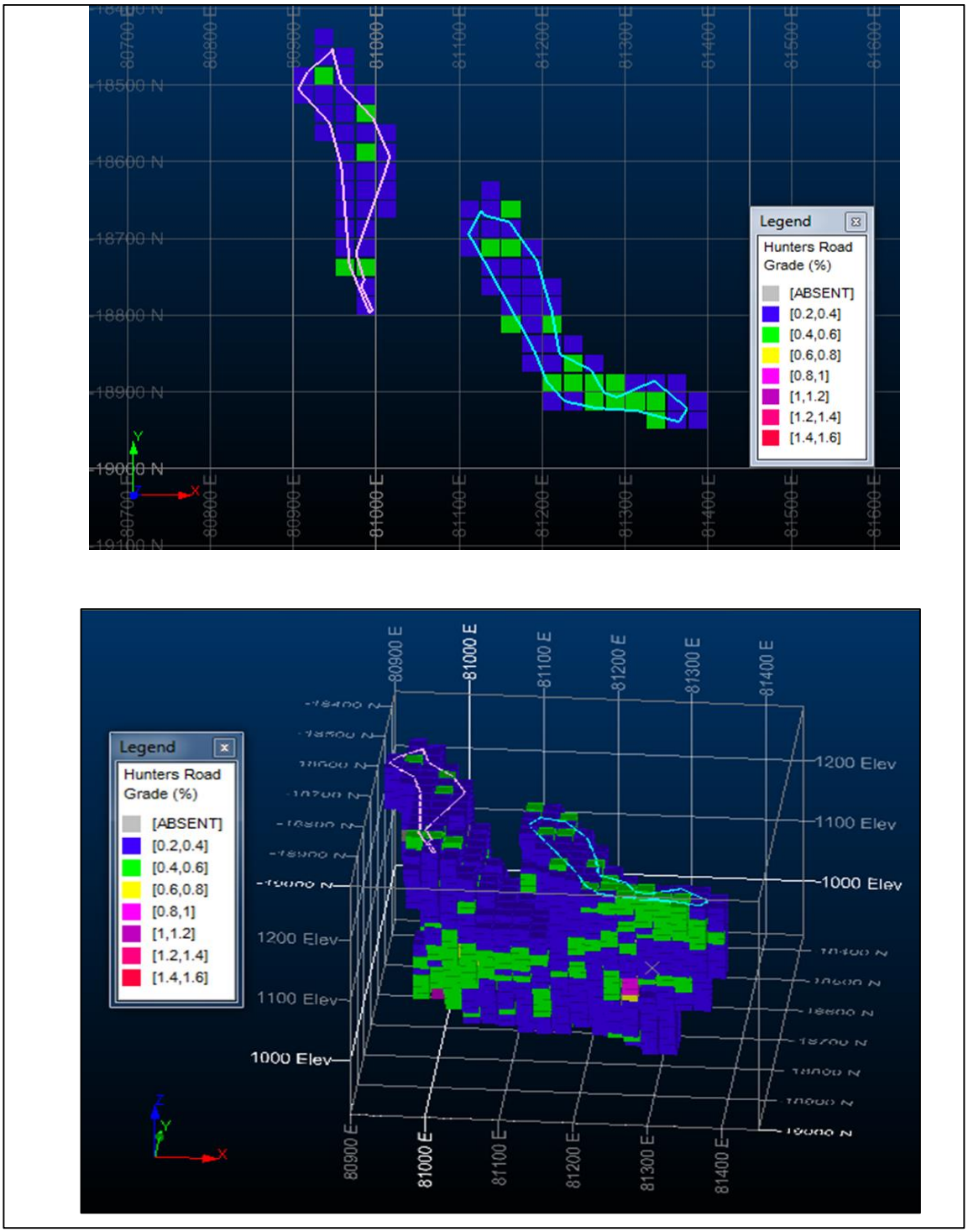

Figure 35: P10 probability map and block model for the Eastern and Western domains

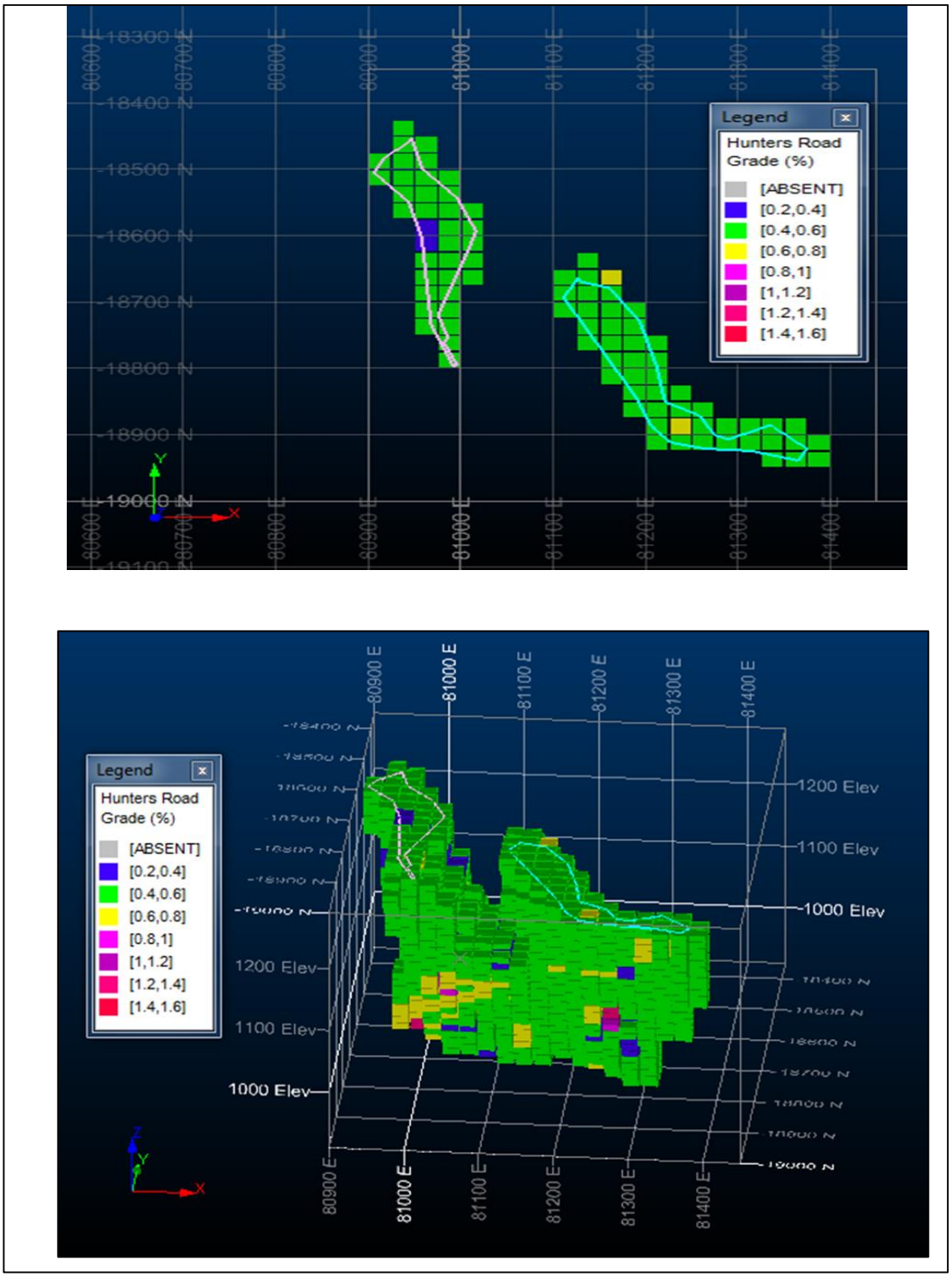

Figure 36: P50 probability map and block model for the Eastern and Western domains.

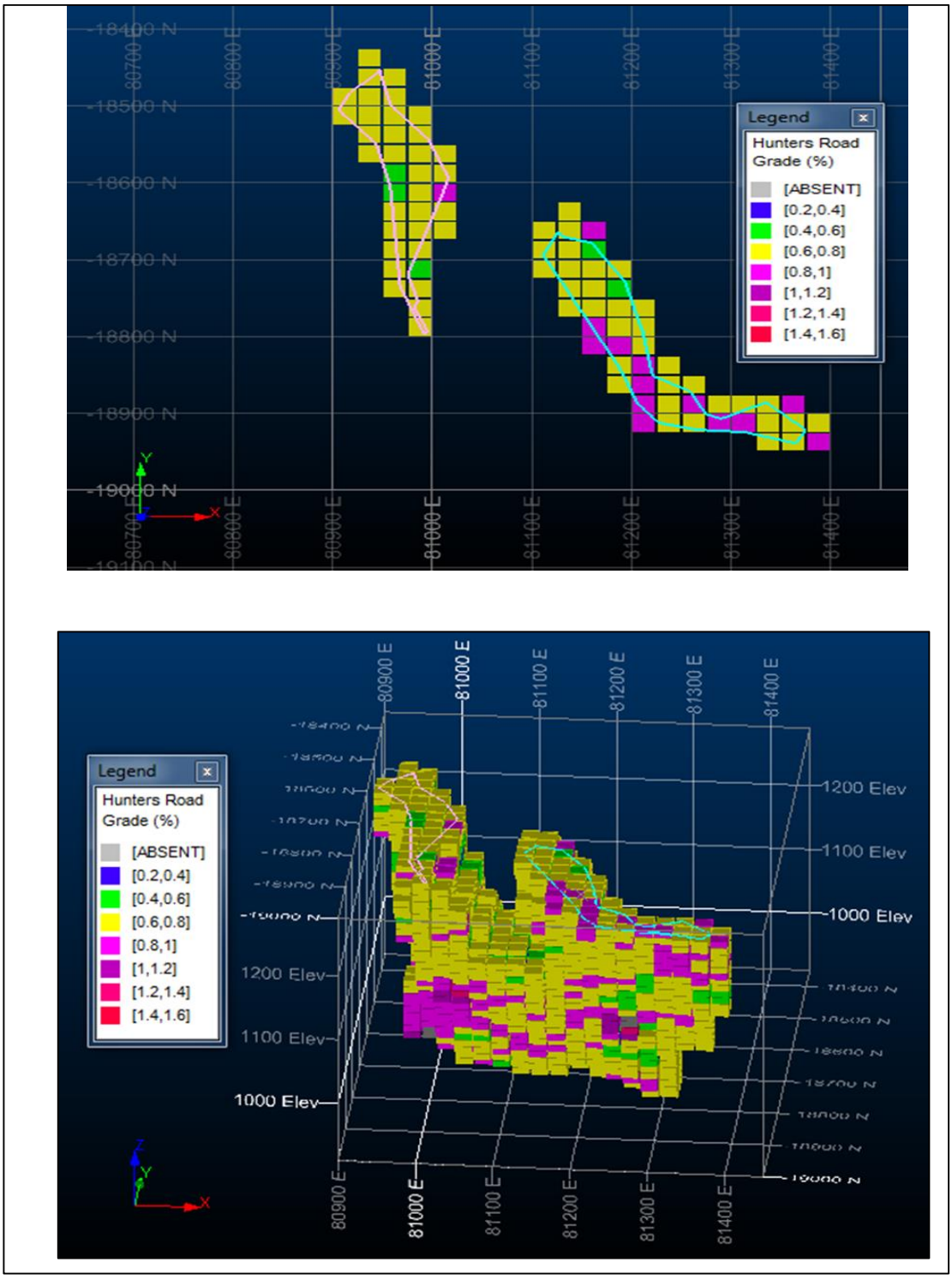

Figure 37: P90 probability map and block model for the Eastern and Western domains.

The P10 probability map shown in Figure 35 shows areas that are really higher with grades above 0.40%Ni. The map shows that while there are grades above 0.60%Ni, the most dominant high grade range is the 0.40%Ni to 0.60%Ni range. The P50 probability map and block model (Figure 36) shows most of the simulated grades falling within the 0.40%Ni to 0.60%Ni grade range with few portions above the 0.60%Ni. The P50 map is a map of medians meaning that that there is a 50% chance of the true value being over or below the value on the map.

Analysis of the P90 map shown in Figure 37 reveals that there are few areas that are certainly low grade areas. The image shows very few areas that are within the 0.40%Ni and 0.60%Ni grade range with the majority of the simulated grades being above 0.60%Ni. A higher quantile map like the P90 identifies areas that are surely low in Ni grades with each grid point having a 90% chance of the true value being lower than the values on the map.

Further analysis of the output of CSMODEL focused on conditional variances. A plot of the conditional variances for the Eastern and Western domain are shown in Figure 38. The plot shows a generally low variability within the two domains although the Eastern domain is more variable. Conditional variances are generally below 0.02 with few isolated portions having higher variances up to 0.2.

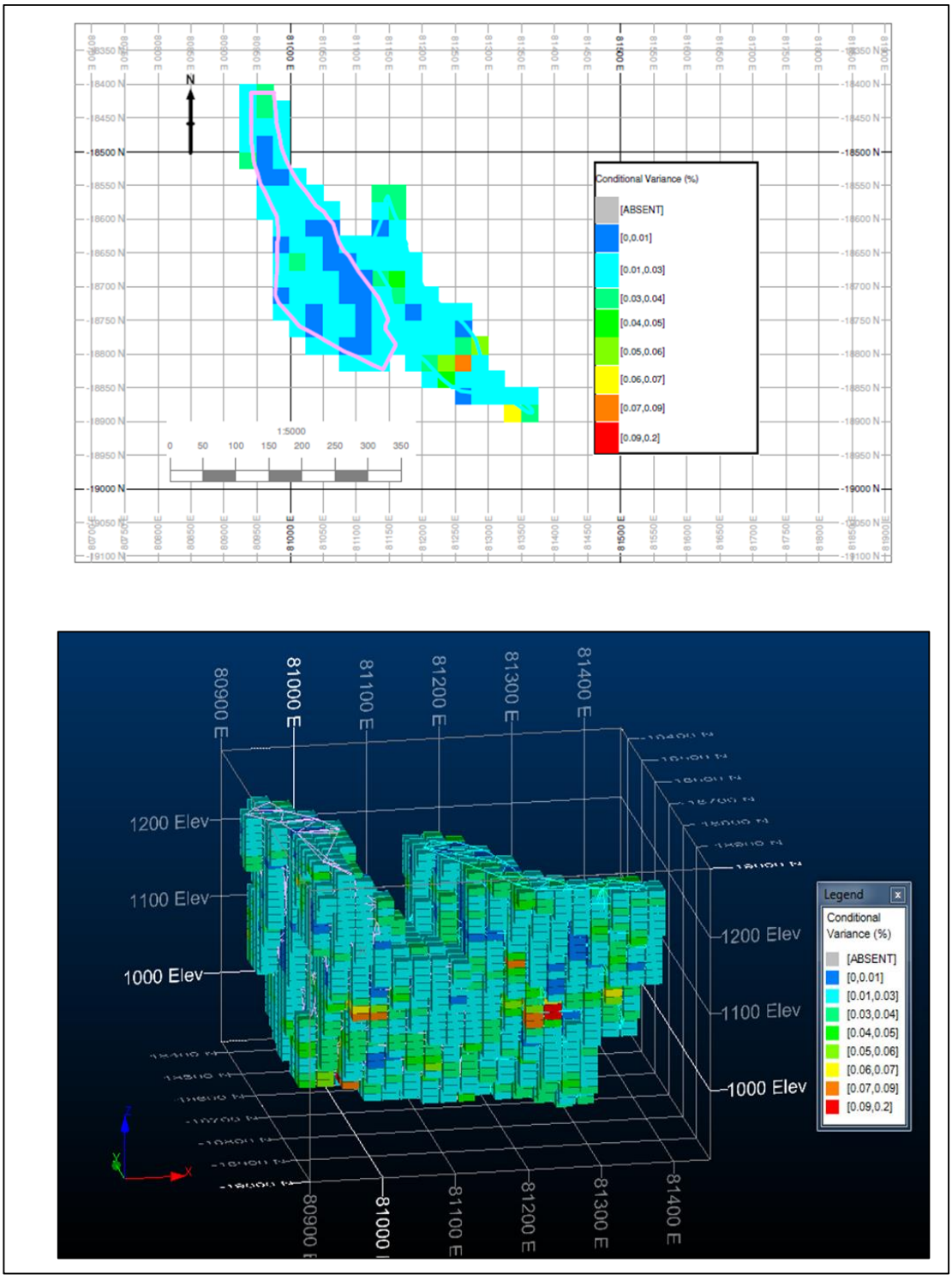

Figure 38: Map and block model showing conditional variances for the Eastern and Western domains.

7.2.2.2 SGSIM Parent Cell Confidence Levels.

Datamine Studio RM module, through its CELLCONF command, is able to calculate confidence associated with the parent cells in a block model created by CSMODEL. The statistical model produced by the CSMODEL process was used in estimating grade confidence levels per parent cell per given grade interval. A summary of the results for the Eastern and Western domains are shown in Tables 23 and 24 respectively. In addition, graphical representation of grade confidence for parent cells for the Eastern and Western domains are shown in Figures 39 and 40 respectively.

Table 23: Confidence levels for Eastern domain parent cells at various grade intervals.

Grade range	1	2	3	4	5	6
Minimum (%Ni)	0	0.20	0.40	0.60	0.80	1.00
Maximum (%Ni)	0.20	0.40	0.60	0.80	1.00	>1
Number of cells	0	38	1190	208	24	7
Number of cell (%)	0	2.6	81.1	14.2	1.6	0.5
Mean (%Ni)	-	0.36	0.53	0.65	0.89	1.14
PC10	-	0.27	0.37	0.47	0.65	0.83
PC20	-	0.30	0.41	0.51	0.71	0.91
PC30	-	0.32	0.44	0.55	0.76	0.98
PC40	-	0.34	0.47	0.58	0.81	1.03
PC50	-	0.35	0.50	0.62	0.86	1.10
PC60	-	0.37	0.54	0.66	0.91	1.17
PC70	-	0.39	0.57	0.71	0.98	1.25
PC80	-	0.42	0.63	0.78	1.06	1.36
PC90	-	0.45	0.71	0.88	1.19	1.49
PC100	-	0.65	1.11	1.34	1.68	1.98

NB PC# represents percentile such that PC10 = 10th percentile value (%Ni)

Analysis of the parent cell data has shown that 81% of the parent cell grades lies within a grade range from 0.40%Ni to 0.60%Ni. For a cell whose estimated value lies between 0.40%Ni and 0.60%Ni, there is a 10% probability that the actual grade will be less than 0.37%Ni and a 10% probability that it will be

above 0.71%Ni. Table 23 above shows that there are no parent cells with grade below 0.20%Ni and 3% of the parent cells have grade less than 0.40%Ni. An estimated 14% of the parent cell grade lies between 0.60% and 0.80%Ni with a 10% probability that the grade will be below 0.47%Ni and 10% probability than it will be above 0.88%Ni. In all the grade ranges considered, the P50 which is the median is lower than the parent cell mean indicating a positively skewed distribution of the estimated block values.

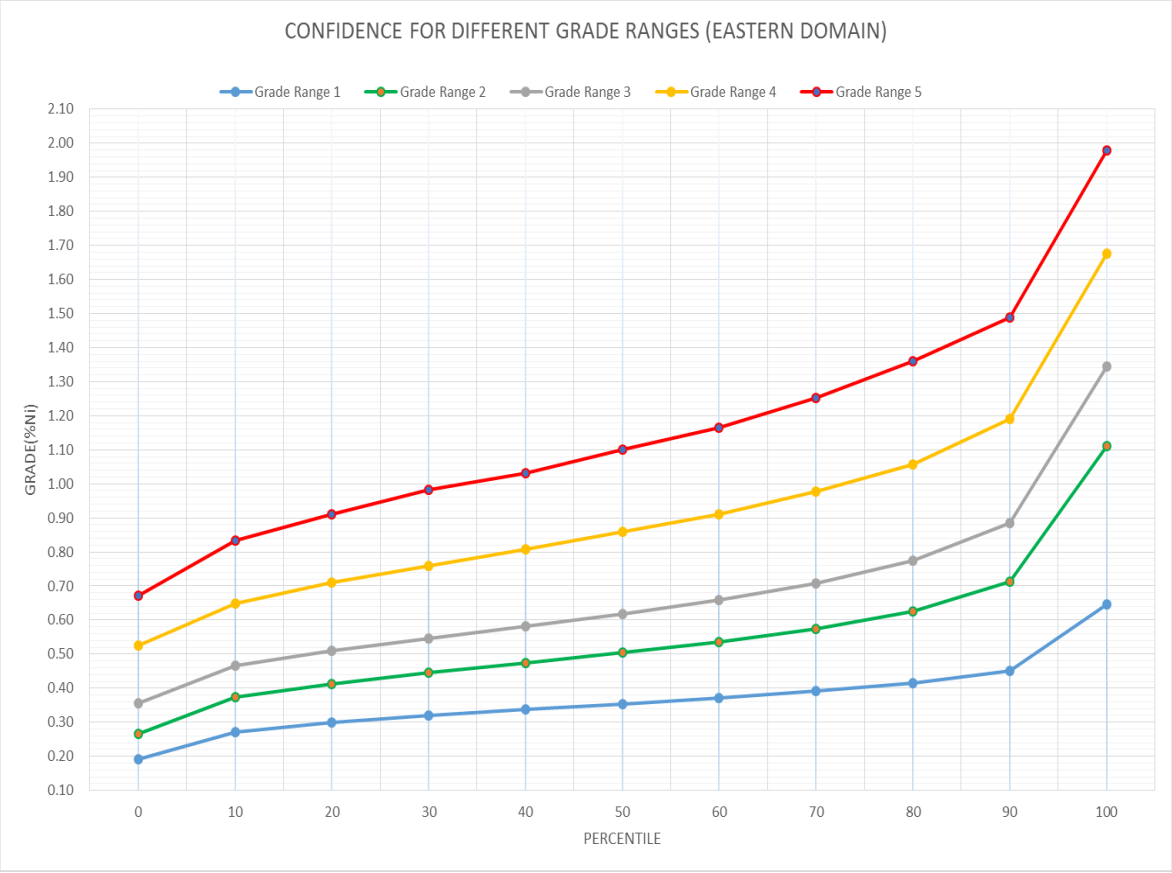

Figure 39: Confidence graph for parent cells of the Eastern domain block model.

Table 24: Confidence levels for Western domain parent cells at various grade intervals.

Grade Range	1	2	3	4	5	6
Minimum(%Ni)	0	0.2	0.4	0.6	0.8	1
Maximum(%Ni)	0.2	0.4	0.6	0.8	1	>1
Number of cells	6	140	1397	500	68	13
Number of cell(%)	0.3	6.6	65.8	23.5	3.2	0.60
Mean (%Ni)	0.16	0.36	0.52	0.66	0.87	1.14
PC10	0.11	0.24	0.36	0.49	0.66	0.90
PC20	0.12	0.28	0.41	0.54	0.72	0.97
PC30	0.14	0.31	0.44	0.58	0.76	1.02
PC40	0.15	0.33	0.47	0.61	0.80	1.07
PC50	0.16	0.35	0.51	0.65	0.84	1.12
PC60	0.17	0.38	0.54	0.68	0.89	1.17
PC70	0.18	0.40	0.57	0.72	0.94	1.22
PC80	0.20	0.43	0.62	0.78	1.01	1.30
PC90	0.22	0.48	0.69	0.86	1.11	1.44
PC100	0.29	0.63	0.98	1.23	1.59	1.76

NB PC# represents percentile such that PC10 = 10th percentile value (%Ni).

Western domain cell confidence results in Table 24 show that 65.8% of the parent cells had grades lying within the grade range from 0.40% to 0.60%Ni. At 65.8%, the number of parent cells within the stated grade range are lower than the 81% obtained in the Eastern domain. In addition, 23.5% of the parent cells in the Western domain have grades lying within the bin grade range from 0.60% to 0.80%Ni. At 23.54%, the number of parent cells lying within the stated grade range are higher than the 14% obtained in the Eastern domain. Parent cells with grades above 0.80% were estimated to be 3.81% while parent cells below the 0.40%Ni were close to 7%. The proportion of parent cells below 0.40%Ni was higher than the 3% obtained for the Eastern domain.

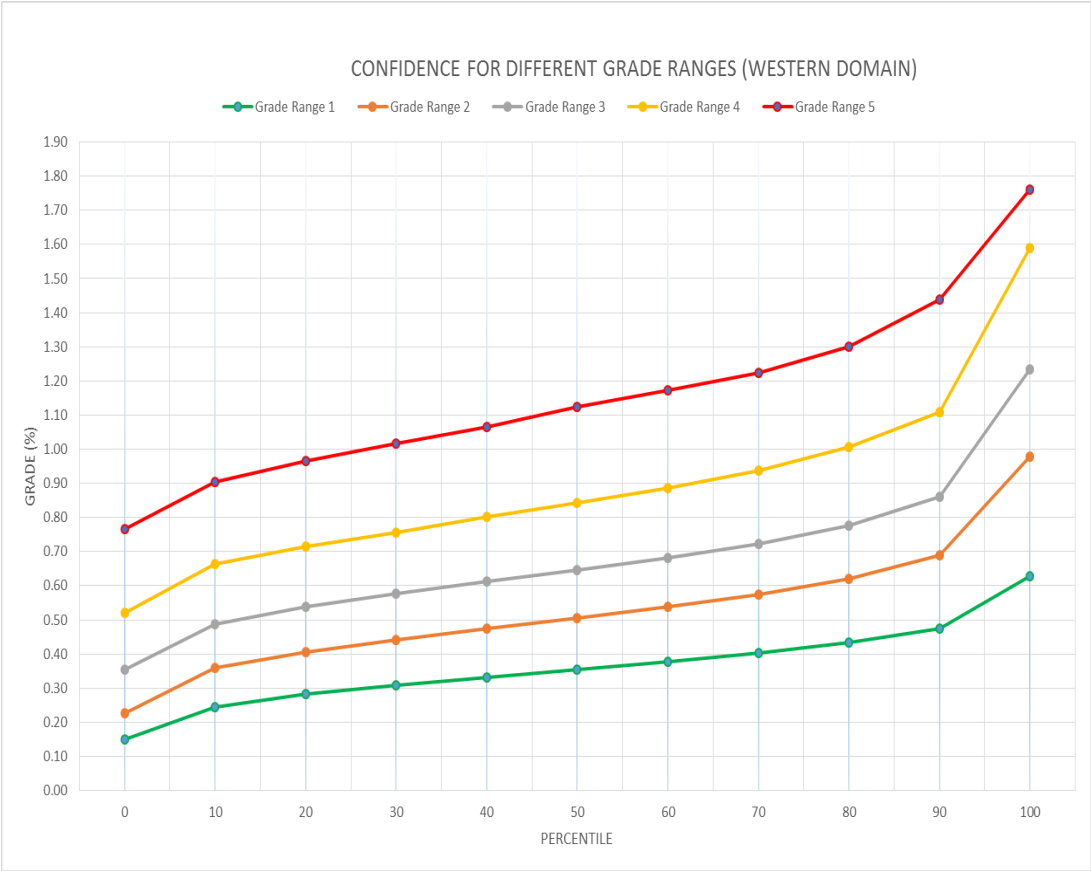

Figure 40: Confidence graph for parent cells of the Western domain block model

Confidence plots in Figure 40 show that for parent cells who have grades lying between 0.40%Ni and 0.60%Ni, there is a 10% probability that the true grade will be below 0.36%Ni and a 10% probability that it will be greater than 0.69%Ni. For a bin grade between 0.60% and 0.80% Ni, there is a 10% probability that the true grade will be below 0.49%Ni and a 10% probability that it will exceed 0.86%Ni. The results indicate high probability of getting grades above 0.40%Ni cut-off grade for both domains but with greater risk of dilution from grades below the 0.40%Ni in the Western domain. The Western domain has higher proportion of high grades than the Eastern domain hence there is a higher probability of getting a higher average grade above the cut-off grade.

7.2.2.3 SGSIM Block Grades Confidence Levels Results

The last part of the conditional simulation post processing and analysis was the calculation of the confidence level for the total grade through the MODCONF process. The algorithm allows calculation of confidence levels of tonnage and grade estimates of a block model. Before focusing on the results of the process, it is important to further identify the two “E-Type” estimates that will appear in the results tables as well as confidence plots. E1 estimate represents the average of all simulations within a cell while E2 represents an average of all simulations for the entire block model under consideration. While the process is able to calculate confidence levels for tonnage and metal content, the main purpose of the study is the assessment of nickel grade uncertainty. A summary of confidence levels of nickel grades per cut-off grade for the Eastern and Western domains is shown in Tables 25 and 26 respectively.

7.2.2.4 Block Model Confidence Results for the Western Domain

Confidence calculation results for the Eastern domain shows that for a cut-off grade of 0.40%Ni, the best estimate for grade is 0.59%Ni based on E2 estimate value and 0.55%Ni based on E1. Based on E2 estimate, there is a 90% probability that the average grade above a cut-off grade of 0.40%Ni will be above 0.57% but less than 0.60%Ni. If a cut-off grade of 0.30% Ni is chosen, E1 and E2 best estimate of the grade is the same at 0.55%. For a 0.30% cut-off grade, there is 90% probability that the average grade above cut-off grade will range between 0.53%Ni% (P10 value) and 0.57%Ni (P90 value). A plot of the confidence levels and E-TYPE estimates per cut-off grade in Figure 33 shows that at cut-off grade above 0.30% E1 estimate values are below the P10 values of E2.

Table 25: Block model grade confidence levels per cut-off grade for the Eastern domain.

Cut-off (%Ni)	E1 (%Ni)	E2 (%Ni)	PC10 (%Ni)	PC20 (%Ni)	PC50 (%Ni)	PC80 (%Ni)	PC90 (%Ni)
0.00	0.54	0.54	0.53	0.53	0.54	0.56	0.56
0.10	0.54	0.54	0.53	0.53	0.54	0.56	0.56
0.20	0.54	0.54	0.53	0.53	0.54	0.56	0.56
0.30	0.55	0.55	0.53	0.54	0.55	0.56	0.57
0.40	0.55	0.59	0.57	0.58	0.59	0.60	0.60
0.50	0.57	0.66	0.64	0.65	0.66	0.67	0.68
0.60	0.67	0.76	0.74	0.74	0.76	0.77	0.78
0.70	0.82	0.86	0.84	0.84	0.86	0.88	0.90
0.80	1.00	0.97	0.93	0.94	0.96	1.00	1.02
0.90	1.10	1.08	1.02	1.04	1.07	1.11	1.14
1.00	1.23	1.18	1.12	1.13	1.18	1.23	1.26
1.10	1.25	1.28	1.20	1.22	1.27	1.34	1.38

NB: E1 and E2 are E-Type estimates representing average grades above cut-off. PC# represents percentile such that PC10 = 10th percentile value (%Ni).

Analysis of the MIK estimate at 0.40%Ni COG versus the confidence levels shown in Table 25 and Figure 41 revealed that, the MIK grade estimate of 0.54%Ni for the Eastern Domain, is outside the confidence limits defined using E2 estimate at similar cut-off grade. However, if falls within the confidence limits defined using a lower cut-off grade of 0.30%Ni.

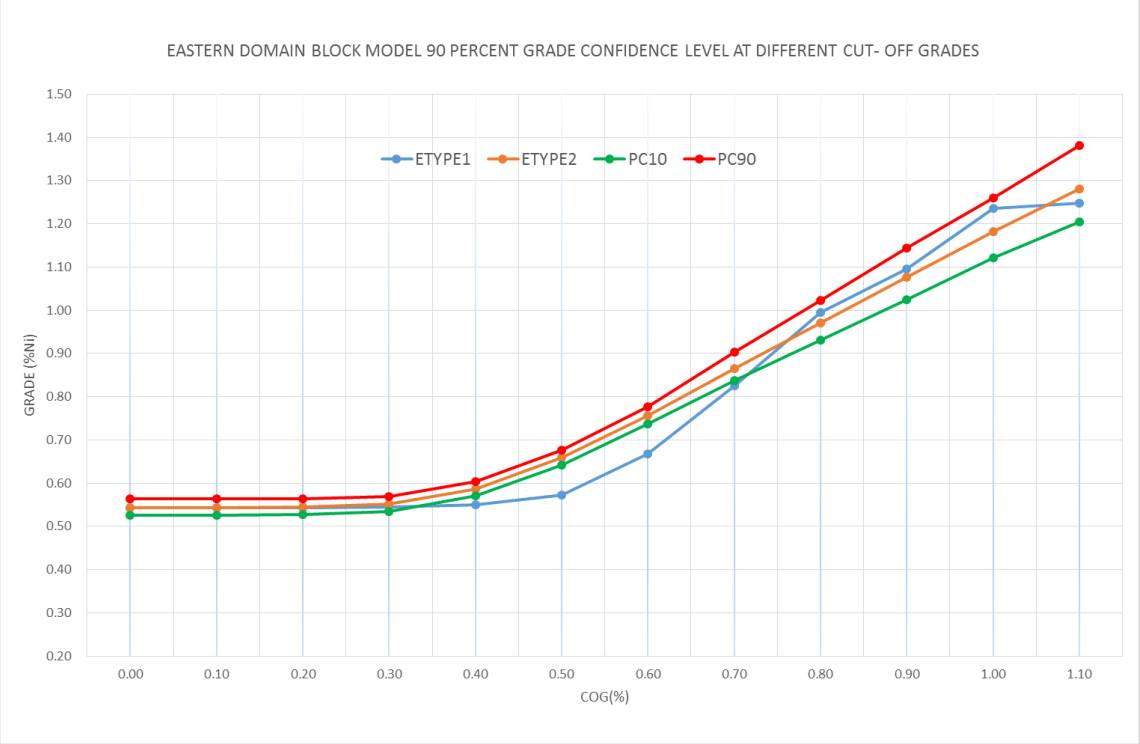

Figure 41: Block model grade confidence level plot for the Eastern domain.

7.2.2.5 Block Model Confidence Results for the Western Domain

Analysis of Western domain block model total grade based on a cut-off grade of 0.40%Ni revealed that the best estimate of the grade is 0.61%Ni (E2) while E1 grade is 0.57%Ni (see Table 26). At this cut-off grade, there is a 90% probability that the average grade above cut-off (0.40%Ni) will be between 0.60%Ni (PC10 value) and 0.62%Ni (PC90 value). If a lower cut-off grade of 0.30%Ni is considered, the best estimate of the grade above cut-off is 0.57%Ni and there is a 90% probability that the grade will be between 0.56%Ni (PC10 value) and 0.58%Ni (PC90 value) (see Table 26). A confidence plot for the Western domain at various cut off grades is shown in Figure 34.

Table 26 : Block model grade confidence levels per cut-off grade for the Western domain.

Cut-off (%Ni)	E1 (%Ni)	E2 (%Ni)	PC10 (%Ni)	PC20 (%Ni)	PC50 (%Ni)	PC80 (%Ni)	PC90 (%Ni)
0.00	0.55	0.55	0.54	0.54	0.55	0.56	0.57
0.10	0.55	0.55	0.54	0.54	0.55	0.56	0.57
0.20	0.55	0.56	0.54	0.54	0.56	0.57	0.57
0.30	0.55	0.57	0.56	0.56	0.57	0.58	0.58
0.40	0.57	0.61	0.60	0.60	0.61	0.62	0.62
0.50	0.60	0.67	0.66	0.66	0.67	0.68	0.68
0.60	0.69	0.75	0.74	0.74	0.75	0.77	0.77
0.70	0.83	0.85	0.83	0.84	0.85	0.87	0.88
0.80	0.94	0.96	0.94	0.94	0.96	0.98	1.00
0.90	1.10	1.08	1.03	1.05	1.07	1.10	1.12
1.00	1.23	1.18	1.13	1.14	1.18	1.22	1.25
1.10	1.29	1.29	1.22	1.24	1.28	1.34	1.39

NB: E1 and E2 are EType estimates representing average grades above cut-off. PC# represents percentile such that PC10 = 10th percentile value (%Ni)

A plot in Figure 42 shows the E2 estimate being significantly higher than the E1 estimate from 0.40%Ni. This is expected as highlighted earlier on but the magnitude of the deviation is worrying. A comparison of MIK grade estimate of 0.58%Ni indicates that although the estimate is slightly higher than E1 estimate, it is outside the confidence limits defined by E2 estimate at 0.40%Ni cut-off grade. However, if a lower cut-off grade of 0.30%Ni is used, the MIK and E2 grade estimates are highly comparable. Block model grade confidence results of the two domains show that although the margins are very narrow, there is higher probability of getting higher grades in the Western domain than the Eastern domain. The E1 estimate is highly comparable with MIK estimate in both domains with the latter being within 2% of E1.

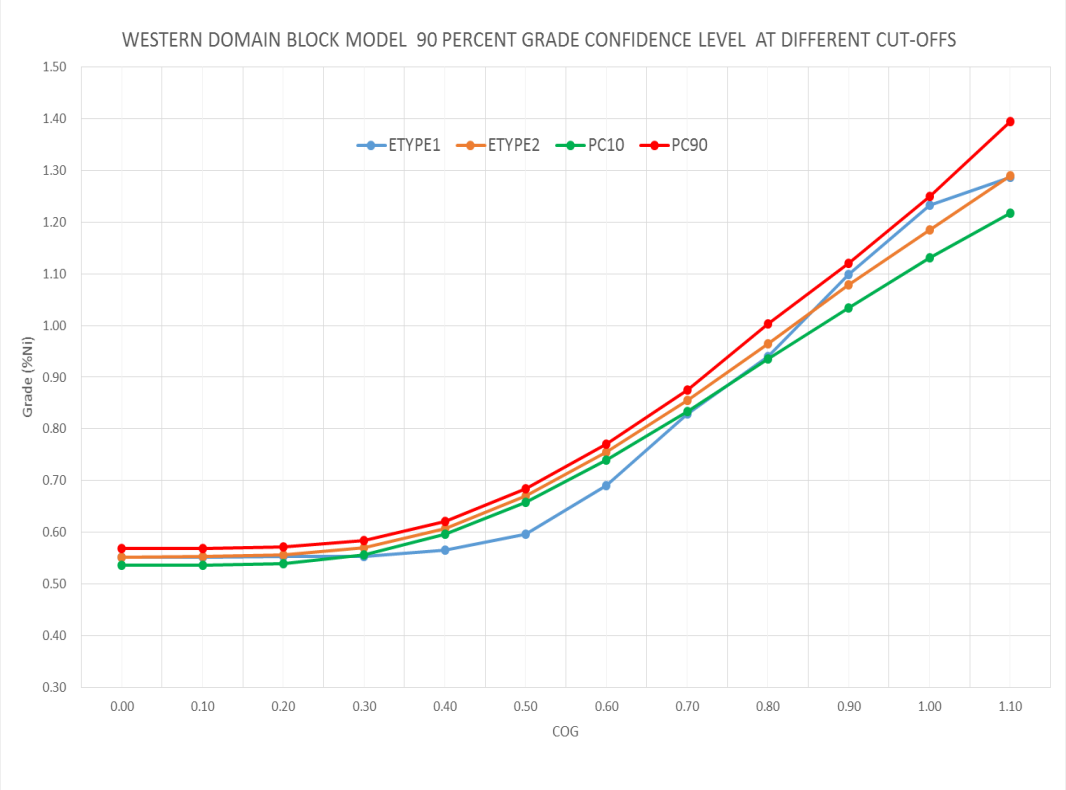

Figure 42: Block model grade confidence level plot for the Western domain.

7.2.2.6 E-type Grade Tonnage Curve

In order to get an insight into the E-Type estimate produced by simulation, an estimate of grade and tonnage without calculating the confidence was done at various cut off grades. The results for both the Eastern and Western domain were plotted as grade tonnage curves in Figures 43 and 44 respectively. The Eastern domain shows approximately 13.24Mt at an E-type average above cut-off grade of 0.57%Ni at a cut-off grade of 0.40%Ni. Increasing COG to 0.50%Ni result in 10.75Mt at a grade of 0.59%Ni which is similar to E-type 2 estimate given earlier on for the same domain.

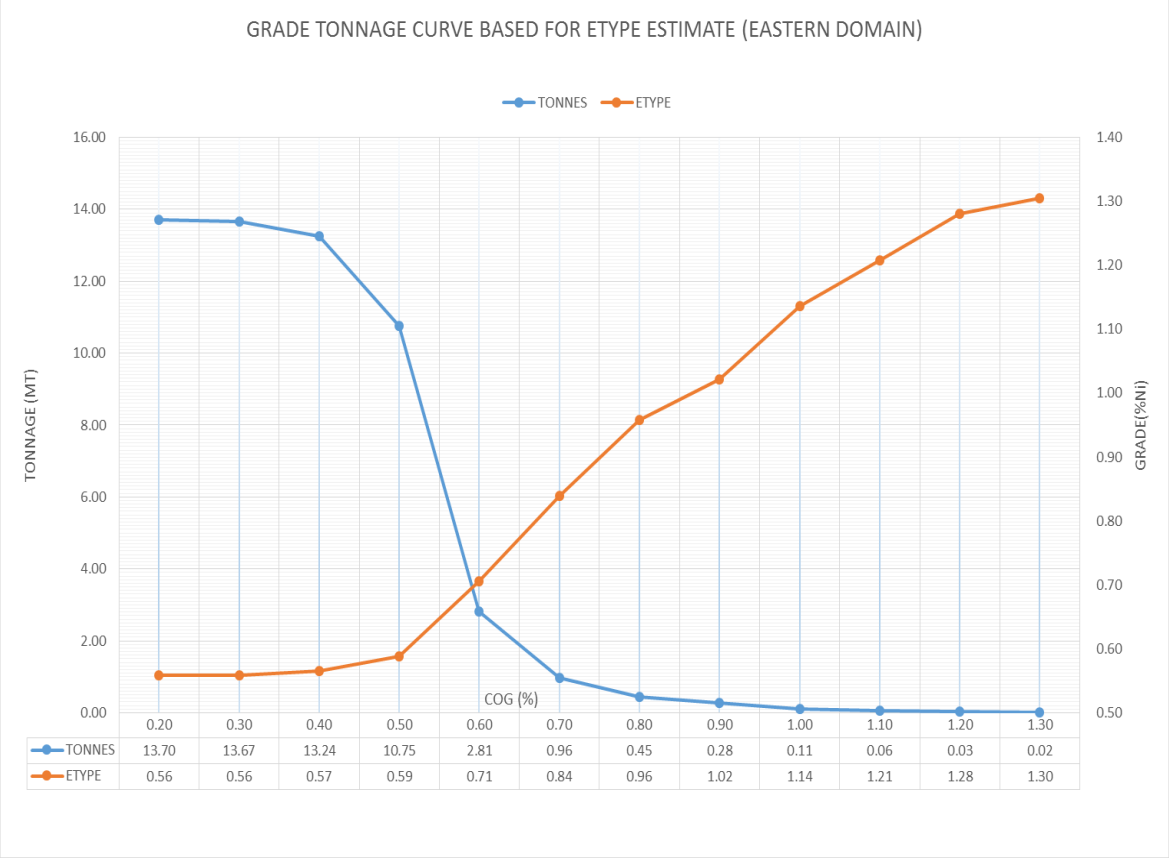

	0.20	0.30	0.40	0.50	0.60	0.70	0.80	0.90	1.00	1.10	1.20	1.30
TONNES	13.70	13.67	13.24	10.75	2.81	0.96	0.45	0.28	0.11	0.06	0.03	0.02
ETYPE	0.56	0.56	0.57	0.59	0.71	0.84	0.96	1.02	1.14	1.21	1.28	1.30

Figure 43: Grade tonnage curve based on various cut off grades of E-Type estimate for the Eastern domain (Block size: 25m x 25m x 10m).

The Western domain grade tonnage curve (Figure 44) shows 21.1Mt at an average grade of 0.58%Ni above a COG of 0.40%Ni. If the COG is increased to 0.50%Ni, 16.07Mt at an average grade of 0.62%Ni is obtained. The estimated resource tonnage of 21.1Mt at a grade of 0.58%% is comparable to MIK estimate of 20.1Mt at a grade of 0.58%Ni. In this situation, MIK and simulation produced similar E-type estimates at 0.40% Ni cut-off grade.

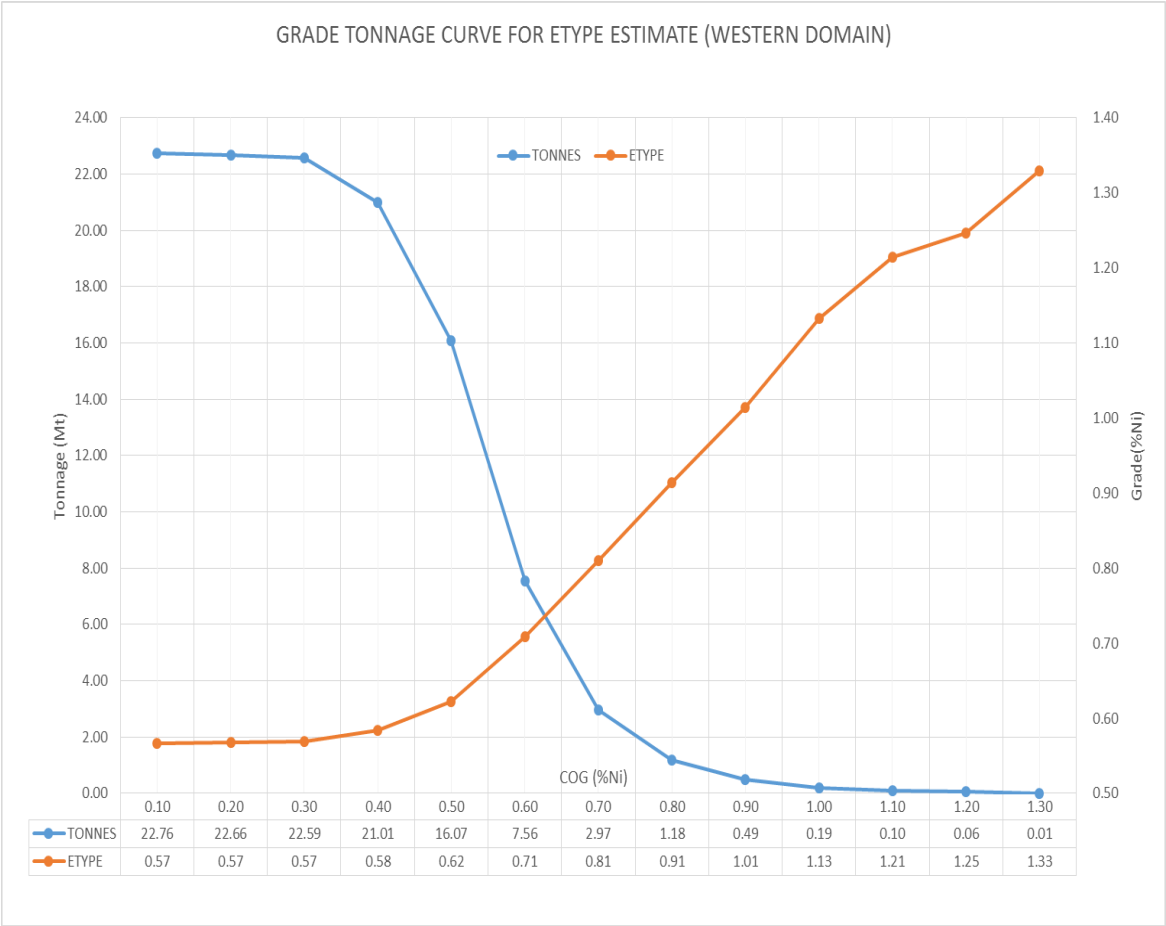

	0.10	0.20	0.30	0.40	0.50	0.60	0.70	0.80	0.90	1.00	1.10	1.20	1.30
TONNES	22.76	22.66	22.59	21.01	16.07	7.56	2.97	1.18	0.49	0.19	0.10	0.06	0.01
ETYPE	0.57	0.57	0.57	0.58	0.62	0.71	0.81	0.91	1.01	1.13	1.21	1.25	1.33

Figure 44: Grade tonnage curve based on various cut off grades of E-Type estimate for the Western domain (Block size: 25m x 25m x 10m).

7.3 Analyses of SGS Results

7.3.1 Eastern Domain Analysis

Block model confidence results for the Eastern domain shown in Table 25 indicate that the best estimate of grade (E2) is 0.59%Ni based on a 0.40%Ni COG. At that grade, there is 90% confidence that the true grade will exceed 0.57%Ni and a 90% probability that it will be below 0.60%Ni. The E1 estimate, which is an average of all simulations within a cell, gave an average grade of 0.55%Ni which is 7% lower than E2 estimate. Based on the PC10 and PC90 values at 0.40%Ni COG, in 90% of the cases, the estimated block grade is

expected to be within 3% of the true value. On the contrary, MIK based grade estimate of 0.54%Ni for the Eastern domain, falls outside the grade confidence limits defined using E2 estimate. However, by considering a lower COG of 0.30%Ni, the MIK estimate will be within a PC10 value of 0.53%Ni and a PC90 value of 0.57%Ni. In this case, in 90% of the cases, the estimated block grade is expected to be within 4% of the true value. The grade variability observed in both cases is very narrow.

Parent cell confidence shows that 81% of the parent cell grades lies between 0.40%Ni and 0.60%Ni, with an average grade of 0.53%Ni (see Table 23).Within this grade range, there is 10% probability that the grade will be below 0.37%Ni and, similarly,10% probability that it will exceed 0.71%Ni. The second most dominant grade range is the 0.60% to 0.80%Ni, with 14% of the parent cells having grades within this range. For those cells, the mean grade was 0.65%Ni, with a 10% probability that the grade will be below 0.47%Ni and a 10% probability that it will exceed 0.88%Ni. It would be appropriate to consider confidence levels that take into consideration the 0.37%Ni highlighted by parent cell results. In that context, block grades uncertainty is properly defined by 0.30%Ni cut off grade with a 90% probability that the average grade above cut-off (0.30%Ni) for the Eastern domain is between 0.53%Ni and 0.57%Ni. At 0.30%Ni COG, the E2 and E1 estimates are within the confidence limits defined by PC10 and PC90 as shown in Figure 41.

7.3.2 Western Domain Analysis

Block model grade confidence results shown in Table 26 indicate that the best estimate of the grade (E2) is 0.61%Ni while E1 estimated grade was 0.57Ni%. At 0.61%Ni, the E2 grade is 7% higher than E1 estimate and 5% higher than MIK estimate. At 0.61% Ni, there is 90% confidence that the grade of the resource will exceed 0.60%Ni and will be below 0.62%Ni. The grade

confidence limits indicated by PC10 and PC90 values show that the true grade will be within 2% of the block grade. If a lower COG of 0.30%Ni is considered in the same context highlighted earlier on, an E2 estimate of 0.57%Ni is obtained with a 90% probability that the average grade above cut-off for the Western domain is be between 0.56%Ni and 0.58% Ni. In 90% of the cases, the true grade will be within 2% of the estimated block grade. This is quite a narrow margin of variability compared to the Eastern domain. This is indicative of intense drilling conducted in the Western domain.

In support of the block model grade confidence results, E-Type estimate grade tonnage curve in Figure 44 shows a 0.58%Ni grade which is similar to the MIK estimates for the Western domain. The lowest grade obtained is 0.57%Ni at a much lower COG of 0.10%Ni. In addition, an analysis of the parent cell grades indicated that 66% of the cells have grades that lie between 0.40%Ni and 0.60%Ni while 24% of the cells have average grades lying between 0.60%Ni and 0.80%Ni (see Table 24). There is a significant increase in cells with higher grades and a reduction in cells with low grades compared to the Eastern domain for the same grade ranges.

Parent cell confidence results indicated that for cells with estimated grades that lie between 0.40%Ni and 0.60%Ni, there is a 10% probability that the actual grade will be less than 0.36%Ni and a 10% probability that it will exceed 0.69%Ni. The mean grade for this grade range is 0.52%Ni which is 2% lower than Eastern domain mean grade for the same range. For cells with an estimated grade that lies between 0.60%Ni and 0.80%Ni, there is 10% probability that the grade will be below 0.49%Ni and a 10% probability that it will exceed 0.69%Ni with a mean grade of 0.66%Ni. This means that there is 90% probability that the parent cells for the Western domain will have grades ranging between 0.36% Ni and 0.86%Ni as defined by the most dominant grade ranges. In summary, the best estimate of the grade above cut-off for the

Western domain is 0.57%Ni with a 90% probability of the average grade above cut-off being between 0.56%Ni and 0.58%Ni. Simulation results confirm higher confidence in grade for the Western domain which is supported by the number of samples used. The Eastern domain, due to less number of samples, has higher grade variability around the mean grade. SGS results also supported MIK findings that the Western domain has higher grades than the Eastern domain.

7.4 Chapter Summary

This section presented SGS results for the two domains focussing on the E-type estimates, probability maps and the probability to exceed a series of cut-off grades. A total of 100 realisations per domain were generated using the same parameters obtained from NS semi variogram. SGS was able to reproduce histogram and semi variogram of the input NS transformed data.

Analysis of SGS realisations through a transfer functions resulted in the production of E-type estimate of the mean and analysis of both cell and block model grade confidence level. The results showed that estimate of the mean for the Eastern domain is 0.55%Ni with a 90% probability that the average above cut-off grade will be between 0.53%Ni and 0.57%Ni. The Western domain simulation results showed that the average grade above cut-off is 0.57%Ni with a 90% probability that it will be between 0.56%Ni and 0.58%Ni. MIK estimate of 0.54%Ni and 0.58%Ni for the Eastern and Western domains respectively are within the 90% confidence limits obtained through SGS. E-type estimate for the Eastern domain obtained 13.24Mt at an average grade of 0.57%Ni while Western domain had 21.01Mt at 0.58%Ni. Western domain E-type estimates are similar to MIK E-type estimate of both grade and tonnage while Eastern domain estimates are different. The next section will focus on discussing key findings of the research.

CHAPTER 8: DISCUSSION

8.1 Introduction

Chapter 6 and 7 focussed on the representation of MIK and conditional simulation results thereby establishing the basis for discussion of the results. This chapter will focus on discussing the results obtained with reference to what is already known about the problem. The main argument of the study is that OK estimates did not reflect both local and spatial uncertainty associated with nickel grades at Hunters Road. The discussion will focus on estimation of recoverable resources, assessment of grade uncertainty and comparison of historical estimates with current estimates.

8.2 Estimation of Recoverable Resources Using Indicator Kriging (IK)

Estimation of recoverable resources using IK was one of the objectives of the study. The argument being that, historical estimates were based on OK which produces smoothed estimates (Yamamoto, 2005) that underestimates the variability associated with regionalised variables. Secondly, OK estimates only gives a single estimate (Vann, et al., 2000) instead of conditional expectation and distribution of grades inside a SMU. EDA and variogram modelling using deciles of sample distribution as cut-off grades enabled the selection of MIK as the best method for estimation of recoverable resources. This was mainly due to noticiable difference in the shape of indicator variogram at various cut-off grade such that the spatial variability could not be approximated by single indicator variogram. This was in accordance with Isaaks and Srivastava (1989) observations regarding MIK. The use of MIK was time consuming especially modelling of the three (3) variograms per every cut-off grade.

Recoverable resources for the two domains namely, the Eastern and Western domains combined were estimated at 32.30Mt at an average grade of 0.57%Ni based on a 0.40%Ni cut-off grade. The resources were also reported per

domain in Chapter 7. The reported MIK estimates are E-type estimates obtained from the composite ccdf ($F_{Z_{UL|(n)}}(z)$) by averaging the proportions of point values within the block which do not exceed a given cut-off grade (Rossi and Deutsch, 2014). A true block ccdf which gives the probability of exceeding a given cut-off grade of 0.40%Ni was not done. This was mainly due to unavalibility of change of support module on the software which is applied as a post processing step (Vann, et al., 2000). The problem was partially addressed through conditional simulation. However, conditional simulation only focussed on grade uncertainty hence it did not address uncertainty associated with resource tonnages. Post processing of MIK composite ccdf through affine correction algorith is required in order to produce block ccdf.

8.3 Assessment and Quantification of Grade Uncertainty at Hunters Road

Grade uncertainity at Hunters Road was assessed through SGS based on decomposition of the multivarate probability distribution function into a series of conditional distributions (Isaaks, 1991). The assessment was based on 100 realisations per domain. Although SGS was able to produce 100 realisations, interpreting these realisations in 3D was a challenge. The use of an algorithim which produces animated display of realisation as suggested by Goovaerts (1997) could have assisted in visual inspection of the realisation. Given the complexity associated with 3D realisations, analysis of uncertainty relied more on E-type mean, probability maps and block confidence. The analysis is in line with suggestions made by Goovaerts (1997) and Deutsch and Journel (1998).

The results showed that the best estimates of block confidence or uncertainty were obtained when a lower cut-off grade of 0.30%Ni was used. This cut-off grade does not imply that this will be the economic cut-off grade for reporting recoverable mineral resources. The E-type estimate for the Eastern domain was 0.55%Ni with a 90% probability that the average grade above cut-off will

be between 0.53%Ni (P10) and 0.57% Ni(P90). Western domain E-type estimate was 0.57%Ni with a 90% probability of the average grade above cut-off being between 0.56%Ni (P10) and 0.58%Ni(P90). While the results are indicative of low variability and therefore low uncertainity associated with nickel grades at Hunters Road, the difference between E1 and E2 at 0.40%Ni cut off grade (Table 25 and 26) is a cause for concern regarding post procesing of SGS realisations when moving from point to block simulations. E1 is an average of all simulations within a cell while E2 is the average of all simulations for the entire model. Although the E2 estimate was expected to be higher than E1 estimate for cut-off grade above 0%Ni, at a COG of 0.40% Ni, E1 estimate were very low such that they were outside the PC10 limit(P10) (Figure 41 and 42).

Further analysis of SGS results especially estimation of block confidence for both grade and tonnage using a different software can be used to validate block model grade confidence results. However, the results from the two domains indicate very low uncertainty around the nickel grades at Hunters Road especially the Western domain. The finding that there is low grade uncertainty at Hunters Road desposit is supported by parent cell confidence results which revealed that there is 10% probability of grade being below 0.37%Ni and 0.36%Ni for the Eastern and Western domain respectively.

8.4 Comparison of Historical OK Estimates with Current Estimates

The third objective of the study was the comparison of historical OK based estimates with the MIK based estimates. Given the fact that OK estimates are single estimates, the comparison of the results was based on E-type estimates of MIK and conditional simulation. A comparison between MIK and OK estimates in Chapter 6 showed similarity with 2001 OK estimates by AACS although the grade was slightly higher at 0.59%Ni compared to 0.57%Ni (see

Table 14). The resource tonnages are highly comparable at 32.30Mt (MIK estimate) compared to 32.64Mt (AACS, 2001 OK estimate). The BNC OK based estimates dated May 2006 resource tonnage was 13% higher than the current MIK estimate while the grade was 4% lower. Due to inconsistencies in the estimation protocol and application of cut-off grade, the BNC May 2006 resources estimates do not reflect the true grades and resource tonnages at Hunters Road. This has led to overstating of Hunters Road resource.

Similarity between OK estimates and MIK estimates for the years under review is consistent with Rossi and Deutsch (2014) argument that for less variant variables, the E-type estimate produced by MIK can be similar to estimates produced by linear geostatistical techniques. Statistical analysis of sample composites in Chapter 4 revealed that the two domains were positively skewed with a COV of 0.63 and 0.54 for the Eastern and Western domains respectively. Journel (1983) considered variables with COV above 2 to be highly variable, hence with such low COV, OK and MIK estimates are not very different. The only difference is that MIK E-type estimate is a conditioned mean derived from composite ccdf rather than a block average grade. The weights allocated to samples by MIK are a function of the actual grades rather than being independent of specific values at their locations (Vann, et al., 2000). In that context as well as the fact that the two distributions were positively skewed, MIK resource estimates are more reliable than BNC OK based estimates.

SGS block confidence limits highlighted earlier on supported MIK E-type estimates in the sense that they all fall within the 90% confidence limits. However, E-type estimate derived from block model produced through SGS transfer functions reported 13.24Mt at an average grade of 0.57%Ni for the Eastern domain compared to 12.16Mt at an average grade of 0.54%Ni derived through MIK. Simulated grade is higher than MIK although they all fall within the defined confidence limits of the block model. SGS E-type estimate for the

Western domain had similar grade of 0.58%Ni while the tonnages were slightly different at 21.01Mt for SGS compared to 20.14Mt estimated through MIK. The resource tonnages were expected to be higher due to the fact that simulation blocks did not strictly follow the defined boundary. In order to properly validate grade and tonnage results from MIK, post processing of composite ccdf through a change of support model should be performed in order to produce block ccdf. This will allow comparison of block ccdf produced through SGS to the one produced through MIK.

This section has discussed results of MIK and SGS against the three key objectives of the study. The next chapter summaries the findings, draws conclusions from the study and makes recommendations for continuous improvement and further studies.

CHAPTER 9: CONCLUSION AND RECOMMENDATION

9.1 Conclusion

The problem statement of the current study stated that the historical estimates which were based on OK did not reflect both local and spatial uncertainty associated with regionalised variables. Application of MIK which is a non-parametric estimation technique resulted in production of risk quantified estimates which took into consideration local uncertainty. The use of several cut-off grade defined by decile of sample distribution resulted in the production of cumulative conditional distribution function (ccdf), which described a range of possible values an estimate can take. This is in contrast to single point estimates that characterised historical estimates.

Due to unavailability of change of support module on the software used, only E-type estimates were produced using MIK. Recoverable resources for Hunters Road based on 0.40%Ni COG was estimated at 32.30Mt at an average grade of 0.57%Ni equivalent to 183,13kt of nickel metal. The estimated resource tonnage is lower than BNC May 2006 estimate of 36.44Mt at an average grade of 0.55%Ni equivalent to 199.80kt of nickel metal. MIK based estimates were highly comparable to AACS‘s January 2001 estimates which had a merged Bottom zone below 1080m ASL. Based on the inconsistencies observed in BNC estimates dated May 2006, they do not reflect the expected grades and tonnages at Hunters Road Nickel Project.

Although MIK E-type estimates were considered to be better, QAQC data covering a period from 1992 to 1993 showed presumed contamination of samples and systematic bias. Poor QAQC results affects the integrity of the data used in the estimation process. Additional work is required in order to increase confidence in sampling information. In addition, boundary analysis of the orebody wireframes revealed that the orebody boundary defined using

0.40%Ni did not properly delineate the resource. A lower COG of 0.30%Ni accompanied by a geological model could have improved delineation of the resources.

Grade uncertainty which was assessed through Sequential Gaussian Simulation (SGS) showed that there is very low variability and therefore low uncertainty around the grades with 90% probability that the true grade will be within +/-3% of the estimated grade. The SGS derived estimate of grade above cut-off for the Eastern domain is 0.55%Ni with a 90% probability that the average grade above cut-off grade will be between 0.53%Ni and 0.57%Ni. Western domain block grade confidence limit indicated that the best estimate of the average grade above cut-off is 0.57%Ni with a 90% probability that the grade above cut-off will be between 0.56%Ni and 0.58%Ni. The MIK estimated grades for the Eastern and Western domains falls within the 90% block model grade confidence limits defined through SGS. The results shows that there is low uncertainty in grade with the Eastern domain being more variable than the Western domain.

In conclusion, the MIK produced better estimates than OK which took into consideration local uncertainty associated with nickel grades. Conditional simulation using SGS allowed assessment of spatial uncertainty associated with nickel grades at Hunters Road Nickel Project. In this regard, the three objectives of the study were achieved. However, there are grey areas which this study did not clearly unravel and these are covered in the following section.

9.2 Recommendation

The discussion on the findings of this study highlighted some grey areas which were not covered and needs continuous improvement. The following recommendations are meant to address noted deficiencies.

1) **Post processing of MIK results through affine correction or other relevant change of support algorithm.**
   This will be done in order to generate block ccdf which gives the probability of exceeding specific cut-off grades for the entire block model. The results will assist in the assessment of local uncertainty associated with nickel grades.

2) **The use of a different SGS algorithm in post processing realisations. Isatis and GSLIB POSTSIM algorithms are recommended for this purpose**.
   Analysis of SGS block confidence results indicated huge difference between E1 and E2 estimate for cut-off grades above 0.30%. The difference may have been associated with the creation of block models from point simulations.

3) **Conditional simulation of both grade and tonnage.**
   The current simulation focussed on grade uncertainty. There is need to carry out simulation of both grade and tonnage so that the ccdf generated can be compared with MIK based ccdf. This is important in understanding uncertainty around resource tonnage and metal content.

4) **Discontinuation of the use of BNC May 2006 resources estimates.**
   Irregularities identified during the current study regarding the methodology and reported grades and tonnages shows that the resource tonnages and

grades are not an accurate representation of expected grades in the Western Orebody of Hunters Road nickel project.

5) **Remodelling of the orebody wireframes using both geological model and a lower cut-off grade of 0.30%Ni.**

   The use of a higher cut-off grade of 0.40%Ni in defining the orebody outline resulted in poor definition of the mineralised envelope. Its subsequent use in reporting the resources estimates created confusion in the final estimates reported by different organisations at 0.40%Ni cut-off grade. Hence there is need to lower the COG and allow grade interpolation method to estimate unsampled zones and report blocks that have grades above a specific economic COG.

6) **There is a need to drill twinned holes in order to validate QAQC results.**

   QAQC analysis for holes drilled between 1992 and 1993 showed contamination and systematic bias in the assays. Given the fact that most of the cores for Hunters Road project have been washed away, drilling of twinned holes would assist in validating QAQC data.

7) **Classification of the resource based on both geometric criteria supported by probabilistic criteria derived from conditional simulation.**

   This can only be done after addressing QAQC issues highlighted earlier on in the report.

10 REFERENCES

Abzalov, M. Z., 2006. Localised uniform conditioning (LUC): A new approach for direct modelling of small blocks. *International Association for Mathematical Geology,* 38(4), pp. 393-411.

Anglo American, 1987. *Bindura Nickel Corporation Limited,*: Anglo American. pp 3

Anglo American Corporation of South Africa (AACS), 1996. *Hunters Road nickel project local mineral resource estimates for nickel,*.: Anglo American Corporation of South Africa Limited.

Anglo American Corporation of South Africa (AACS), 2002. *Hunters Road study phase 0: Validation of business proposal.* Bindura: Anglo American, pp 11

Badel, M., Angorani, S. & Panahi, M. S., 2011. The application of median indicator kriging and neural network in modeling mixed population in an iron ore deposit. *Computers &Geosciences,* 37(2011), pp. 530-540.

Basante, F. G., Ordonez, C., Taboada, J. & Matias, J. M., 2008. Comparison of indicator kriging , conditional indicator simulation and multiple-point statistics used to model slate deposits.. *Engineering Geology,* 98(2008), pp. 50-59.

Bindura Nickel Corporation (BNC), 2006. *Hunter's Road Project Phase O (A)-Part 2.* Bindura: Bindura Nickel Corporation.

Cheshire, P. E., Leach, A. & Milner, S. A., 1980. *The geology of the country between Gwelo and Redcliff.* 86 ed. Harare: Geological Survey of Zimbabwe Bulletin 86.

Chiles, J. P. and Delfiner, P., 2012. *Geostatistics: modelling spatial uncertainty.* New York: Wiley.

Clark, I. and Harper, W. V., 2007. *Practical Geostatistics 2000.* Columbus , Ohio USA: Ecosse North America.

Deutsch, C. V. and Journel, A. G., 1998. *Geostatistical software library and user's guide.* 2nd ed. New York: Oxford University Press.

De-Vitry, C., Vann, J. & Arvidson, H., 2007. *A guide to selecting the optimal method of resource estimation for multivariate iron ore deposit.* [Online] Available at: http://citeseerx.ist.psu.edu/viewdoc/download?doi=10.1.1.83.5590&rep=rep1&type=pdf[Accessed 26 August 2016].

Dimitrakopoulos, R., Farrelly, C. T. & Godoy, M., 2002. *Moving forward from traditional optimisation :grade uncertainty and risk effects in open -pit design.* [Online] Available at: www.tandfonline.com/doi/abs/10.1179/mnt.2002.111.1.82[Accessed 27 August 2016].

Dohm, C., 2015. *Geostatistical methods in mineral resource evaluation (Lecture Notes).* Johannesburg: University of the Witwatersrand, Johannesburg.

Duke, J. H. and Hanna, P. J., 2014. Geological interpretation for resource modelling and estimation. In: *Mineral Resource and Ore Reserve estimation .The AusIMM guide to good practice.* 2nd ed. Carlton Victoria: The Australasian Institute of Mining and Metallurgy, pp. 145-153.

Emery, X., 2005. Simple and ordinary multigaussian kriging for estimating recoverable reserves. *Mathematical Geology,* 37(2), pp. 295-319.

Emery, X., Ortiz, J. M. & Rodriguez, J. J., 2006. Quantifying uncertainty in mineral resources by use of classification schemes and conditional simulations. *Mathematical Geology,* 38(4), pp. 445-464.

Emery, X. and Pelaez, M., 2011. Assessing the accuracy of sequential Gaussian simulation and cosimulation. *Computer Geosciences,* 2011(15), pp. 673-689.

Ghahramani, Z., 2001. An introduction to hidden Markov models and Bayesian networks.. *International Journal of pattern recognition and artificial intelligence,* 15(1), pp. 9-42.

Glacken , I. and Trueman, A., 2014. Overview- Mineral Resource Estimation. In: *Mineral Resource and Ore Reserves Estimation. The AusIMM guide to good practice.* 2nd ed. Carlton Victoria: The Australasian Insitute of Mining and Metallurgy, pp. 263-276.

Goovaerts, P., 1997. *Geostatistics for natural resource evaluation.* New York: Oxford University Press.

Harrison, N. M., 1970. *The geology of the country around Que Que..* s.l.:Gological Survey of Rhodesia Bulletin 65.

Hill, D., Mueller, U. and Bloom, L., 1998. Comparison of median and full indicator kriging in the analysis of gold mineralisation. In: *Beyond ordinary kriging - Non-Linear Geostatistical Methods in Practice.* Perth: The Geostatistical Association of Australasia, pp. 50-62.

Isaaks, E. H., 1991. *The application of Monte Carlo methods to the analysis of spatially correlated data (PHD Thesis).* [Online] Available at: http://www.worldcat.org/title/application-of-monte-carlo-methods-to-the-analysis-of-spatially-correlated-data/oclc/79823910 [Accessed 8 March 2017].

Isaaks, E. H. and Srivastava, R. M., 1989. *Applied Mining Geostatistics.* New York: Oxford University Press.

Journel , A. G., 1983. Nonparametric estimation of spatial distributions. *Mathematical Geology,* 15(3), pp. 445-468.

Journel , A. G., 1988. New distance measures- the route towards truly non-Gaussian geostatistics.. *Mathematical Geology,* 20(5), pp. 459-475.

Journel, A. G., 1982. The indicator approach to estimation of spatial distribution. *In Proceedings 17th APCOM,* pp. 793-806.

Keogh, A. and Moulton, C., 1998. Median Indicator kriging : A case study of iron ore. In: *Beyond ordinary kriging: Non-Linear Geostatistical Methods in Practice.* Perth: The Geostatistical Association of Australasia, pp. 106-120.

Krige, D. G., 1994. *An analysis of some essential basic tenets of geostatistics not always practiced in ore valuations.* [Online] Available at: http://www.saimm.co.za/Conferences/DanieKrige/DGK40.pdf [Accessed 4 July 2015].

Krige, D. G., 1996. *A basic perspective on the role of classical statistics ,data search routines , conditional biases and information and smoothing effects in ore block valuations.* [Online] Available at: www.saimm.co.za/Conferences/DanieKrige/DGK41.pdf [Accessed 23 June 2015].

Krige, D. G., 1997. A practical analyses of the effects of spatial structure and of data available and accessed on conditional biases in ordinary kriging. In: E. Y. Baafi & N. A. Schofield, eds. *Geostatistics Wollongong '96.* Dordrecht: Kluwer Academic Publishers, pp. 799-810.

Lipton , I., Gaze, R., Horton, J. & Khosrowshahi, S., 1998. Practical application of multiple indicator kriging and conditional simulation to recoverable resource estimation for the Halley's lateritic nickel deposit. In: *Beyond ordinary kriging -Non-Linear Geostatistical Methods in Practice.* Perth: The Geostatistical Association of Australasia, pp. 88-105.

Lloyd, C. D. and Atkinson, P. M., 2001. Assessing uncertainty in estimates with ordinary and indicator kriging. *Computers & Geosciences,* 27(2001), pp. 929-937.

Manchuk, J. G. and Deutsch, C. V., 2012a. Implementation aspects of sequential Gaussian simulation on irregular points. *Comput Geosci,* 2012(16), pp. 625-637.

Manchuk, J. G. and Deutsch, C. V., 2012b. A flexible sequential Gaussian simulation program: USGSIM. *Computers & Geosciences,* 41(2012), pp. 208-2016.

Manchuk, J. G., Leuangthong, O. & Deutsch, V. C., 2007. *The proportional effect of spatial variables -CCG.* [Online]
Available at: www.ccgalberta.com/ccgresources/report09/2007-126_proportional_effect.pdf[Accessed 12 January 2017].

Matheron, G., 1971. *The theory of regionalized variables and its application.* [Online] Available at:
http://cg.ensmp.fr/bibliotheque/public/MATHERON_Ouvrage_00167.pdf
[Accessed 25 June 2016].

Mudau, M., 2014. *Linear and non linear resources estimation techniques applied in the Kanzi phosphate project in Democratic Republic of Congo,* Johannesburg: University of the Witwatersrand.

Ortiz, J. M. and Deutsch, C. V., 2003. *Uncertainty Upscaling.* [Online]
Available at: www.ccgalberta.com/ccgresources/repoert05/2003-124-upscaling.pdf [Accessed 25 August 2016].

Prendergast, M. D., 2001. Komatiite-hoisted Hunters Road nickel deposit, central Zimbabwe: Physical volcanology and sulfide genesis. *Australian Journal of Earth Sciences,* 2001(48), pp. 681-694.

Prins, C. and Minnit, R. C. A., 2016. *Theoretical Simulation Techniques (MINN7054) Lecture Notes.* Johannesburg, University of the Witwatersrand .

Rivoirard, J., 1994. *Introduction to disjunctive kriging and non linear geostatistics.* Oxford: Clarendon Press.

Roden , S. and Smith, T., 2014. Sampling and analysis protocols and their role in mineral exploration and new resource development. In: *Mineral Resources and Ore Reserves estimation. The AusIMM Guide to Good Practice.* 2nd ed. Carlton Victoria: The Australasian Institute of Mining and Metallurgy, pp. 53-60.

Rossi, M. E., 1999. *Improving the estimates of recoverable reserves.* [Online] Available at: www.onemine.org/documents [Accessed 12 March 2017].

Rossi, M. E. and Deutsch, C. V., 2014. *Mineral Resource Estimation.* Dordrecht: Springer.

Safikhani, M., Asghari, O. & Emery, X., 2016. *Assessing the accuracy of sequential gaussian simulation through statistical testing,* Verlag Berlin Heidelberg: Springer.

SRK Consulting Zimbabwe, 2002. *Investigation of the structural metamorphic control of nickel sulphide mineralisation in Zimbabwe (unpublished).* Harare: SRK Consulting Zimbabwe.

Statios, n.d. *GSLIB Help: POSTSIM - Statios.* [Online] Available at: http://www.statios.com/help/postsim.html [Accessed 12 March 2017].

Tinofirei, J., 1996. *A geological report on the Hunters Road nickel project,* s.l.: Unpublished.

Vann, J. and Guibal, D., 1998. Beyond ordinary kriging- An overview of non linear estimation. In: Perth: The Geostatistical Association of Australasia, pp. 6-25.

Vann, J., Guibal, D. & Harley, M., 2000. *Multiple Indicator Kriging - Is it suited to my deposit?.* Coolum,Qld, s.n, pp 57

Vann, J., Jackson, S. & Bertoli, O., 2003. *Quantitative kriging neighbourhood analysis for the mining Geologist - A description of the method with worked case examples.* Bendigo, s.n.

Verly, G., 1983. The multigaussian approach and its applications to the estimation of local reserves. *Mathematical Geology,* 15(2), pp. 259-286.

Winter , F., 1994. *A preliminary mineralogical and geochemical study of the Hunters Road deposit, Zimbabwe,* s.l.: Anglo American Research Laboratory Internal Report (Unpubl).

Yamamoto, J. K., 2005. Correcting the smoothing effect of ordinary kriging estimates. *International Association for Mathematical Geology,* 37(1), pp. 69-94.

APPENDIX 1: QAQC CONTROL CHARTS FOR 1992 TO 1993 EXPLORATION PROGRAM.

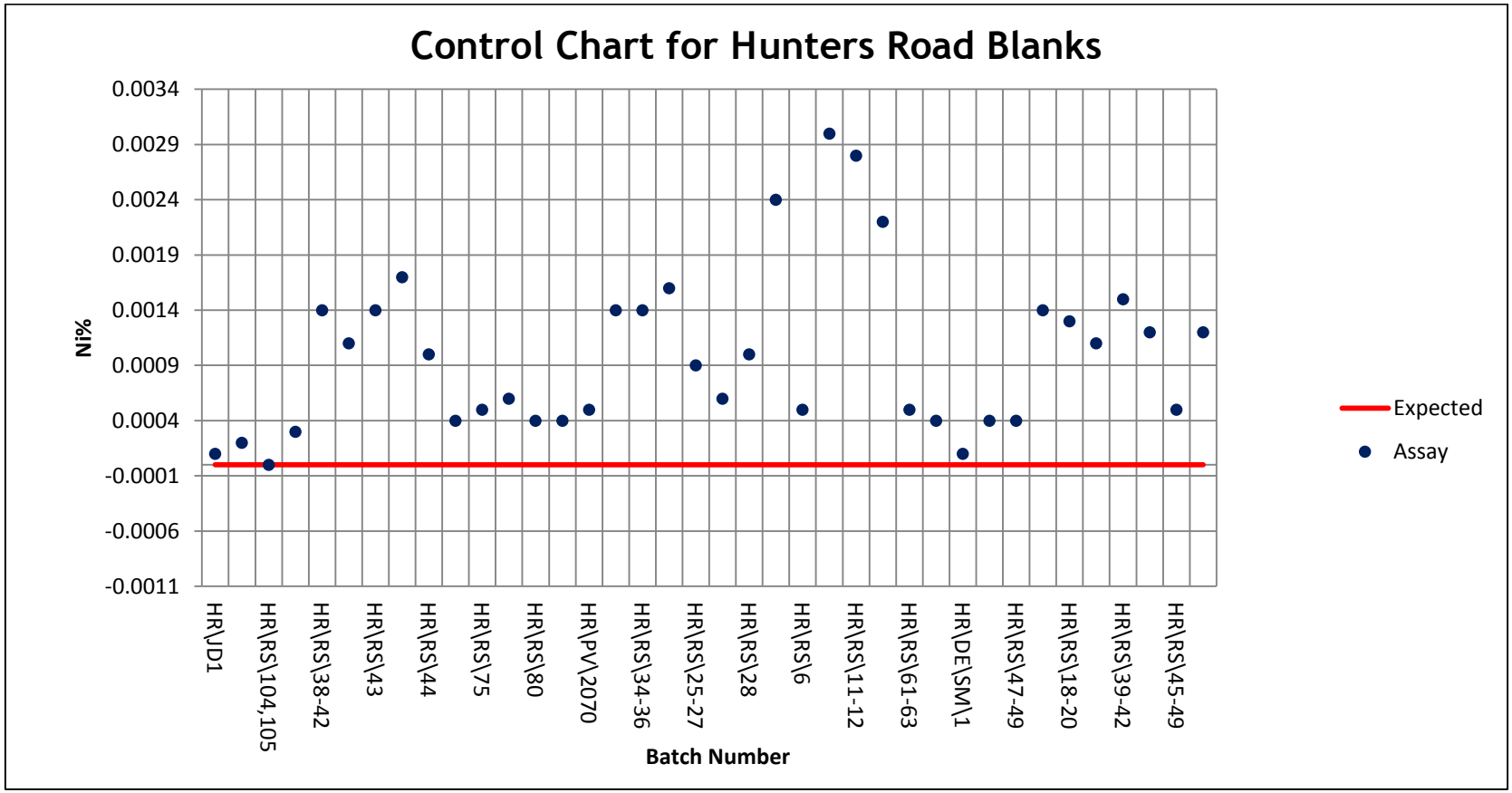

Figure A 1: Control chart for blanks.

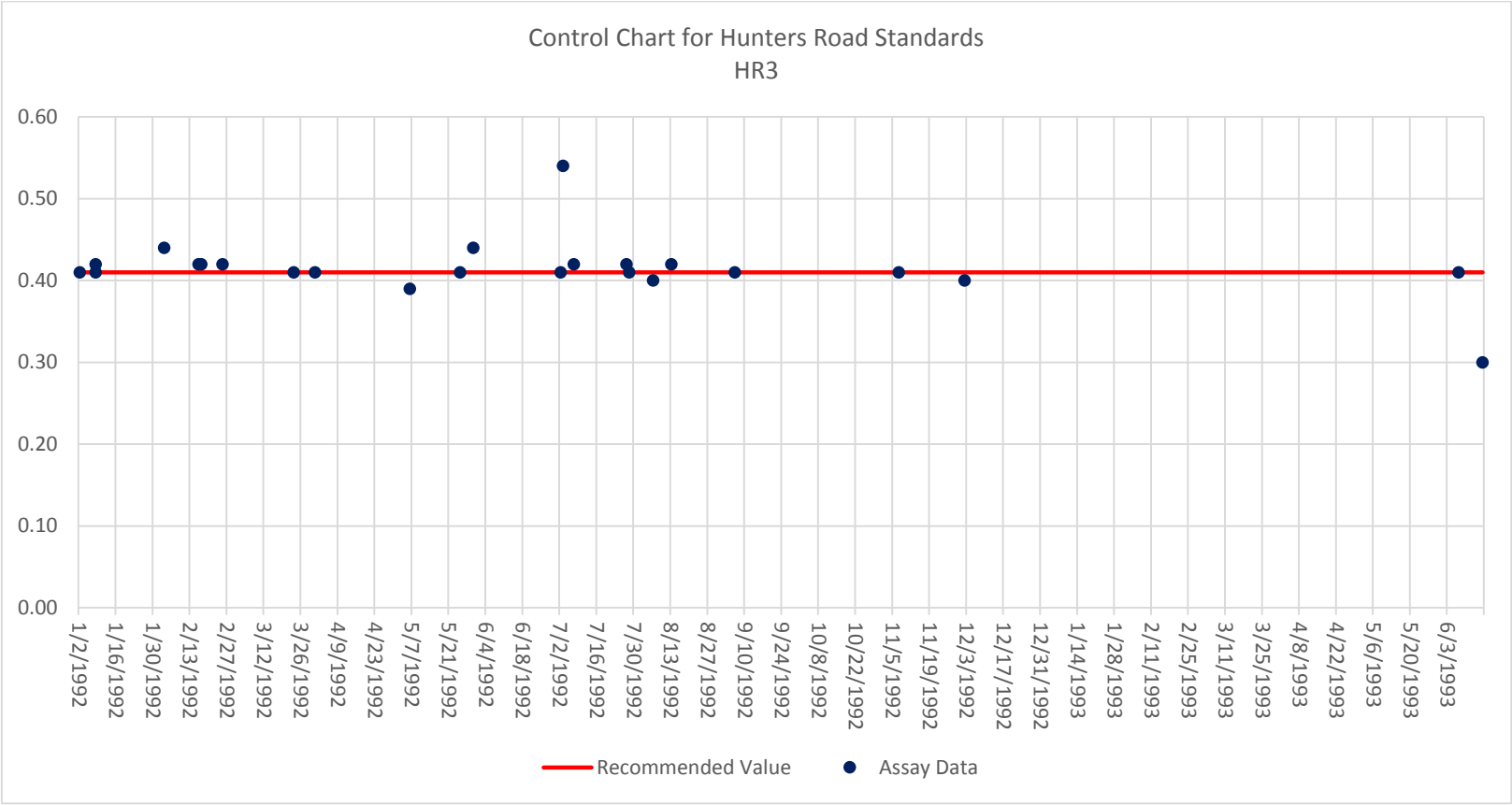

Figure A 2: Control chart for Standard HR3 with recommended value of 0.41% Ni.

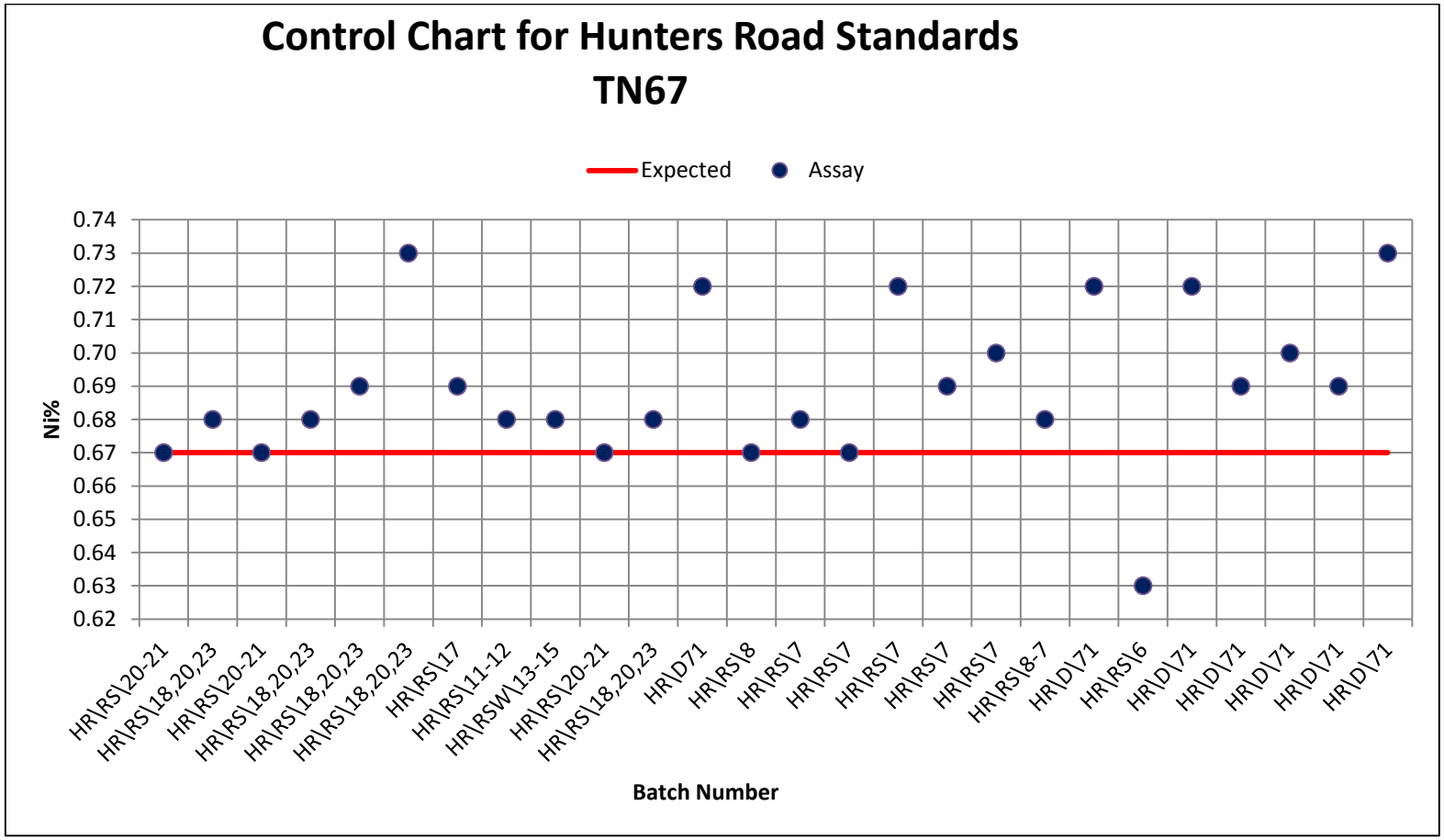

Figure A3: Control chart for Standard TN67 with recommended value of 0.67% Ni.

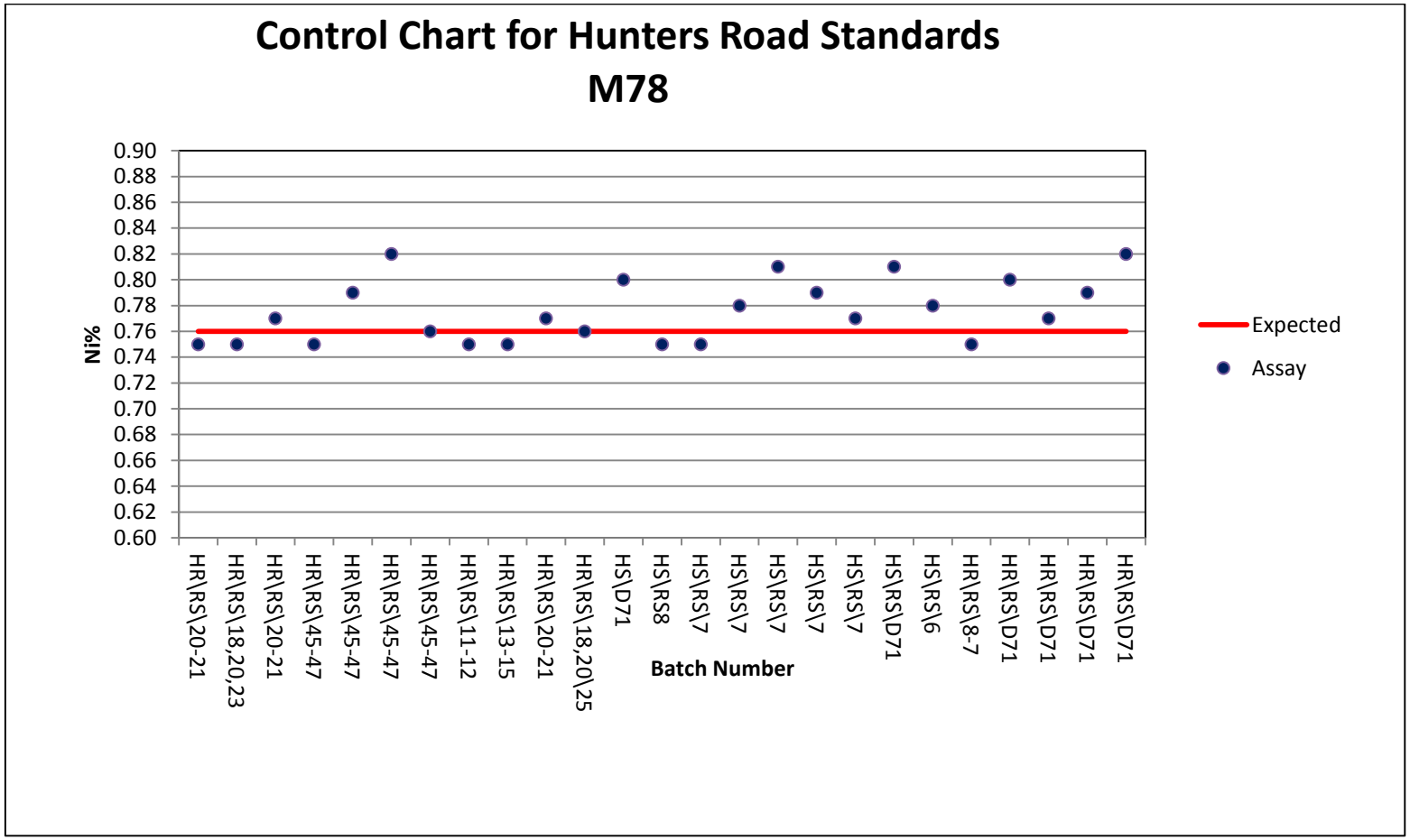

Figure A4: Control chart for Standard M78 with recommended value of 0.76% Ni.

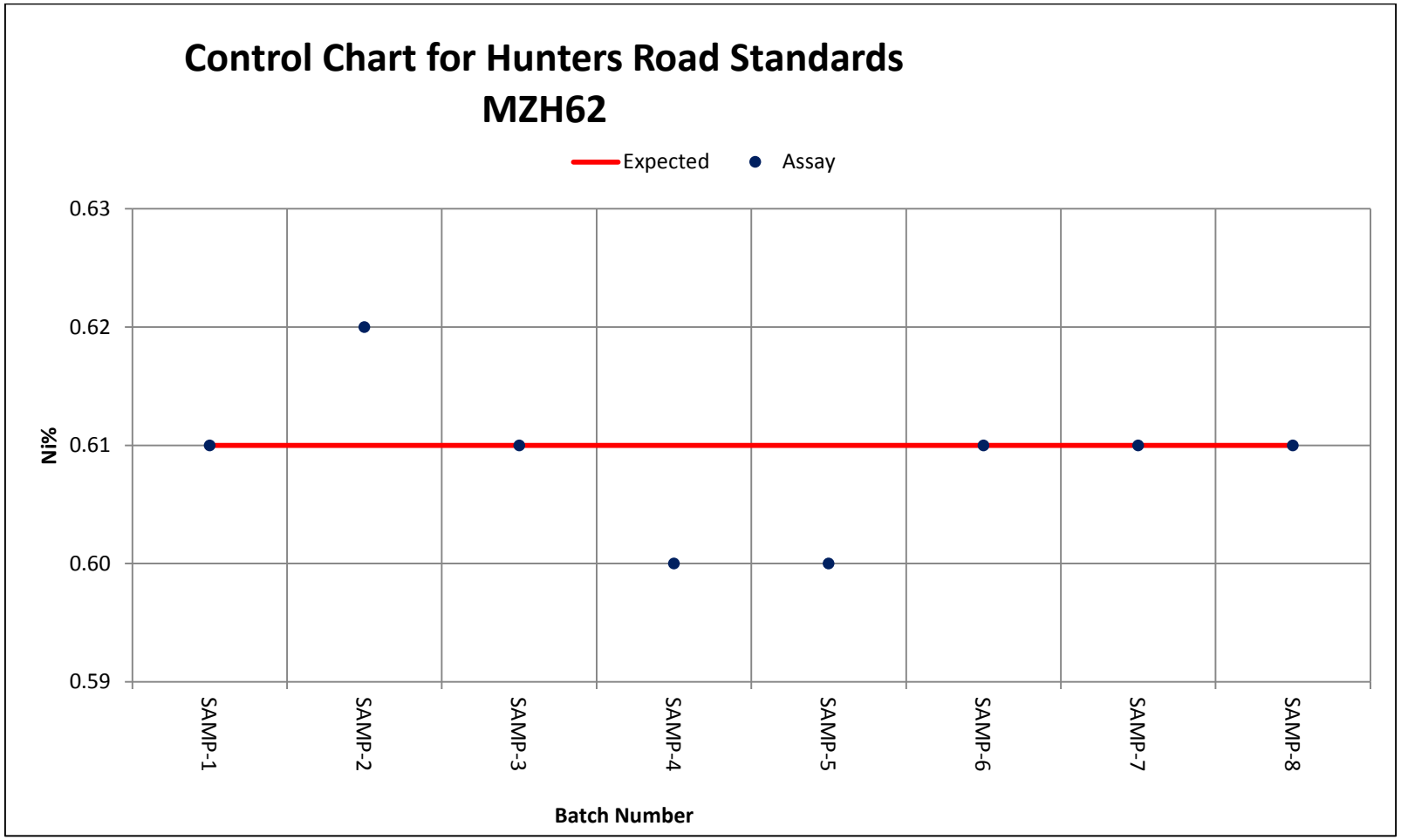

Figure A5: Control chart for Standard MZH62 with recommended value of 0.61% Ni.

APPENDIX 2: VARIOGRAM MODELS FOR THE EASTERN DOMAIN OF THE WESTERN OREBODY OF HUNTERS ROAD NICKEL PROJECT.

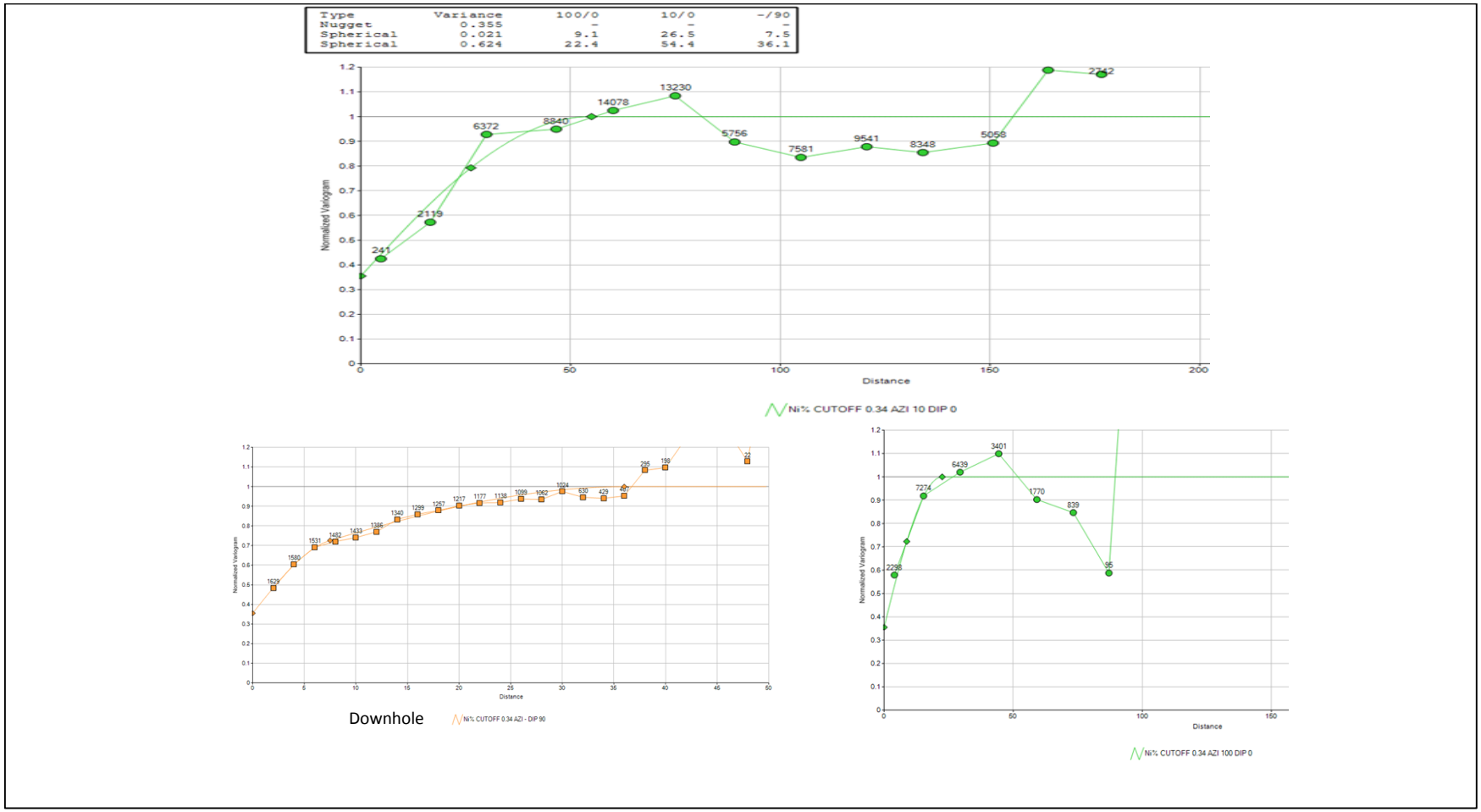

Figure A6: Eastern domain Indicator semi variogram at 0.34%Ni cut off grade.

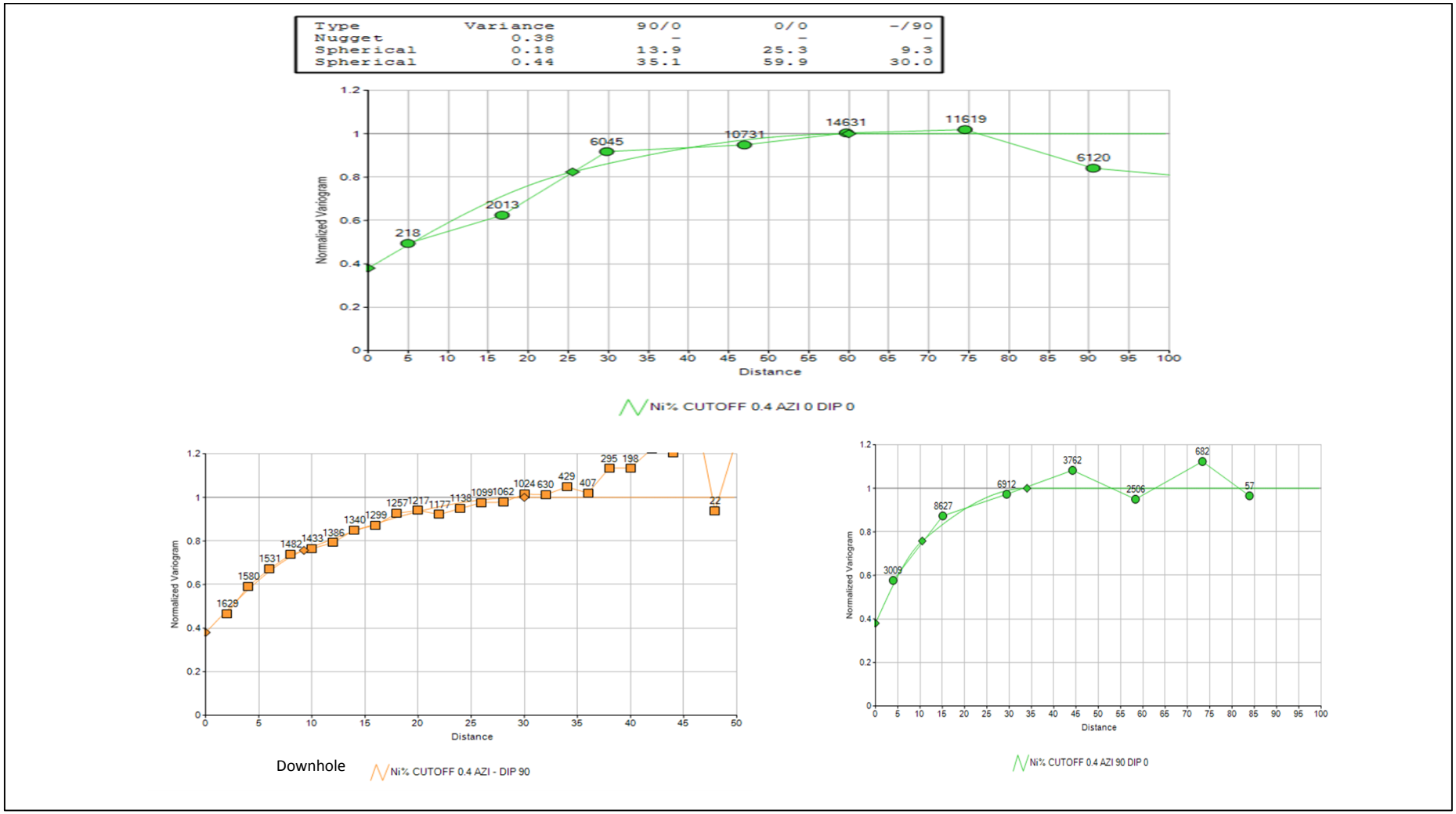

Figure A7: Eastern domain Indicator semi variogram at 0.40%Ni cut off grade.

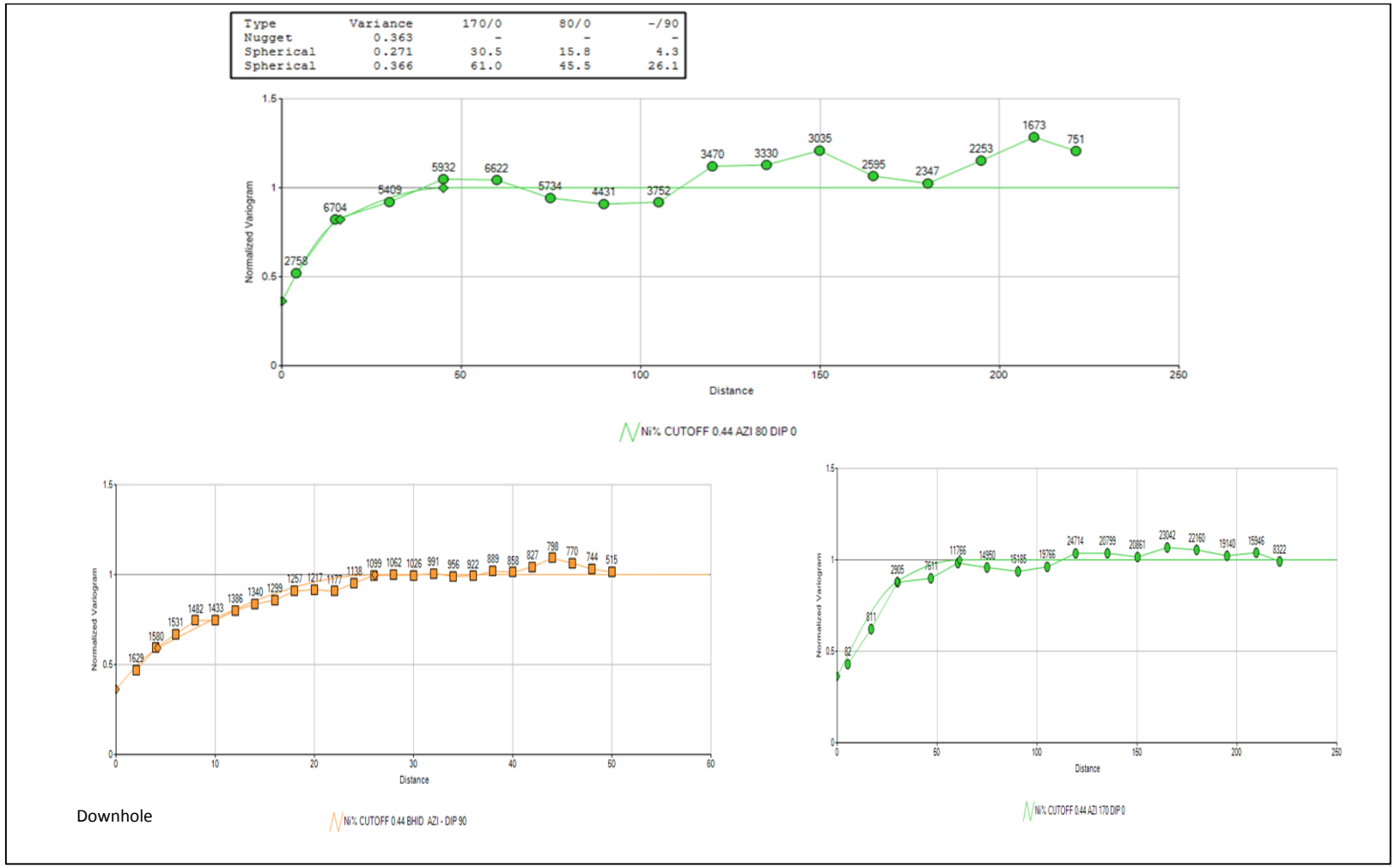

Figure A8: Eastern domain Indicator semi variogram at 0.44%Ni cut off grade.

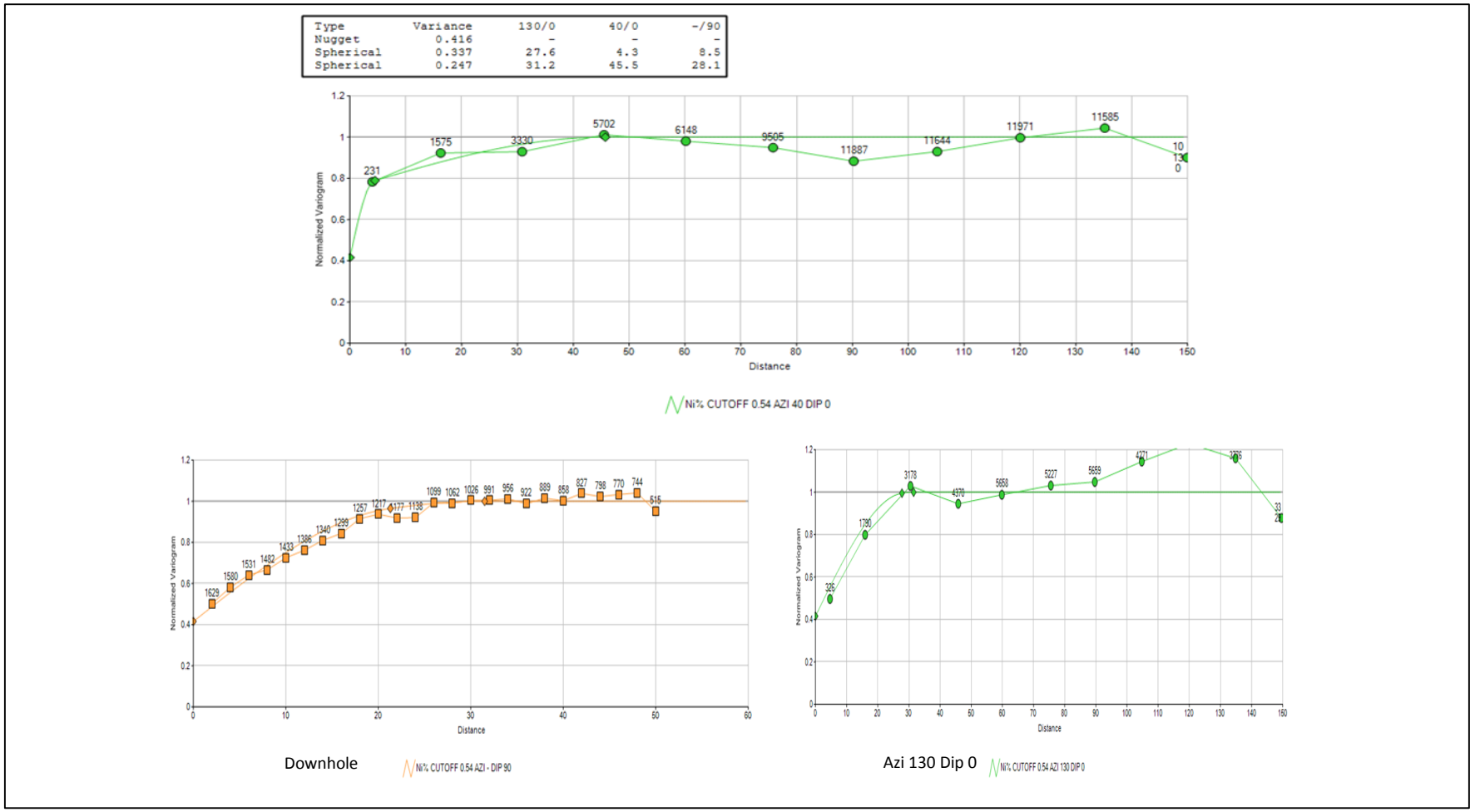

Figure A9: Eastern domain Indicator semi variogram at 0.54%Ni cut off grade.

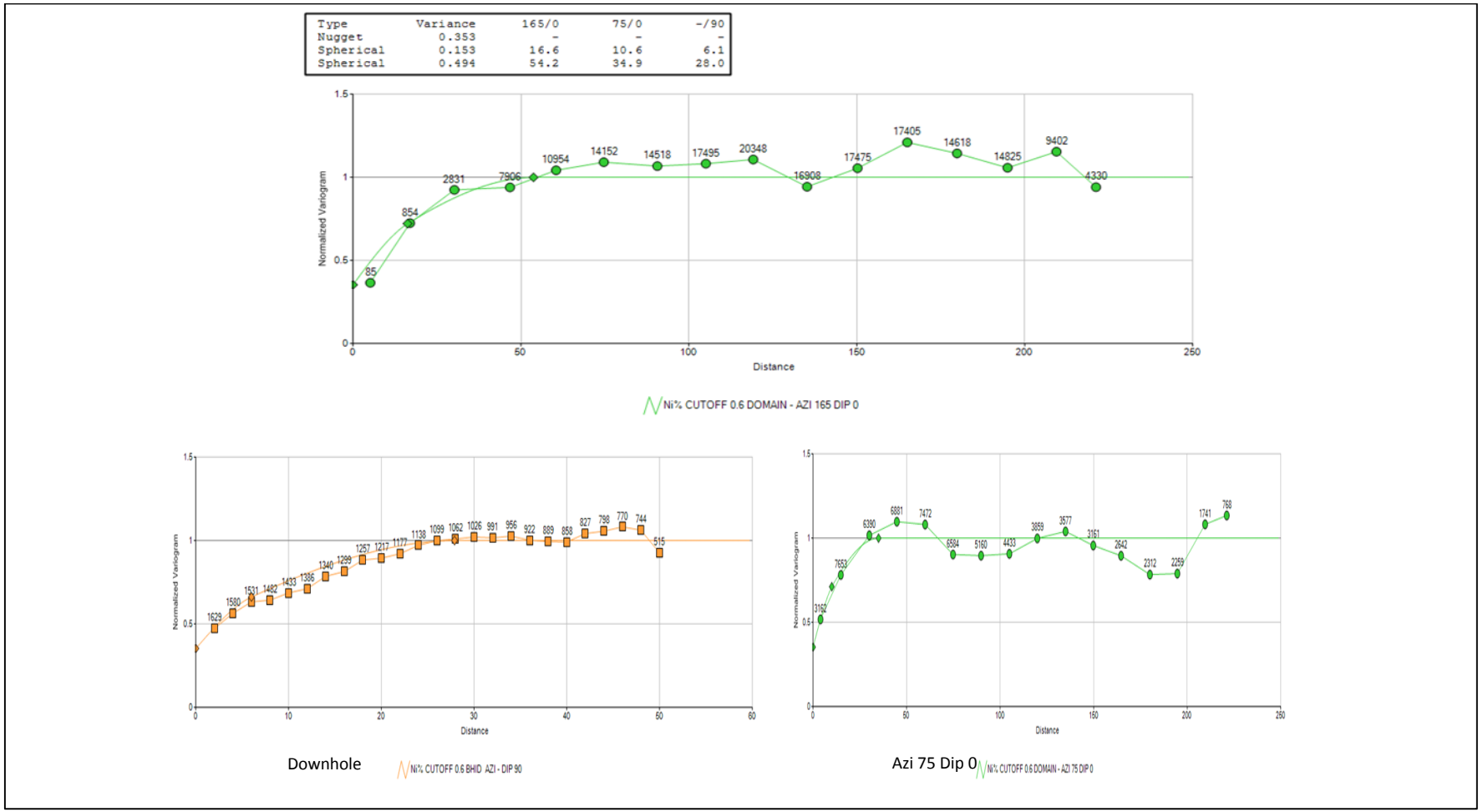

Figure A10: Eastern domain Indicator semi variogram at 0.60%Ni cut off grade.

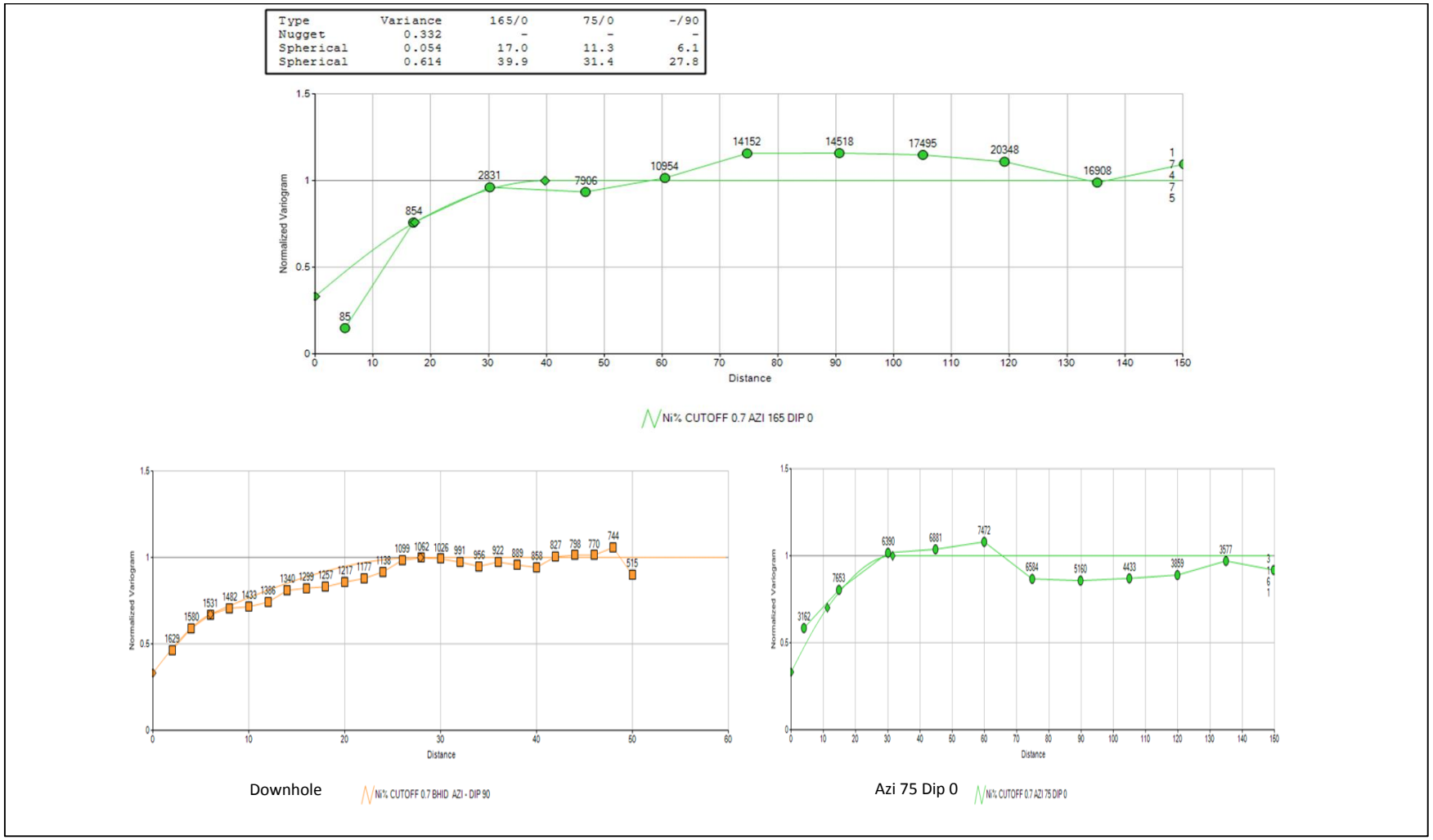

Figure A11: Eastern domain Indicator semi variogram at 0.70%Ni cut off grade.

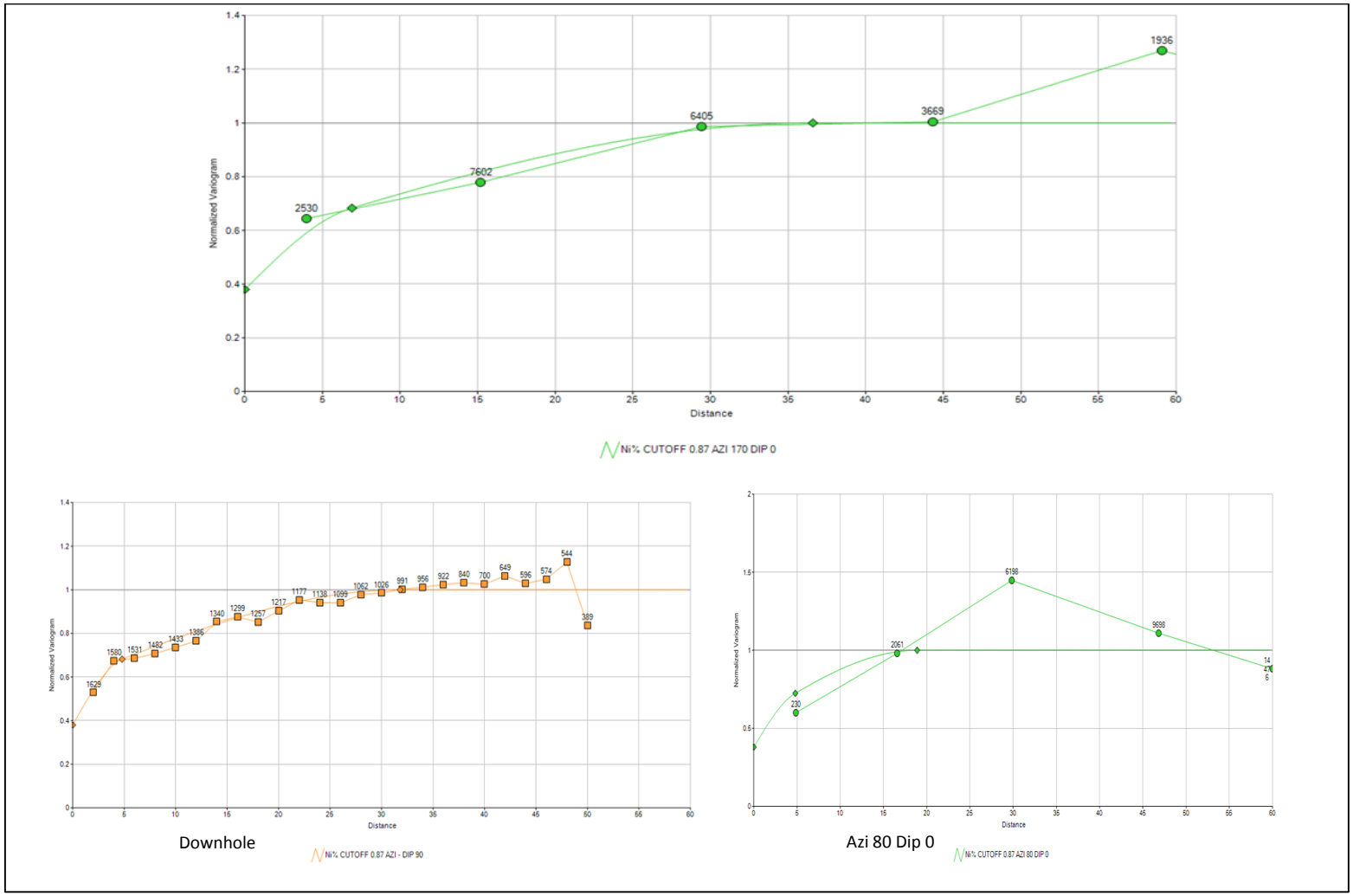

Figure A12: Eastern domain Indicator semi variogram at 0.87%Ni cut off grade.

APPENDIX 3: VARIOGRAM MODELS FOR THE WESTERN DOMAIN OF THE WESTERN OREBODY OF HUNTERS ROAD NICKEL PROJECT.

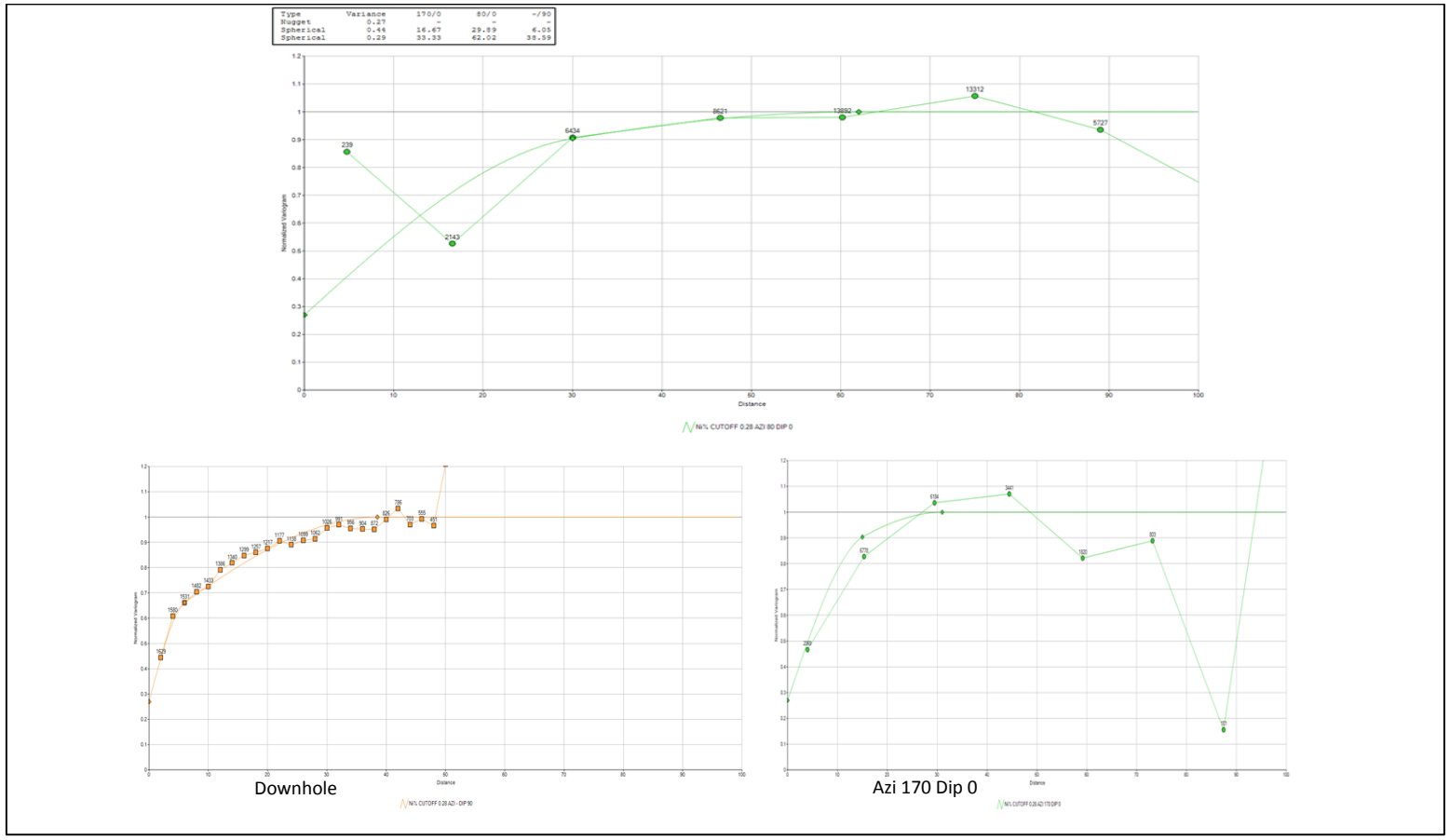

Figure A13: Western domain Indicator semi variogram at 0.28%Ni cut off grade.

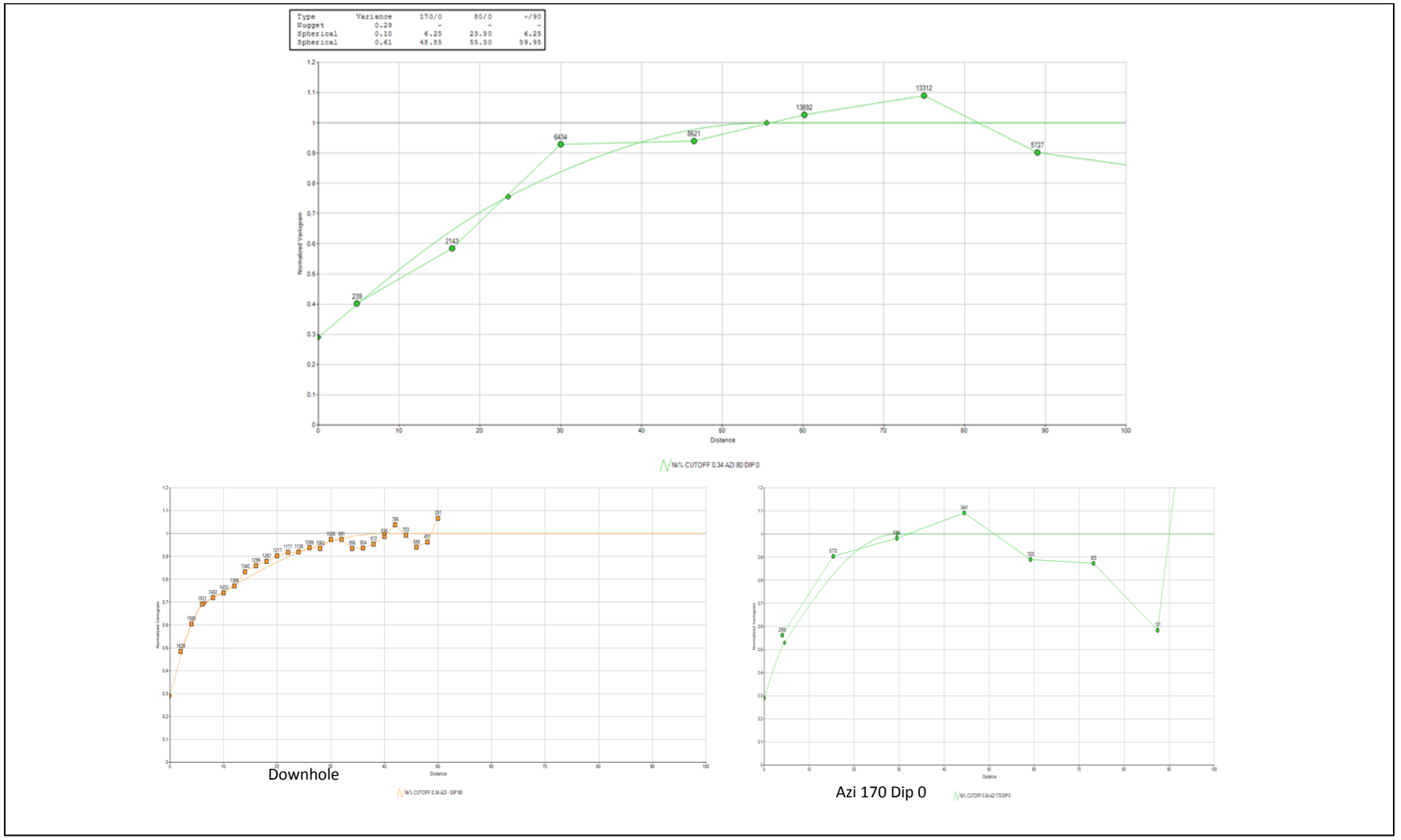

Figure A14: Western domain Indicator semi variogram at 0.34%Ni cut off grade.

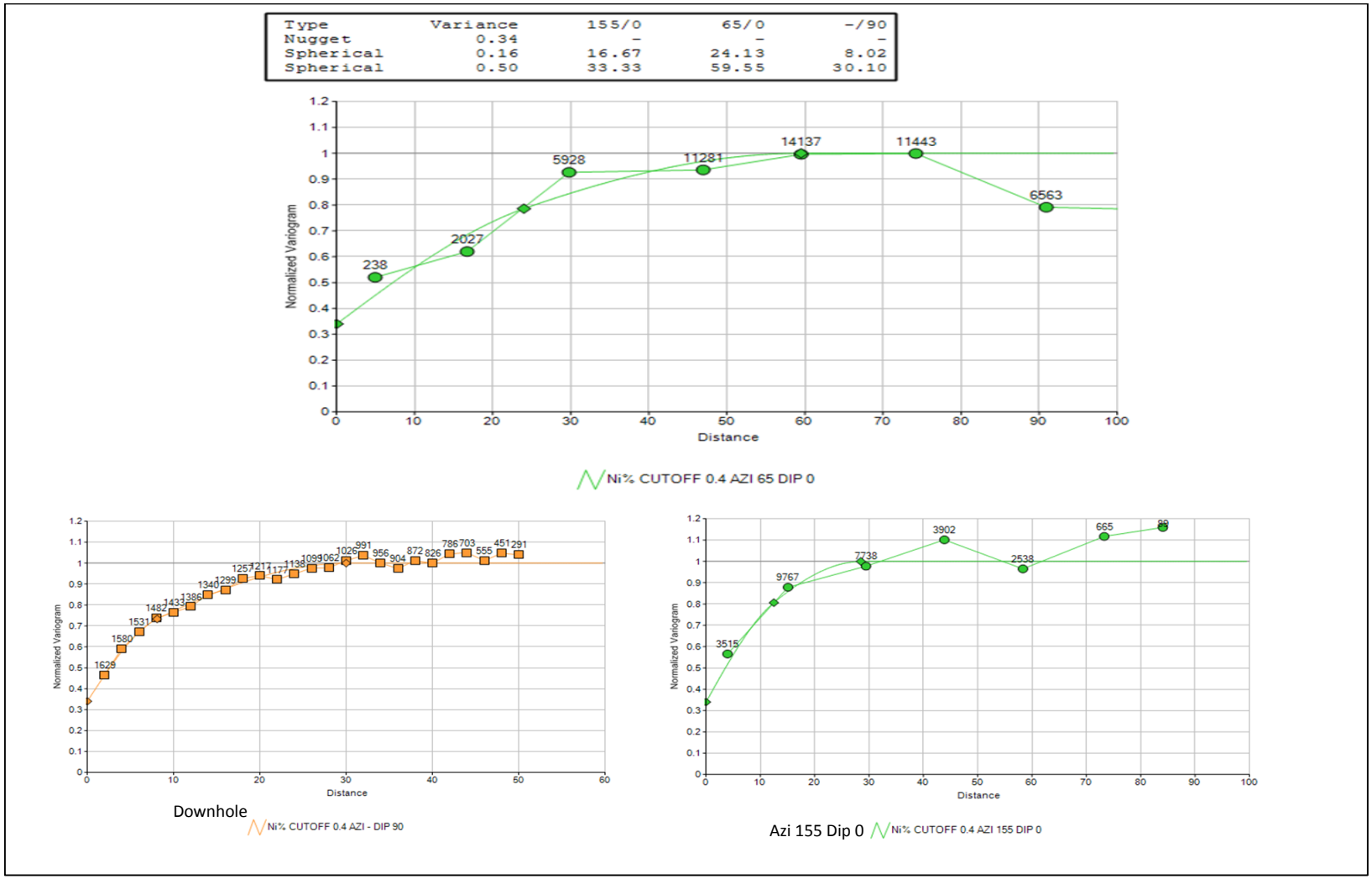

Figure A15: Western domain Indicator semi variogram at 0.40%Ni cut off grade.

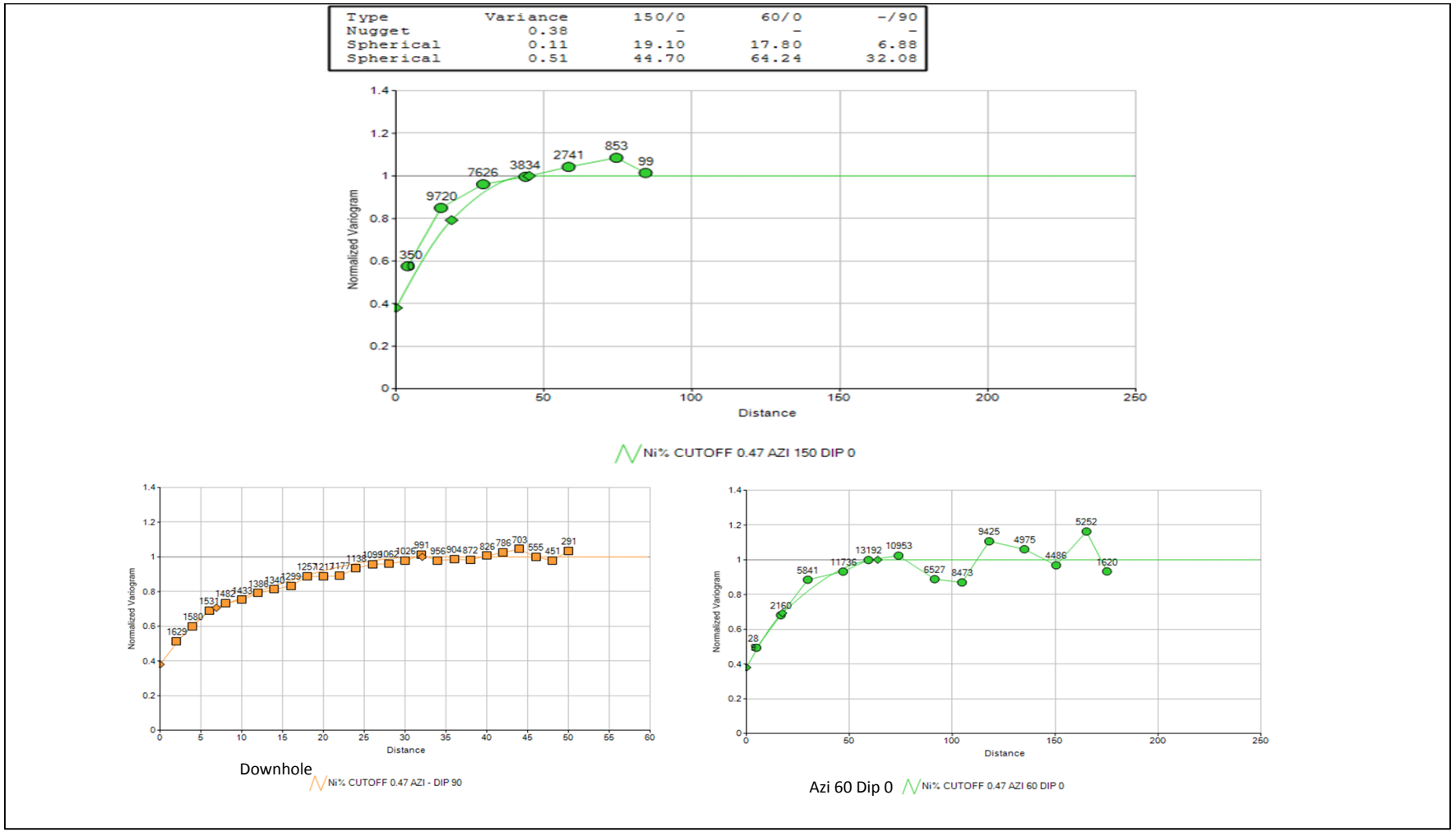

Figure A16: Western domain Indicator semi variogram at 0.47%Ni cut off grade.

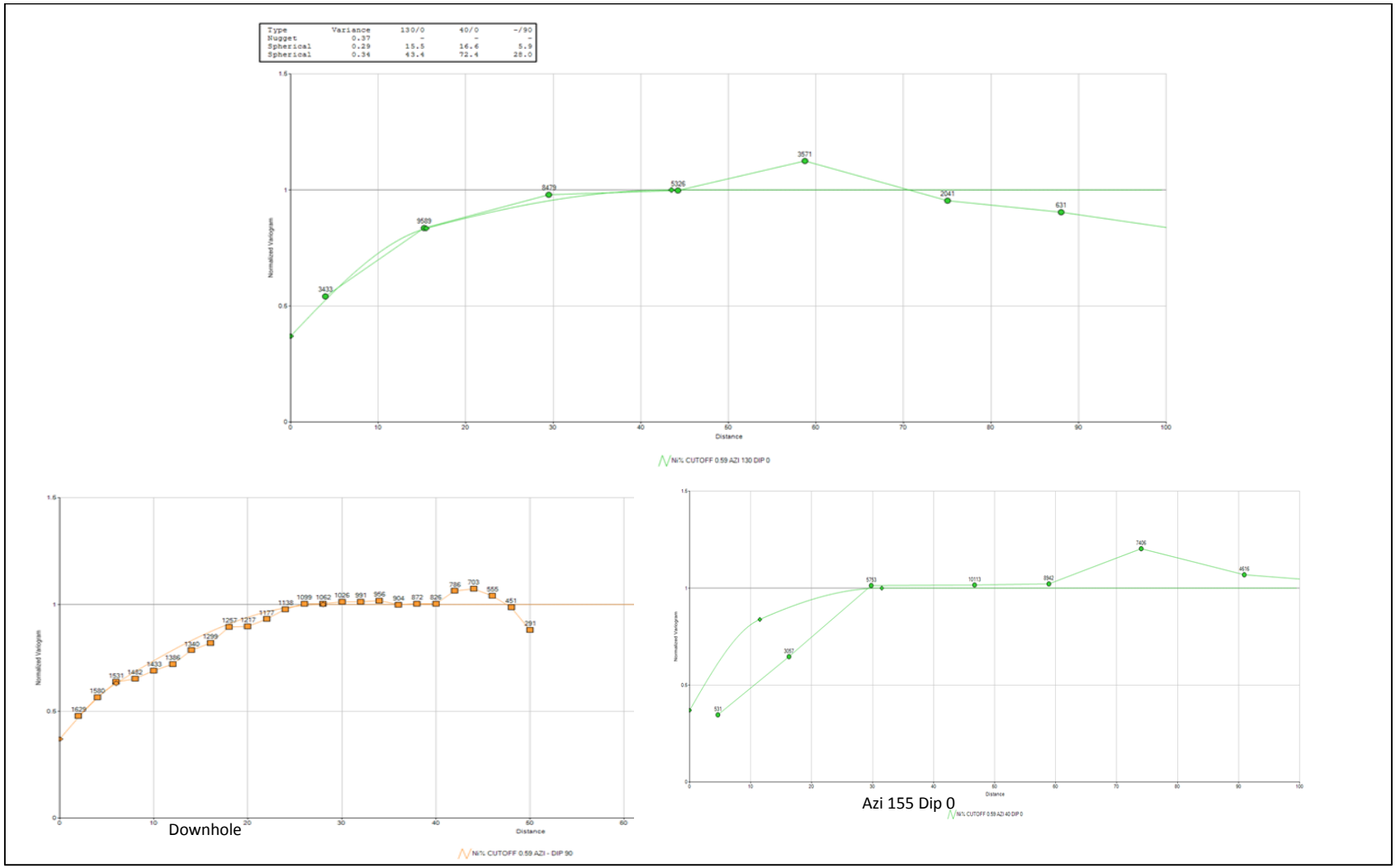

Figure A17: Western domain Indicator semi variogram at 0.59%Ni cut off grade.

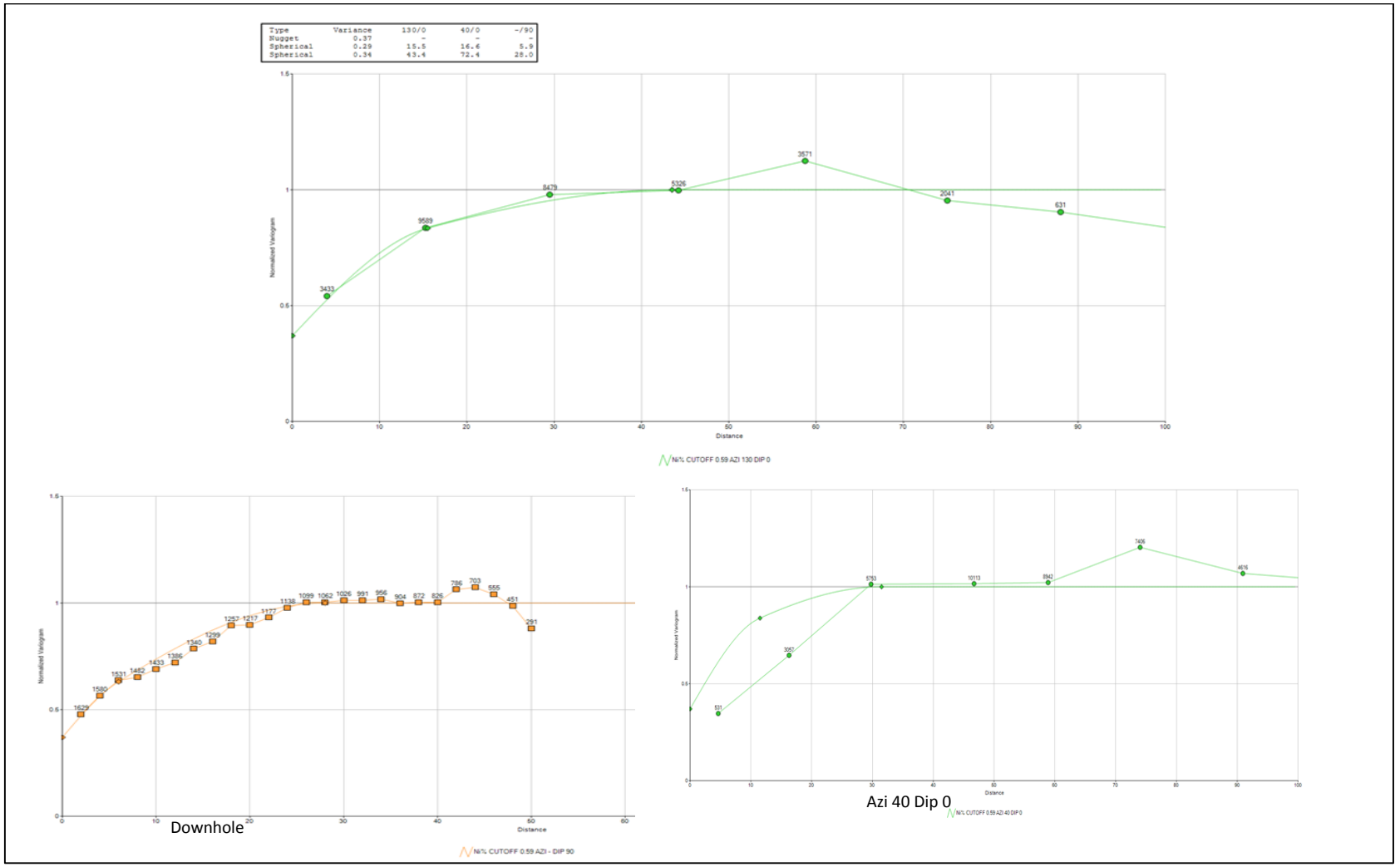

Figure A18: Western domain Indicator semi variogram at 0.66%Ni cut off grade.

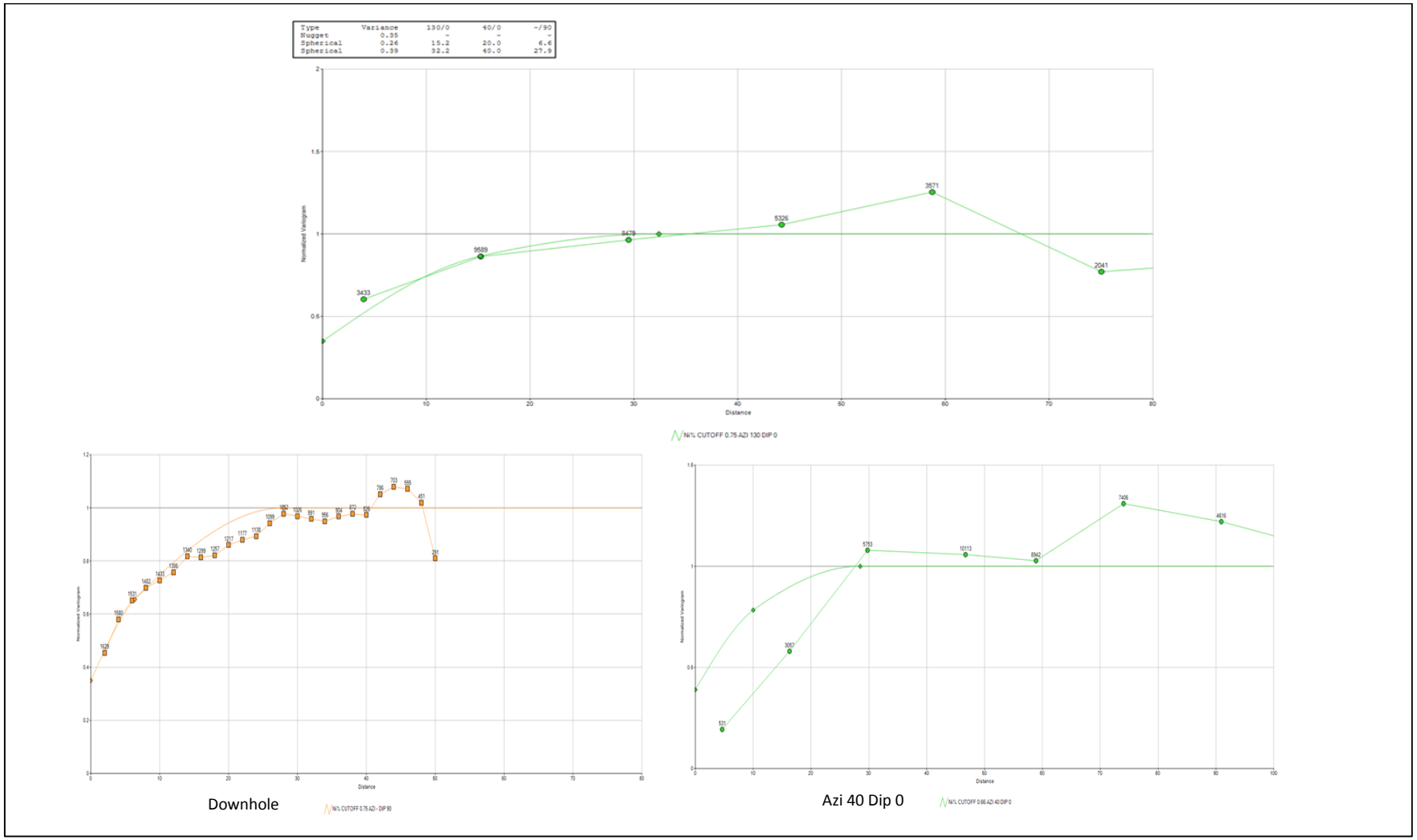

Figure A19: Western domain Indicator semi variogram at 0.75%Ni cut off grade.

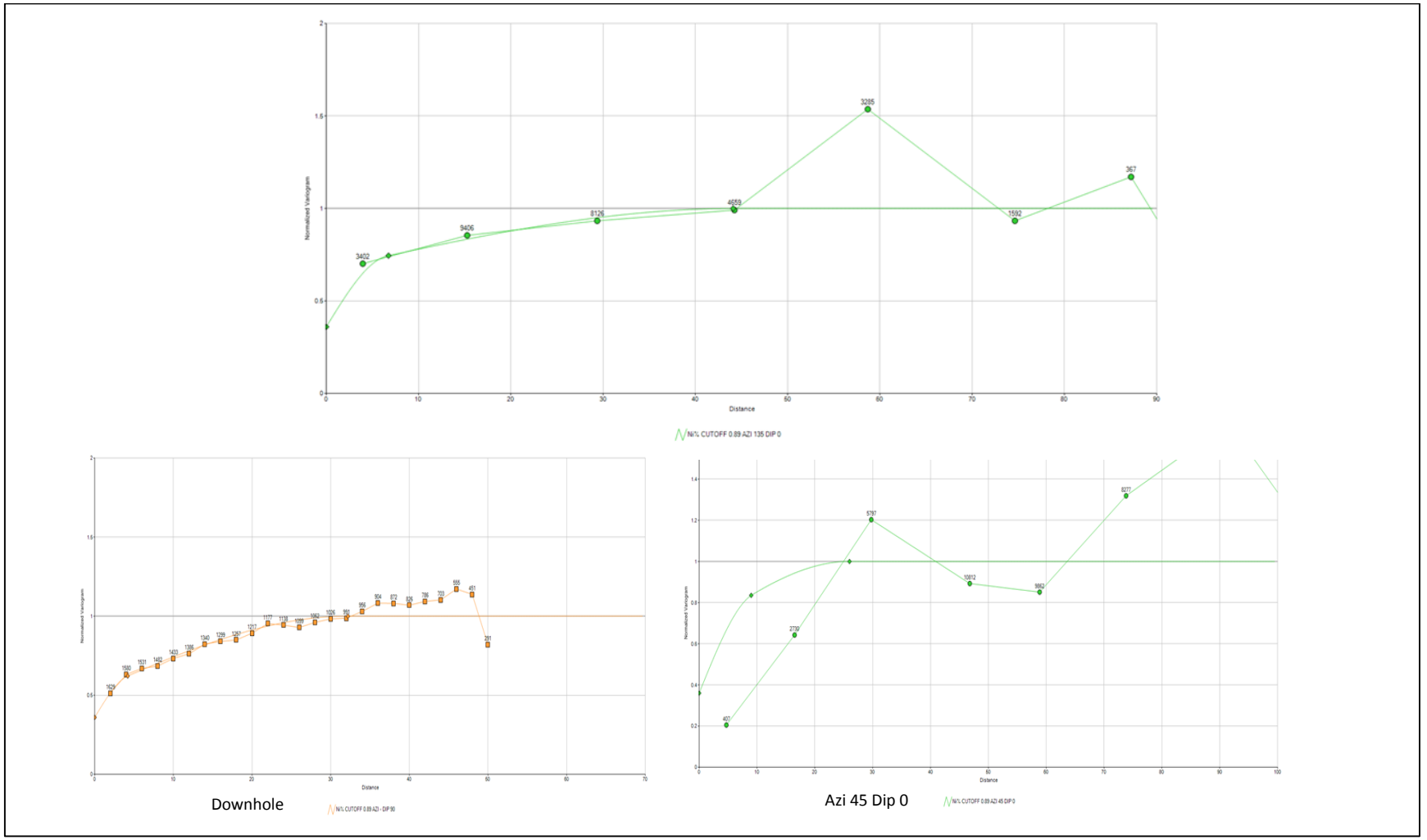

Figure A20: Western domain Indicator semi variogram at 0.89%Ni cut off grade.

APPENDIX 4: MINERAL RESOURCES PER BENCH FOR THE EASTERN AND WESTERN DOMAINS.

Table A 1: Eastern Domain Resources per bench using 0.40% COG

Bench (m)	Volume (m^3)	Tonnes (t)	Relative Density (t/m^3)	Grade (%Ni)	Metal Content (t)
1240	140,749	365,946	2.6	0.49	1792.13
1230	134,738	350,319	2.6	0.53	1863.34
1220	169,683	441,176	2.6	0.51	2233.87
1210	176,228	458,194	2.6	0.51	2353.54
1200	172,649	448,888	2.6	0.52	2332.75
1190	179,643	467,072	2.6	0.52	2447.70
1180	166,110	431,887	2.6	0.54	2331.08
1170	169,746	441,341	2.6	0.49	2183.05
1160	156,073	405,790	2.6	0.47	1907.69
1150	170,008	442,021	2.6	0.51	2262.65
1140	191,199	497,117	2.6	0.52	2591.12
1130	194,255	505,064	2.6	0.54	2731.70
1120	193,316	502,623	2.6	0.57	2875.24
1110	184,056	478,545	2.6	0.57	2744.08
1100	177,128	460,533	2.6	0.58	2652.92
1090	183,155	476,204	2.6	0.57	2695.49
1080	184,557	479,848	2.6	0.59	2854.86
1070	173,902	452,144	2.6	0.61	2742.17
1060	173,139	450,161	2.6	0.59	2648.70
1050	176,119	457,911	2.6	0.58	2642.73
1040	167,029	434,275	2.6	0.58	2523.28
1030	140,776	366,018	2.6	0.56	2053.08
1020	119,214	309,956	2.6	0.53	1638.53
1010	112,623	292,820	2.6	0.57	1678.16
1000	109,240	284,025	2.6	0.59	1687.77
990	87,313	227,014	2.6	0.56	1279.86
980	86,540	225,003	2.6	0.54	1216.61
970	95,559	248,454	2.6	0.53	1322.18
960	94,481	245,651	2.6	0.53	1303.99
950	81,931	213,020	2.6	0.54	1145.03
940	64,022	166,456	2.6	0.51	857.05
930	53,202	138,326	2.6	0.5	694.00
Total	**4,678,386**	**12,163,802**	**2.6**	**0.54**	**66286.36**

Table A 2: Western Domain Resources per bench using 0.40% COG

Bench (m)	Volume (m^3)	Tonnes (t)	Relative Density (t/m3)	Grade (%Ni)	Metal Content (t)
1240	90,911	236,370	2.60	0.49	1,153.73
1230	100,232	260,602	2.60	0.52	1,363.21
1220	103,632	269,443	2.60	0.48	1,280.23
1210	107,368	279,158	2.60	0.48	1,338.97
1200	99,826	259,549	2.60	0.46	1,200.89
1190	140,920	366,393	2.60	0.47	1,715.25
1180	154,054	400,541	2.60	0.51	2,050.01
1170	186,779	485,625	2.60	0.5	2,412.24
1160	181,293	471,362	2.60	0.52	2,469.85
1150	161,168	419,036	2.60	0.49	2,038.38
1140	186,805	485,693	2.60	0.51	2,452.87
1130	227,700	592,021	2.60	0.49	2,929.61
1120	226,508	588,920	2.60	0.5	2,946.95
1110	272,901	709,542	2.60	0.53	3,728.93
1100	271,094	704,844	2.60	0.53	3,737.75
1090	307,918	800,588	2.60	0.51	4,117.43
1080	318,979	829,344	2.60	0.54	4,509.02
1070	325,867	847,254	2.60	0.58	4,898.72
1060	313,987	816,366	2.60	0.61	4,978.45
1050	331,193	861,102	2.60	0.62	5,315.40
1040	325,603	846,568	2.60	0.64	5,448.82
1030	321,329	835,455	2.60	0.64	5,344.22
1020	309,582	804,913	2.60	0.64	5,139.12
1010	308,440	801,945	2.60	0.63	5,083.97
1000	300,054	780,142	2.60	0.63	4,934.60
990	314,033	816,485	2.60	0.64	5,204.26
980	315,946	821,460	2.60	0.64	5,297.02
970	308,243	801,432	2.60	0.63	5,037.77
960	303,091	788,036	2.60	0.66	5,238.20
950	299,618	779,006	2.60	0.65	5,037.35
940	283,739	737,722	2.60	0.62	4,538.77
930	246,834	641,768	2.60	0.61	3,905.83
Total	7,745,648	20,138,686	2.60	0.58	116,847.83